



UNIVERSIDAD NACIONAL AUTÓNOMA DE MÉXICO
POSGRADO EN CIENCIAS BIOLÓGICAS
FACULTAD DE CIENCIAS
ECOLOGÍA

**MODELACIÓN MATEMÁTICA DE LA DINÁMICA DE LA COBERTURA VEGETAL
EN LA RESERVA ECOLÓGICA DEL PEDREGAL DE SAN ÁNGEL**

TESIS

(POR ARTÍCULO CIENTÍFICO)

**PREDICTING DYNAMIC TRAJECTORIES OF A PROTECTED PLANT COMMUNITY UNDER
CONTRASTING CONSERVATION REGIMES: INSIGHTS FROM DATA-BASED
MODELLING**

QUE PARA OPTAR POR EL GRADO DE:

MAESTRO EN CIENCIAS BIOLÓGICAS

PRESENTA:

JAIME ACOSTA ARREOLA

**TUTOR: DR. JORGE ARTURO MEAVE DEL CASTILLO
FACULTAD DE CIENCIAS, UNAM**

**COMITÉ TUTOR: DRA. MARIANA BENÍTEZ KEINRAD
LABORATORIO NACIONAL DE CIENCIAS DE LA SOSTENIBILIDAD, UNAM
COMITÉ TUTOR: DR. ROBERTO BONIFAZ ALFONZO
INSTITUTO DE GEOFÍSICA, UNAM**



UNAM – Dirección General de Bibliotecas

Tesis Digitales
Restricciones de uso

DERECHOS RESERVADOS ©
PROHIBIDA SU REPRODUCCIÓN TOTAL O PARCIAL

Todo el material contenido en esta tesis está protegido por la Ley Federal del Derecho de Autor (LFDA) de los Estados Unidos Mexicanos (Méjico).

El uso de imágenes, fragmentos de videos, y demás material que sea objeto de protección de los derechos de autor, será exclusivamente para fines educativos e informativos y deberá citar la fuente donde la obtuvo mencionando el autor o autores. Cualquier uso distinto como el lucro, reproducción, edición o modificación, será perseguido y sancionado por el respectivo titular de los Derechos de Autor.



UNIVERSIDAD NACIONAL AUTÓNOMA DE MÉXICO
POSGRADO EN CIENCIAS BIOLÓGICAS
FACULTAD DE CIENCIAS
ECOLOGÍA

**MODELACIÓN MATEMÁTICA DE LA DINÁMICA DE LA COBERTURA VEGETAL
EN LA RESERVA ECOLÓGICA DEL PEDREGAL DE SAN ÁNGEL**

TESIS

(POR ARTÍCULO CIENTÍFICO)

**PREDICTING DYNAMIC TRAJECTORIES OF A PROTECTED PLANT COMMUNITY UNDER
CONTRASTING CONSERVATION REGIMES: INSIGHTS FROM DATA-BASED
MODELLING**

QUE PARA OPTAR POR EL GRADO DE:

MAESTRO EN CIENCIAS BIOLÓGICAS

PRESENTA:

JAIME ACOSTA ARREOLA

**TUTOR: DR. JORGE ARTURO MEAVE DEL CASTILLO
FACULTAD DE CIENCIAS, UNAM**

**COMITÉ TUTOR: DRA. MARIANA BENÍTEZ KEINRAD
LABORATORIO NACIONAL DE CIENCIAS DE LA SOSTENIBILIDAD, UNAM
COMITÉ TUTOR: DR. ROBERTO BONIFAZ ALFONZO
INSTITUTO DE GEOFÍSICA, UNAM**

COORDINACIÓN DEL POSGRADO EN CIENCIAS BIOLÓGICAS
FACULTAD DE CIENCIAS
DIVISIÓN ACADÉMICA DE INVESTIGACIÓN Y POSGRADO
OFICIO FCIE/DAIP/299/2022
ASUNTO: Oficio de Jurado

M. en C. Ivonne Ramírez Wence
Directora General de Administración Escolar, UNAM
Presente.

Me permito informar a usted que en la reunión ordinaria del Comité Académico del Posgrado en Ciencias Biológicas, celebrada el día **9 de mayo de 2022** se aprobó el siguiente jurado para el examen de grado de **MAESTRO EN CIENCIAS BIOLÓGICAS** en el campo de conocimiento de **Ecología** del (la) alumno(a) **ACOSTA ARREOLA JAIME** con número de cuenta **302050763** por la modalidad de graduación de **tesis por artículo científico** titulado: "**Predicting dynamic trajectories of a protected plant community under contrasting conservation regimes: insights from data-based modelling**", que es producto del proyecto realizado en la maestría que lleva por título "**Modelación matemática de la dinámica de la cobertura vegetal en la Reserva Ecológica del Pedregal de San Ángel**." ambos realizados bajo la dirección del **DR. JORGE ARTURO MEAVE DEL CASTILLO**, quedando integrado de la siguiente manera:

Presidente: DR. LUIS ZAMBRANO GONZÁLEZ
Vocal: DR. ZENÓN CANO SANTANA
Vocal: DR. EDGAR JAVIER GONZÁLEZ LICEAGA
Vocal: M. EN C. EVERARDO GUSTAVO ROBREDO ESQUIVELZETA
Secretario: DRA. MARIANA BENÍTEZ KEINRAD

Sin otro particular, me es grato enviarle un cordial saludo.

ATENTAMENTE
"POR MI RAZA HABLARÁ EL ESPÍRITU"
Ciudad Universitaria, Cd. Mx., a 26 de julio de 2022

COORDINADOR DEL PROGRAMA

DR. ADOLFO GERARDO NAVARRO SIGÜENZA



Agradecimientos institucionales

Al Posgrado de Ciencias Biológicas de la UNAM por la oportunidad de estudiar una maestría de excelencia académica. Al CONACyT, por otorgarme la beca No. 703449, la cual facilitó mi dedicación de tiempo completo a la investigación. A mi tutor, el Dr. Jorge Arturo Meave del Castillo por su apoyo y por su crítica constante y reflexiva. Finalmente, al comité tutor conformado por la Dra. Mariana Benítez Keinrad y el Dr. Roberto Bonifaz Alfonzo; ambos aportaron observaciones y críticas sumamente valiosas para el desarrollo de la investigación durante todos los semestres. Gracias a todo el comité tutor por la confianza en el proyecto.

Agradecimientos personales

Agradezco a la vida por ser tan diversa y al tiempo por hacer que todo cambie...

Quiero agradecer al pueblo de México por pagar mi educación pública y gratuita durante toda mi vida.

Agradezco a los colaboradores y coautores del artículo. Al Dr. Pablo Aguirre por su participación con el cálculo de la separatriz y la propuesta de control del eucalipto, así como por sus comentarios que mantuvieron el rigor matemático. Al matemático Nicolás González por su análisis de los puntos de equilibrio de los modelos. En especial agradezco a la Dra. Elisa Domínguez. Gracias a ella pudimos contar la historia ecológica con el formalismo matemático, las herramientas computacionales y el uso de representaciones visuales de una forma contundente. En especial agradezco a Jorge y a Elisa la revisión exhaustiva del manuscrito. Gracias a ustedes he aprendido mucho sobre cómo realizar una investigación y convertirla en una publicación con altísimos estándares de calidad.

Agradezco a todos los miembros del jurado por los valiosos comentarios y correcciones. Al Dr Zenón Cano por su visión integral y erudita de la REPSA y por su sentido del humor. Al M. en C. Everardo Robredo por su profundo conocimiento de la ecología y las matemáticas. A la Dra. Mariana Benítez por su visión reflexiva y social de los modelos matemáticos en ecología. Al Dr. Luis Zambrano por su conocimiento en la REPSA y en la teoría de estados estables alternativos. A los más de mil comentarios del Dr. Edgar González, a su rigor matemático y a su experiencia y perspectiva al crear diálogos con un lenguaje sencillo y consistente entre la ecología y las matemáticas. También, agradezco la revisión que realizó a esta última versión el Dr. Roberto Bonifaz.

Agradezco al Grupo de Ecología y Diversidad Vegetal y al Biól. Marco Antonio Romero Romero por su incansable y amable labor en el apoyo técnico. Agradezco a Artemisa Miranda Mondragón del grupo de trabajo de Zenón por la revisión bibliográfica.

Agradezco a la UNAM y a la Facultad de Ciencias, que pese a todos sus problemas, siguen siendo la vanguardia en la investigación y en la formación del pensamiento crítico, científico y artístico en México. Ahí he conocido tanto la competencia ruin y la desigualdad por privilegios, como el apoyo mutuo y la belleza de compartir el conocimiento.

Por último, agradezco a mi familia. Sin ellos, nada de esto sería posible.

Dedicado a...

Ma. del Carmen Arreola Sánchez y a su amor infinito...

el Dr. Eduardo Acosta Arreola y a su ternura radical...

la memoria de Jaime Acosta Levet... Papá, gracias por todo...

Índice

<i>Índice</i>	4
<i>Resumen</i>	5
<i>Abstract</i>	6
<i>Introducción</i>	7
Estabilidad y resiliencia.....	8
Estados estables alternativos	9
¿Cuenca de atracción en la Reserva Ecológica del Pedregal de San Ángel?.....	10
<i>Predicting dynamic trajectories of a protected plant community under contrasting conservation regimes: insights from data-based modelling</i>	13
<i>Discusión general</i>	119
<i>Conclusiones</i>	123
<i>Referencias bibliográficas</i>	124

Resumen

La modelación del comportamiento dinámico de comunidades ecológicas basada en datos es un gran reto en la ecología de sistemas y en la conservación biológica. Ante el aumento de los disturbios por distintos factores, la implementación de estos modelos para predecir escenarios futuros potenciales es clave para la toma de decisiones en las reservas ecológicas. Construimos una familia de modelos (mediante el uso de sistemas de ecuaciones diferenciales ordinarias) para reconstruir sus interacciones dinámicas a partir de datos demográficos y ecológicos de tres especies arborescentes de la Reserva Ecológica Pedregal de San Ángel (REPSA; Ciudad de México, México). Los primeros dos modelos consideraron dos especies nativas (*Pittocaulon praecox* y *Buddleja cordata*) y sus posibles interacciones ecológicas antagónicas de competencia o de cooperación. Estas especies son consideradas ingenieros ecosistémicos ya que son capaces de determinar varios atributos de la comunidad vegetal. Estos modelos predicen la transición de un estado estacionario estable dominado por *P. praecox* (como se informó en la década de 1950) a la comunidad actual, cuya estructura aparentemente está cambiando a un estado estable alternativo dominado por *B. cordata*. El segundo par de modelos incorpora también al árbol exótico australiano *Eucalyptus camaldulensis*, el cual ejerce efectos negativos en todas las especies de plantas nativas. Este modelo predice un estado dominado por *E. camaldulensis* en el que las especies nativas de la reserva son desplazadas. Esta predicción supone que esta especie exótica seguirá las tendencias actuales de crecimiento poblacional sin intervención externa para controlar su crecimiento. El análisis de bifurcación de este último modelo nos permitió diseñar racionalmente estrategias de intervención óptimas que potencialmente podrían desviar la trayectoria de una configuración con solo *E. camaldulensis* hacia una donde sea posible la coexistencia estable de las especies nativas. Al igual que con los modelos de dos especies, hicimos dos versiones para los de tres especies, una solo incluyendo interacciones competitivas y otra que incluyó una interacción de facilitación entre *B. cordata* y *P. praecox*. Nuestro análisis muestra que la facilitación conduce a una coexistencia estable entre las dos especies nativas, incluso en presencia de los eucaliptos. Los modelos construidos, los cuales integran numerosas fuentes de datos, ayudan a esclarecer información empírica contradictoria sobre posibles mecanismos ecológicos. Además, permiten hacer predicciones para fortalecer los futuros programas de manejo y control de eucaliptos antes de que sus efectos negativos modifiquen irreversiblemente el funcionamiento y la biodiversidad de la comunidad biótica protegida en la REPSA.

Palabras clave: Conservación dinámica, Eco-modelación, Manejo de reservas ecológicas, Control de especies exóticas, Planificación de la conservación basada en modelos; Protección sostenible de la naturaleza.

Abstract

Data-based modelling of the dynamic behavior of ecological communities is a big challenge in systems ecology and conservation biology. Implementing these models to forecast potential future scenarios is key for supporting decision-making in ecological reserves, given the ever-increasing disturbance threatening their future. Using demographic and dynamic data for three tree (or tree-like) species from the Pedregal de San Ángel Ecological Reserve (PSAER; Mexico City, Mexico), we constructed a family of dynamical models (using systems of ordinary differential equations) to reconstruct their dynamic interactions. The first two models considered two native species (*Pittocaulon praecox* and *Buddleja cordata*), with either antagonistic or cooperative ecological interactions between them. These species are alleged ecosystem engineers playing different roles in the system and determining several plant communities attributes. These models predict the transition from a stable steady state dominated by *P. praecox* (as reported in the 1950s) to the current community whose structure is apparently shifting to an alternative stable state dominated by *B. cordata*. The second pair of models additionally incorporate the exotic Australian tree *Eucalyptus camaldulensis*, which exerts negative effects on all native plant species. The prediction of this model is an *E. camaldulensis*-dominated state with the exclusion of the native species from the reserve, provided this exotic species follows current population growth trends, without external intervention to check this process. Bifurcation analysis of the latter model allowed us to rationally design optimal intervention strategies that could potentially deviate the trajectory from converging to an *E. camaldulensis*-only configuration into the stable coexistence of the native species. For the two-species and three-species models we made two versions, one with only competitive interactions and another one including a facilitation interaction between *B. cordata* and *P. praecox*. Our analysis shows that facilitation leads to a stable coexistence between the two native species, even in the presence of *E. camaldulensis*. The models constructed here, which integrate multiple data sources, help clarify conflicting empirical information regarding potential ecological mechanisms, and allow making predictions for strengthening the future management and *E. camaldulensis* control programs before its effects irreversibly modify the functioning and biodiversity of the biotic community protected in the PSAER.

Keywords: Dynamic conservation; Eco-modelling; Ecological reserve management; Exotic species control; Modelling-based conservation planning; Sustainable nature protection

Introducción

Cuando creamos un modelo intentamos generar una representación que nos ayude a entender la realidad. Aunque no son reales en sí mismos, los modelos tienen una gran utilidad, tanto teórica como práctica, e incluso son capaces de generar cambios de paradigmas que impactan a la realidad. Ejemplos de algunos modelos relevantes han sido los de la Tierra y del Sistema Solar, el modelo del árbol evolutivo de Charles Darwin, o el modelo logístico de Thomas Robert Malthus. De estos tres ejemplos, el primero representa la escala de nuestro sistema planetario y es gráfico. El segundo también es un modelo gráfico sobre el tiempo y la evolución de las especies. El tercero es un modelo representado por una ecuación matemática que dibuja una curva que muestra el cambio de una variable ecológica en el tiempo. Los tres han cambiado la forma en la que vemos al mundo.

La modelación de los procesos ecológicos y su formalización mediante el uso de las matemáticas ha sido uno de los grandes retos al que los ecólogos nos hemos enfrentado. Aunque los modelos estadísticos presentan una gran cantidad de cualidades descriptivas, siguen siendo limitados en las predicciones que pueden generar. Por ello, el enfoque de los sistemas dinámicos con base en modelos estadísticos podría generar predicciones más robustas sobre procesos ecológicos. La modelación de las interacciones y el análisis de su estabilidad en el tiempo y de sus implicaciones en la estructuración del sistema se han vuelto acciones urgentes en un mundo cada vez más afectado por el cambio climático y por la actividad humana en general. Ante esta perspectiva, nos interesa saber si las cualidades de un sistema se mantendrán o si cambiarán. Conocer su trayectoria podría arrojar luz sobre su posible futuro y a la vez esto nos permitiría tomar decisiones encaminadas a la sostenibilidad y la conservación.

Las bases teóricas para conocer las trayectorias de los sistemas se establecen de una forma más clara con el concepto de *sucesión* propuesto por Frederic Clements (1916):

“Succession is the universal process of formation development. It has occurred again and again in the history of every climax formation and must recur whenever proper conditions arise”.

El concepto de la comunidad clímax representaba una idea sumamente atractiva, sin embargo, es unidireccional. Todas las comunidades sin limitantes ecológicas deberían llegar al mismo tipo de ensamblaje de especies “clímax”. Sin embargo, Sir Arthur Tansley no estaba satisfecho con esta idea; por el contrario, él consideraba que una misma comunidad presente en dos lugares con condiciones similares podría llegar a estados completamente distintos (van der Valk, 2013). En los años treinta del siglo XX, Tansley preguntó a Arthur Roy Clapham por una palabra que definiera un concepto ecológico que integrara a los organismos, a sus interacciones y al medio ambiente; y éste le sugirió el término “ecosistema” (Willis, 1997). Después de muchas reflexiones, este concepto, junto con otros elementos

teóricos como su interpretación de la sucesión ecológica, fueron publicados en 1935 en un texto modular para la ecología moderna (Tansley, 1935). El autor sostiene que las ideas de clímax de Clements no eran del todo correctas. Sin embargo, usa y expande la analogía del desarrollo de un organismo para hacer notar que una comunidad vegetal puede pasar por diferentes etapas hasta llegar a una con mayor madurez, de la misma forma que un organismo puede llegar a una etapa adulta. Aunque similar a las de Clements, sus ideas difieren en algo fundamental. Las regresiones que se pueden presentar en las comunidades vegetales no son compatibles con el concepto de clímax. Por ejemplo, cuando un bosque pierde la cobertura de árboles por la acción de un disturbio y se convierte en un pastizal. Tansley resuelve esta situación refiriéndose simplemente a ella como un cambio de fases en el desarrollo del ecosistema. Un mismo sistema con las mismas condiciones puede presentar composiciones ecológicas totalmente diferentes dependiendo de su dinámica.

Este acercamiento entre la ecología y el estudio de los sistemas ha sido lento pero ha avanzado con paso firme. En 1966, Bernard Patten vaticinó la incorporación de las herramientas matemáticas de análisis de datos de los sistemas dinámicos a la ecología. Aunque en los últimos 50 años la brecha tecnológica se ha reducido y se han desarrollado enormemente la teoría de sistemas y el poder computacional, los ecólogos no han aprovechado estas herramientas lo suficiente para analizar la complejidad de los sistemas biológicos no lineales. De manera general, persiste un rezago en la construcción de modelos y su corroboración con distribuciones de datos reales. Por ello, existe una enorme necesidad de promover el uso de estas herramientas (Andersen *et al.*, 2009).

Al usar el enfoque de la modelación dinámica podemos encontrar y analizar propiedades emergentes de las interacciones entre los componentes de un ecosistema, fundamentales para entender sus estados transitorios y sus estados estables (Patten, 1966). Esto es de gran utilidad ante la dificultad de separar individualmente los factores que afectan a la vegetación debido a sus sinergismos (Meave y Pérez-García, 2013). El estudio de un sistema complejo con numerosos patrones requiere decidir qué procesos y qué variables serán incluidos para explicarlo de la forma más adecuada (Evans *et al.*, 2013). Una de las grandes interrogantes en la ecología de sistemas complejos es saber si los ecosistemas son estables y resilientes.

Estabilidad y resiliencia

Robert MacArthur (1955) fue uno de los primeros ecólogos en introducir los conceptos de comunidades estables e inestables. Con ellos, él se refería a las primeras como comunidades donde las abundancias de las especies se mantienen constantes, mientras que en las comunidades inestables varían enormemente. Sin embargo, su propuesta para cuantificar la estabilidad hace varios supuestos que

difícilmente se cumplirían en la naturaleza. Por ejemplo, esta propuesta considera solo dos tipos de ecosistemas que presupone como opuestos: por un lado, los ecosistemas tropicales conformados por muchas especies representan la estabilidad; por el otro, los ecosistemas árticos que albergan pocas especies ejemplifican la inestabilidad.

Robert May, quien lamentablemente falleció cuando esta tesis estaba siendo escrita, fue un pilar brillante en la ecología de sistemas. En su libro *Stability and Complexity in Model Ecosystems*, publicado en 1973, puso en perspectiva el análisis ecológico a partir de las biomatemáticas desarrolladas hasta ese momento. May revisó los distintos modelos de crecimiento existentes en su época, incluyendo los modelos de Lotka y Volterra. A partir de estos estudios, mostró la relación existente entre la complejidad y la estabilidad por medio del uso de matemáticas no lineales. Así, él encontró que la complejidad y la estabilidad van de la mano en los sistemas ecológicos. En ese texto fundamental, menciona que los estados estables e inestables alternativos corresponden a puntos de equilibrio donde la diferencial de la variable de interés vale cero. A partir de entonces, los modelos analíticos se han analizado tradicionalmente buscando las soluciones que muestren los equilibrios (Larsen *et al.*, 2016). Hay que considerar que estos modelos comunitarios fueron construidos únicamente a partir de supuestos de interacciones de competencia y de depredación.

El mismo año en que May publicaba su libro, Crawford Stanley Holling (1973) proponía el concepto de *estabilidad* como la habilidad de un sistema para regresar a un estado de equilibrio anterior después de haber sido perturbado temporalmente. Holling fue el primero en introducir el concepto de *resiliencia* a la ecología como una medida de la habilidad de un sistema para absorber cambios en las variables controladoras de estado y en los parámetros, manteniendo las relaciones entre sus elementos. La resiliencia es una propiedad emergente de los ecosistemas y otros sistemas complejos y reconoce que los mismos operan en múltiples cuencas de atracción (Angeler y Allen, 2016). La teoría de estados alternativos considera que un sistema puede tener distintos estados estables en las mismas condiciones ambientales (Scheffer y Carpenter, 2003), tal y como lo había esbozado Tansley (1935) décadas atrás.

Estados estables alternativos

Las ideas desarrolladas por Clements, Tansley, Holling y May, entre otros, desembocaron en la teoría de estados estables alternativos. Estos modelos de transiciones organizan la complejidad y describen la dinámica de la vegetación en respuesta a distintos factores (Briske *et al.*, 2005). Con ellos, se ha propuesto que los grandes cambios en un ecosistema están asociados a estados estables alternativos y a puntos de inflexión críticos (Scheffer *et al.*, 2001; Scheffer y Carpenter, 2003; Rietkerk *et al.*, 2004; van Nes y Scheffer, 2007). Los estados estables alternativos pueden definirse como las múltiples

cuenca de atracción de un sistema, cada una de ellas caracterizadas por distintos ensambles de especies (Suding y Hobbs, 2009). Una acotación que más adelante haría May (1977) es que, si un sistema solo tiene un único estado estable, entonces los efectos históricos no tienen importancia, pero si hay varios estados estables alternativos localmente, los accidentes históricos pueden tener una enorme significancia.

Se ha definido una cuenca de atracción como la región donde todos los valores iniciales en la variable de estado generan trayectorias que llevan al estado estable (Schröder *et al.*, 2005). Cuando la resiliencia es baja, cerca del punto de inflexión, la vasija o cuenca de atracción se aplana perdiendo profundidad, lo que genera una reducción en la tasa de recuperación; de esta manera, un pequeño disturbio estocástico podría llevar al sistema a una cuenca de atracción distinta (van Nes y Scheffer, 2007; Dakos *et al.*, 2010; Nazarimehr, 2018).

¿Cuenca de atracción en la Reserva Ecológica del Pedregal de San Ángel?

La historia natural y la intensidad con la que se ha estudiado el Pedregal de San Ángel lo hacen un sistema natural idóneo para intentar modelar sus estados alternativos. Este derrame de lava y el ecosistema que allí se desarrolla existen a partir de una erupción volcánica que comenzó hace aproximadamente 1690 años en el sur del Valle de México (Siebe, 2009). Al enfriarse la lava, comenzó un proceso sucesional que en la actualidad sostiene una comunidad con una diversidad única al combinar especies adaptadas a climas fríos con especies originadas y adaptadas a climas tropicales. La sucesión primaria se define como el proceso de desarrollo mediante el cual una comunidad en un nuevo hábitat se modifica conforme pasa el tiempo hasta presentar una organización estructural generalmente más compleja y estable (Cano-Santana y Meave, 1996). El proceso sucesional que ha tenido lugar en el Pedregal de San Ángel ha sido estudiado al menos desde 1954 con el trabajo pionero de Jerzy Rzedowski. A principios de la década de 1980 se creó la Reserva Ecológica del Pedregal de San Ángel (REPSA) con la finalidad de proteger una parte remanente de este interesante ecosistema. La REPSA se ubica en el área del Pedregal de San Ángel que Rzedowski (1954) clasificó como la comunidad *Senecionetum praecoxis*, debido a la abundancia del *palo loco* [*Senecio (=Pittocaulon) praecox* (Cav.) Rob. & Brettell]. Rzedowski observó una asociación entre el *palo loco* y el pirul (*Schinus molle* L.), un árbol originario de Sudamérica introducido a México hace siglos, en casi todo el pedregal. En ese trabajo, hipotetizó que dicha comunidad se transformaría hacia una vegetación del tipo *Schinetum molle*, es decir, dominada por el pirul, para eventualmente seguirse desarrollando hacia una comunidad de encinos sobre estrato basáltico y finalmente a una de encinos con suelo más

desarrollado, en una etapa sucesional mucho más avanzada. Esta propuesta no representa otra cosa que una teorización predictiva de los estados estables alternativos en la zona del pedregal.

Desde hace tres décadas, investigadores y académicos que han trabajado en este ecosistema comenzaron a reportar un aumento considerable en el número de individuos de *tepozán* (*Buddleja cordata* Kunth). Tomando en cuenta estos antecedentes relacionados con procesos ecológicos observados y cuantificados en este ecosistema, el presente estudio se enfocó en la reconstrucción de la dinámica y la trayectoria de la vegetación a partir del incremento del *tepozán* y la aparente disminución del elemento dominante anterior, el *palo loco*. Se puede considerar que estas especies son clave en el funcionamiento de la REPSA y pueden determinar la estructura y la composición de la comunidad vegetal. Además, en una fase posterior de la modelación decidimos incluir al eucalipto (*Eucalyptus camaldulensis* Dehn.), ya que es el árbol exótico más abundante con numerosos efectos negativos sobre las plantas nativas (Segura-Burciaga y Meave, 2001 Segura-Burciaga, 2009).

A partir de esta propuesta planteamos tres hipótesis:

- i) “Hipótesis de la dominancia del pirul” propuesta por Rzedowski (1954). Esta hipótesis fue descartada de entrada ya que no encontramos datos en la literatura que la respaldaran, ni en cuanto a su aporte de biomasa (Cano-Santana, a1994) ni en cuanto su aporte de semillas (Mendoza Hernández, 2002; Martínez-Orea et al., 2010) u otras observaciones de campo.
- ii) “Hipótesis de la dominancia del *tepozán*”. Se sustenta en numerosos estudios demográficos y ecosistémicos.
- iii) “Hipótesis de la dominancia del eucalipto”. Incorpora el posible efecto de este árbol exótico invasor.

Debido a que los datos en la bibliografía sí apoyan la posibilidad de la dominancia de tepozanes y de eucaliptos, construimos cuatro modelos para ponerlas a prueba. Los primeros modelos fueron construidos para dos especies nativas, el *tepozán* y el *palo loco*. Uno de los modelos sólo presentaba una interacción de competencia entre estas especies, mientras que el otro se modificó, introduciendo un efecto de facilitación del *tepozán* sobre el *palo loco*.

A continuación, construimos otros dos modelos donde incorporamos al eucalipto y la regulación negativa de las especies nativas. De igual forma que con los primeros modelos, en este caso propusimos dos versiones, una solo con competencia y otra incorporando la facilitación del *tepozán* sobre el *palo loco*. Todas las propuestas de interacciones de los cuatro modelos se basan en datos cualitativos y cuantitativos de la REPSA. El planteamiento del modelo parte de un análisis exhaustivo de la literatura que incluye información de las características morfológicas y fisiológicas de las especies focales, de su comportamiento demográfico y de las interacciones entre ellas. Una vez construidos los modelos gráficos, se procedió a construir los sistemas de ecuaciones diferenciales ordinarias acopladas

para realizar un análisis matemático que permitiera poner a prueba las hipótesis. De esta manera, fue posible determinar los posibles estados estables de cada sistema de manera analítica. Para este modelo se hizo, de forma adicional, un análisis de bifurcaciones con la finalidad de proponer un método de control del eucalipto que permitiera pasar de un estado estable caracterizado por la dominancia de este árbol exótico a uno donde la coexistencia de las distintas especies focales sea posible. A partir de este procedimiento, la intención final fue generar una propuesta de control para el eucalipto invasor con el fin de brindar una herramienta para la toma de decisiones en el plan de manejo de la REPSA. A continuación, presento el artículo que se contruyó a partir de esta investigación y que fue enviado a la revista *Ecological Modelling*.

Predicting dynamic trajectories of a protected plant community under contrasting conservation regimes: insights from data-based modelling

Jaime Acosta-Arreola^{1,4}, Elisa Domínguez-Hüttinger^{2*}, Pablo Aguirre³, Nicolás González³, Jorge A. Meave^{1*}

¹Departamento de Ecología y Recursos Naturales, Facultad de Ciencias, Universidad Nacional Autónoma de México, Ciudad Universitaria, Coyoacán 04510, Ciudad de México, México

²Departamento de Biología Molecular y Biotecnología, Instituto de Investigaciones Biomédicas, Universidad Nacional Autónoma de México, Ciudad Universitaria, Coyoacán 04510, Ciudad de México, México

³Departamento de Matemática, Universidad Técnica Federico Santa María, Casilla 110-V, Valparaíso, Chile

⁴Posgrado en Ciencias Biológicas. Unidad de Posgrado, Circuito de Posgrados, Universidad Nacional Autónoma de México, Ciudad Universitaria, Coyoacán 04510, Ciudad de México, México

* Corresponding authors. E-mails: jorge.meave@ciencias.unam.mx;
elisa.dominguez@iibiomedicas.unam.mx

Abstract

Data-based modelling of the dynamic behavior of ecological communities is a big challenge in systems ecology and conservation biology. Implementing these models to forecast potential future scenarios is a key for supporting decision-making in ecological reserves, given the ever-increasing disturbance threatening their future. Using demographic and dynamic data for three tree (or tree-like) species from the Pedregal de San Ángel Ecological Reserve (PSAER; Mexico City, Mexico), we constructed a family of dynamical models (using systems of ordinary differential equations) to reconstruct their dynamic interactions. The first two models considered two native species (*Pittocaulon praecox* and *Buddleja cordata*), with either antagonistic or cooperative ecological interactions between them. These species are alleged ecosystem engineers playing different roles in the system and determining several plant communities attributes. These models predict the transition from a stable steady state dominated by *P. praecox* (as reported in the 1950s) to the current community whose structure is apparently shifting to an alternative stable state dominated by *B. cordata*. The second pair of models additionally incorporate the exotic Australian tree *E. camaldulensis*, which exerts negative effects on all native plant species. The prediction of this model is an *E. camaldulensis*-dominated state with the exclusion of the native species from the reserve, provided this exotic species follows current population growth trends, without external intervention to check this process. Bifurcation analysis of this latter model allowed us to rationally design optimal intervention strategies that could potentially deviate the trajectory from converging to an *E. camaldulensis*-only configuration into the stable coexistence of the native species. For the two-species and three-species models we made two versions, one with only competitive interactions and another one including a facilitation interaction between *B. cordata* and *P. praecox*. Our analysis shows that facilitation leads to a stable coexistence between the two native species, even in the presence of eucalyptus. The models constructed here, which integrate multiple data sources, help clarify conflicting empirical information regarding potential ecological mechanisms, and allow

making predictions for strengthening the future management and *E. camaldulensis* control programs before its effects irreversibly modify the functioning and biodiversity of the biotic community protected in the PSAER.

Keywords:

Dynamic conservation; Eco-modelling; Ecological reserve management; Exotic species control; Modelling-based conservation planning; Sustainable nature protection

1. Introduction

As the human footprint on Earth deepens (Williams et al., 2020), good management of nature reserves for biological conservation and ecosystem function maintenance becomes increasingly important as an instrument to prevent losses in our planet's biological legacy (Suding and Hobbs, 2009; Venter et al., 2016; Schuwirth et al., 2019). Uncertainty about the efficacy of nature protection areas stems from the difficulty to ensure the continuity of the biota and the overall ecosystem health they are supposed to safeguard (Cano-Santana et al., 2006; Shrestha et al., 2021). Integrating information on the past, present, and future dynamics of protected areas allows assessing whether such continuity is being achieved or else if the system is shifting towards unknown new states. Such information would provide an important decision-making tool, allowing to adjust or to improve current management of a protected area by ensuring that decisions are based on sound knowledge on the dynamics of species occurring in the community (Schuwirth et al. 2019). Identifying the roles of those species contributing the most to community structure and functioning should enable the prediction of future scenarios for protected areas based on quantitative ecological relationships (Suding and Hobbs 2009). To this purpose, mathematical modelling offers a very useful tool. Computing (*in silico*) experiments are a cheaper and faster option vis-à-vis field experiments, as they assist in searching for optimized solutions to ecological problems (Borenstein, 2012). For example, the control of exotic species, a central topic in conservation biology, could strongly benefit from this approach.

Exotic species invasions of nature reserves may gradually lead to communities that have little in common with the original ones. To examine this possibility, the alternative stable states theory offers an adequate theoretical framework. The notion of alternative stable states has its roots in Tansley's (1935) work, who suggested that ecosystems transit through different development stages without ever reaching the "community climax"; these multiple stages were later recognized by May

(1973) as alternative attracting equilibrium points. These early ideas prompted a rapidly growing field of research, in which the current debate largely focuses on the issue of ecosystem stability in the event of disturbances. Central to this topic is the concept of ecological resilience, defined as the measure of the magnitude of a disturbance required to trigger a transition into a qualitatively different state (Holling, 1973; Peterson et al., 1998; Gunderson, 2000; Suding and Hobbs, 2009). Each of these states is associated to a different basin of attraction (Scheffer and Carpenter, 2003; Suding and Hobbs, 2009; Angeler and Allen, 2016). Often, big changes observed in ecosystems are associated to transitions (Scheffer et al., 2001; Scheffer and Carpenter, 2003; Rietkerk et al., 2004; van Nes and Scheffer, 2007). Crossing the boundaries between basins of attraction of alternative steady states is possible when disturbances are strong enough to push the trajectories beyond the separatrix (Scheffer et al., 2001; Scheffer and Carpenter, 2003; Guttal and Jayaprakash, 2008; Angeler and Allen, 2016). The stability of stable steady states is roughly associated to feedback loops that maintain and sustain the system's functionality (Angeler and Allen, 2016). A bifurcation of a dynamical system has been defined as a topological change in the phase space that results from smooth changes in a bifurcation parameter (Andersen et al., 2009). Saddle node bifurcations, in which a stable steady state disappears when it collapses with an unstable branch (Guttal and Jayaprakash, 2008; Dakos et al., 2012; Nazarimehr et al., 2018) are amongst the most common ecologically relevant bifurcations (saddle node bifurcations are also known as thresholds; Scheffer et al., 2009; Kéfi et al., 2014; Angeler and Allen, 2016). The stability of an attractor decreases in the vicinity of a bifurcation point, a phenomenon associated to a decrease in the size of the corresponding basin of attraction and a slower recovery of the system from transient perturbations (referred to as “critical slowing down” in dynamical systems theory) and thus to reduced resilience, increasing the system’s vulnerability and therefore the likelihood of flickering between states (van Nes and Scheffer, 2007; Dakos et al., 2010; Nazarimehr et al., 2018).

Forty years ago, a natural conservation area was created in southern Mexico City which offers

an excellent system to test ideas related to alternative stable states theory. This nature protection area, the Pedregal de San Ángel Ecological Reserve (hereafter PSAER; we will use the colloquial name as San Ángel Reserve, SAR), is located within the main campus of the National Autonomous University of Mexico (Universidad Nacional Autónoma de México; UNAM). As the natural vegetation in SAR hosts a very rich flora and fauna, and due to its proximity to UNAM's Faculty of Sciences, the Institute of Biology and the Institute of Ecology, many students and scholars have been engaged in numerous biological research programs, making SAR one of the most intensely studied protected areas in Mexico (Carabias-Lillo and Meave del Castillo, 1987; Lot and Cano-Santana, 2009). The natural ecosystem it protects is quite peculiar. For one, it is neither representative of the lacustrine systems once widespread in the bottom of the Basin of Mexico prior to human occupation, nor of the temperate forests occurring on the surrounding mountains. The reason for this apparent anomaly is that this ecosystem develops on a lava field that formed some 1700 years ago with the eruptive event of the Xitle, a monogenetic volcano typical of the Trans-Mexican Volcanic Belt. Primary succession likely began in this area shortly after the eruption ceased, and this process is going on to this date (Siebe, 2009). This successional condition, along with its location within the University's main campus and the concomitant large amount of information available, makes of SAR an ideal place to study successional dynamics. In the mid-20th century, Rzedowski (1954) documented a very rich flora (538 vascular plant species) for the entire area (ca. 80 km²) of this lava field (*pedregal* in Spanish), occurring in a mosaic of nine plant community types spanning a 1,000 m elevational gradient. Mexico City's unchecked urban sprawl since the 1960s took a big toll on this ecosystem's size, so that currently only a small fraction remains, mostly protected in the SAR. Despite the benign climate of this high-elevation location and its potential for temperate forest development, vegetation in SAR is a xerophytic scrub, given its arid condition due to incipient soil development (Cano-Santana and Meave, 1996). A recent account of SAR's vascular flora comprises 373 vascular plant species (Castillo-Argüero et al., 2004, 2009), among which some 10 are trees and the remaining

comprise an array of smaller growth forms. Among these trees, three exotic species are prominent, two eucalypts (*Eucalyptus camaldulensis* and *E. globulus*; Myrtaceae), and the Peruvian peppertree or *Pirul* (*Schinus molle*; Anacardiaceae). Despite its protection status, multiple threats compromise the integrity of SAR and its biota. For one, SAR is situated amidst one of the world's largest urban areas, where the environmental effects of over 20 million people are difficult to overlook (Cano-Santana and Meave, 1996; Cano-Santana et al., 2006). Main disturbances with continuous effects on this ecosystem are landscape fragmentation, squatting, and illegal material dumping (Castellanos Vargas et al., 2017), combined with high tropospheric ozone levels typical of Mexico City's air quality (de Bauer and Hernández-Tejeda, 2007). Lastly, but not least, exotic species invasions represent an additional threat.

The first detailed description of the plant community occurring in the lowest reaches of this lava field, where SAR is located, was provided by Rzedowski (1954). This author classified this community as a xerophytic scrub and, following the European phytosociological tradition, named it *Senecionetum praecocis*, reflecting the high abundance and physiognomic contribution of the tree-like, large shrub *Pittocaulon* (=*Senecio*) *praecox* (Asteraceae), a dominant species in the community until the mid-20th century. Rzedowski also reported the presence of *S. molle*, a short tree native from South America introduced centuries ago to the former New Spain (Ramírez-Albores and Badano, 2013). Based on the success of this species in the central Mexico highlands (Corkidi et al., 1991), Rzedowski hypothesized that this community would eventually turn into a *Schinetum mollis*, i.e., a community dominated by this exotic species. Rzedowski went further and hypothesized that given enough time, this community could eventually become an oak forest, as this is the “climax” vegetation type at this elevation in the Central Mexican highlands (Meave et al., 2016). However, given the scarcity of oak trees in the xerophytic scrub (Castillo-Argüero et al., 2007), this seems a less plausible successional outcome. We discarded Rzedowski's hypothesis predicting the future dominance of *S. molle* (“*S. molle* dominance hypothesis”) due to its lack of empirical support.

As the ecological knowledge on this community advanced, new potential successional scenarios became apparent. First, based on the relentless urbanization around SAR and probably in association with increased air pollution, some authors noted the increasing prevalence of a species whose presence was not emphasized by Rzedowski (1954), namely the short tree *Buddleja cordata* (Scrophulariaceae). Locally known as *Tepozán*, several authors reported an increasing abundance of this species in SAR around the turn of the 21st century (e.g., Hernández Islas, 1984; Cano-Santana, 1994; Flores Vázquez, 2004), to the degree that a “tepozanization” process was suggested (Soberón et al., 1991). On this basis, we formulated the “*B. cordata* dominance hypothesis”, the first one to be tested in our study, which states that the fate of this community would be a *B. cordata*-dominated system.

A second hypothesis derived from conspicuous presence of eucalypts in SAR. The potential ecological effects of the introduction of *Eucalyptus camaldulensis* to this area half a century ago have been amply documented, including strong impacts on community structure and diversity, through competitive effects to allelopathic interference (Segura-Burciaga, 2009; Espinosa-García, 1996; Segura-Burciaga and Meave, 2001). Thus, eucalypts are likely to trigger feedback loops potentially leading to catastrophic, qualitative changes in this community’s successional trajectory. Hence, the “*E. camaldulensis* dominance hypothesis” foresees a future scenario for this community characterized by the dominance of this invasive species.

Based in this background, the following questions emerged: What is the stage of the successional dynamics in this plant community? In which direction is it shifting? What are the effects of the entry of new species to the community? To answer these questions, we analysed the successional dynamics of the plant community present in SAR and tested the two aforementioned hypotheses. We did this by modelling the successional dynamics of this plant community to predict future scenarios for this natural protected area. Our mechanistic mathematical models are dynamical representations of key ecological interactions between the focal species that drive the successional

process. To the extent that this was possible, we derived the ecological mechanisms from empirical observations. To deal with conflicting or missing observations, we constructed a family of mathematical models, representing either the *B. cordata* dominance (type I models) or the *E. camaldulensis* dominance (type II models) hypothesis, and assessed their plausibility (or explanatory capacity) by measuring their ability to reproduce field observations (i.e. by, minimizing a cost function). The rationale behind this modelling approach is that it allows assessing the most plausible ecological interactions between the tree species given empirical data limitations (Schuwirth et al. 2019). We expect that this modelling exercise will prove useful in making informed decisions to manage this ecological reserve, and eventually that this approach will become widespread to promote a sounder management of natural protected areas.

2. Materials and methods

2.1 Selection of focal species

Pittocaulon praecox (Cav.) Rob. & Brettell (common name, *Palo Loco*). This species is a large, dichotomously branched, succulent shrub, usually < 4 m tall but occasionally more, allowing its classification as arborescent or tree-like. The thickened stems of this plant are related to water storage, enabling them to grow under the limiting water conditions derived from the very shallow soils in the ecosystem (Cano-Santana and Meave, 1996). The selection of this species was based on its past dominance in the community (Rzedowski 1954). Despite evidence indicating that the population of this species is still growing (Rodríguez de la Vega, 2003; Pérez Ishiwara, 2011), it seems on its way to becoming a subordinate community component.

Buddleja cordata Kunth (common name, *tepozán*). This species is a very frequent, short tree commonly growing in disturbed areas of temperate forests and xerophytic scrub vegetation in the central highlands of Mexico (Mendoza Hernández, 2003). Trees of this species are evergreen (Meave et al., 1994), despite a continuous foliage turnover in their crowns, thus they cast a deep shade even in the harsh dry springtime typical of Mexico City. This suggests that the concept of ecosystem

engineer (Jones et al. 1994) is suitable for this species, as arguably it is a key modulator of resources and of abiotic factors, impacting the plant community' structure and function in its vicinity.

Eucalyptus camaldulensis Dehnh (common name, *Eucalipto* or eucalypt). The selection of this species (incorrectly reported as *Eucalyptus resinifera* Sm. in previous studies in this area) was based on its high abundance in certain areas of SAR, particularly bordering the inner roads of the University campus and the main city roads that cross it, and because of the alleged impact it is having on this ecosystem (Segura-Burciaga, 2009; Acosta-Arreola, 2015). The abundant information on this species also warrants its recognition as an ecosystem engineer. Normally attaining a much larger height than any other native tree species, eucalypts dominate the upper stratum, reducing light intensity under their crowns (Segura-Burciaga, 2009). In SAR, the experimental remotion of eucalypts resulted in higher species richness compared to control plots covered with eucalypt crowns (Segura-Burciaga and Meave, 2001); this difference was interpreted as a result of volatile allelopathic compounds released by eucalypts with negative effects on the growth and survival of native species (Espinosa-García, 1996). Moreover, the thick litter layer that often accumulates around eucalypt trees decomposes very slowly, apparently deterring the germination of other species' seeds (Segura-Burciaga and Martínez-Ramos, 1994), and increasing fire risk in the dry season. Reports of death bumblebees and bees on the ground of *E. camaldulensis*-dominated zones suggest the presence of lethal secondary metabolites in its nectar (Segura-Burciaga, 2009), although this remains unconfirmed. The rapid growth rates of eucalypts, combined with the lack of native predators and competitors capable of playing a regulatory role of its population, render this species a threat for the future functioning of the entire ecosystem. Three demographic studies covering the 1951–2009 period revealed a rapid growth of the *E. camaldulensis* population over this period, despite the launching of a control program that operated from 1994 to 2001 which resulted in the downing of several thousands of individuals (Segura-Burciaga and Martínez-Ramos, 1994; Segura-Burciaga, 2009; Acosta-Arreola, 2015).

2.2 Sources of empirical data

The starting point for the construction of the models was a thorough review of published sources, including grey literature, to search for morphological and ecological information on the focal species. This search produced 23 studies with relevant information, including 13 academic theses and dissertations, five book chapters, and five articles in specialized journals based on research conducted in this community. These studies were conducted between 1954 and 2015.

Quantitative information sources were of two kinds. The first group comprised empirical descriptions of the ecological interactions involving the model's variables and was used for the construction of the reaction network and hence the mathematical model (Rzedowski 1954; Hernández Islas, 1984; Soberón-M. et al., 1991; Segura-Burciaga and Martínez-Ramos, 1994; Segura-Burciaga, 1995; Cano-Santana and Meave, 1996; Olvera Carrillo, 2001; Segura-Burciaga and Meave, 2001; Mendoza Hernández, 2002, 2003; Rodríguez de la Vega, 2003; Flores Vázquez, 2004; Camacho Altamirano, 2007; Antonio-Garcés et al., 2009; Castillo-Argüero et al., 2009; Valverde and Chávez, 2009; Martínez-Orea et al., 2012; Mendoza Hernández et al., 2013; Santillán Carvantes, 2013). The second group included longitudinal demographic monitoring of the densities of the three species and were used for parameterizing the mathematical model. Data for the calibration of the kinetic relations between the two native species were retrieved from Cano-Santana (1994), who reported demographic data (density) and ecosystem-level information, including biomass production for *B. cordata* and *P. praecox* from 1990 to 1992. The increasing trend of *B. cordata* dominance in the community is supported by much qualitative and quantitative evidence (Soberón-M. et al., 1991; Cano-Santana, 1994; Cano-Santana and Meave, 1996; Mendoza Hernández, 2003; Flores Vázquez, 2004; Camacho Altamirano, 2007; Antonio-Garcés et al., 2009; Cano-Santana et al., 2006; Castillo-Argüero et al., 2009; Valverde and Chávez, 2009; Martínez-Orea et al., 2010; Mendoza Hernández,

2002).

A further set of sources provided information on the Eucalypt's ecology. Demographic information derived mainly from Segura-Burciaga (2009, 1995), Segura-Burciaga and Martínez-Ramos (1994), and Segura-Burciaga and Meave (2001), and was supplemented with a demographic study of this species conducted by one of us in 2011 (Acosta-Arreola, 2015). Interestingly, only five of these studies include demographic matrix modelling: Segura-Burciaga (1995) for the *E. camaldulensis*, Mendoza Hernández (2002) and Flores Vázquez (2004) for *B. cordata*, and Rodríguez de la Vega (2003) and Pérez Ishiwara (2011) for *P. praecox*. All these studies confirmed the growing populational trends for these species. In addition, we gathered information from seed bank and post-fire colonization studies that confirmed the increasing dominance of *B. cordata* in SAR (Hernández Islas, 1984; Martínez Mateos, 2001; Mendoza Hernández, 2002; Martínez-Orea et al., 2010, 2012).

2.3 Construction of the mathematical models

In constructing a model, its assumptions need to be totally explicit to create realistic expectations while avoiding making a black box that can neither be understood nor discussed (Schuwirth et al., 2019). Hence, in these sections we explain in detail how the model was constructed, calibrated and analyzed.

We constructed a family of four mechanistic mathematical models representing the dynamic interactions between the two native species and the exotic species. These four systems of coupled ordinary differential equations represent the positive (*A*) and negative (*B*) dynamic interplay between the two alleged ecosystem engineers in SAR (namely *B. cordata* and *P. praecox*), both in the absence (I) and presence (II) of the exotic *E. camaldulensis*.

First, we explored the dynamic consequences of both positive and negative interactions between *B. cordata* and *P. praecox* to clarify contradicting empirical evidence regarding these two

possible interactions: negative regulation by competition and positive regulation by cooperation between them. We constructed spatially homogeneous and deterministic models based on ordinary differential equations. These models assumed that resources and space are limited; therefore, we refer to our model variables as “eco-dimers”, i.e., the integrated units of space inhabited by a given tree. Given that our model variables are trees or tree-like plants, we posit that the eco-dimer is defined by the area of the canopy projected onto the soil, and hence it has units of area/tree cover. Model construction also assumed total space/resources on SAR to be constant (parameter TS) so that, using conservation equations, the free space can always be represented as an algebraic function (i.e., the constant total space minus the sum of the eco-dimers).

In each of our models, the dynamic variables are given by the 3 (or 2) species of trees, i.e. $\vec{x} = [PS, BS, ES]$ with entries of \vec{x} corresponding to the space in SAR occupied by *Pittocaulon praecox* (PS), *Buddleja cordata* (BS), and *Eucalyptus camaldulensis* (ES), respectively. Our model also implicitly includes the *Free Space* (FS) variable representing the area of SAR not occupied by any of the tree species. The *Total Space* (TS) is given by the algebraic relation $FS = TS - (PS + BS + ES)$ or, equivalent, $TS = FS + PS + BS + ES$. For each species we assumed that growth (or occupation of space) is a first order process linearly dependent on the free space, with parameter α_{x_i} . Death of individuals of any species is also a first order process that leads to the liberation of space with parameter β_{x_i} .

In models *A* (negative regulatory interactions, i.e. competition) we assumed that PS growth is inhibited by BS , representing the asymmetric competition for resources where *B. cordata* is the aggressive competitor. Support for this negative regulatory interaction derives from field observations by Valverde and Chávez (2009) suggesting the existence of regions of SAR strongly dominated by *B. cordata*, where the canopy is relatively closed, and have a poorly lit lower stratum. We assumed a competitive effect for nutrients, water, soil and light. Nonetheless, there is also increasing evidence that facilitation is a key driver of community assembly in high-diversity systems

(Callaway, 1995; Bruno et al., 2003; Valiente-Banuet and Verdú, 2007). Hence, we also included positive interactions: in models *B* (positive regulatory interactions, i.e. cooperation) we assumed that *BS* favours the growth of *PS* through facultative facilitation. Facilitation is a positive interaction from which at least one species benefits without damaging the other. In facilitative interactions the mere presence of one species modifies the environment, often resulting in a benefit for its neighbours (Bruno et al., 2003; Valiente-Banuet and Verdú, 2007; but see Valladares et al., 2008 for a cautionary view).

Based on a review of nearly 200 studies published between 1909 and 1995, Callaway (1995) concluded that facilitation is a key plant community structuring process, particularly through the nursery effect in deserts. In the case of *B. cordata*, facilitation could be inferred if individuals of different species were recruited under a nursing *B. cordata* tree more frequently than expected at random (Valiente-Banuet and Verdú, 2007). Olvera Carrillo (2001) hypothesized that *B. cordata* could serve as the nurse of the cactus *Opuntia tomentosa*; although this author failed to demonstrate specificity in the nursing relationship, she showed that shadier, more humid microsites are key to the successful establishment of plant species in this community. Such conditions may be created by stones, walls and even other plant species. In another sector in the same lava field but outside of SAR, *B. cordata* fails to limit the establishment of new individuals (Ruiz Amaro, 1996), possibly due to nursing effects or microclimatic modifications around *B. cordata* individuals that could lead to increases in *PS*. Mendoza Hernández (2002, 2003, 2013) suggested that *B. cordata* has facilitating effects through the accumulation of soil and humidity around it, promoting seed germination of native species, and highlights its facilitating role for late successional species like oaks. Rodríguez de la Vega (2003) reported that in 1997, following a massive recruitment event of *P. praecox* that started in 1992, 88 % of *P. praecox* seedlings were located under nurse plants in a *B. cordata* - dominated area; in addition, this author showed that 44.4 % of plants growing under nurse plants survived, which contrasts with a 3.8 % survival for seedlings growing under exposed conditions

(Rodríguez de la Vega, 2003). Figueroa-Castro et al. (1998) reported a higher production of reproductive structures for *P. praecox* in shadier, more humid microenvironments. This supports the possibility of a positive, facilitating effect of *B. cordata* on *P. praecox* and probably some other species.

In constructing the type II (three-species) models, we further assumed negative effects of *ES* on the two native species, both by inhibiting their growth and inducing their death. These negative effects are mainly related to competition for nutrients, water and light, and the release of allelopathic compounds. In these models, \emptyset represents the negative effects on the reproduction of native species, mainly related to the physio-chemical barrier represented by a litter layer containing allelopathic compounds in *E. camaldulensis*-dominated areas, preventing seed germination of native species (Segura-Burciaga, 1995), but also to the potential toxic effects of *E. camaldulensis* s on the pollinators of native species (Segura-Burciaga, 1995, 2009). Figure 1 shows the conceptual diagrams for the four models; Table 1 provides a description of model variables, and the equations are given in Table 2.

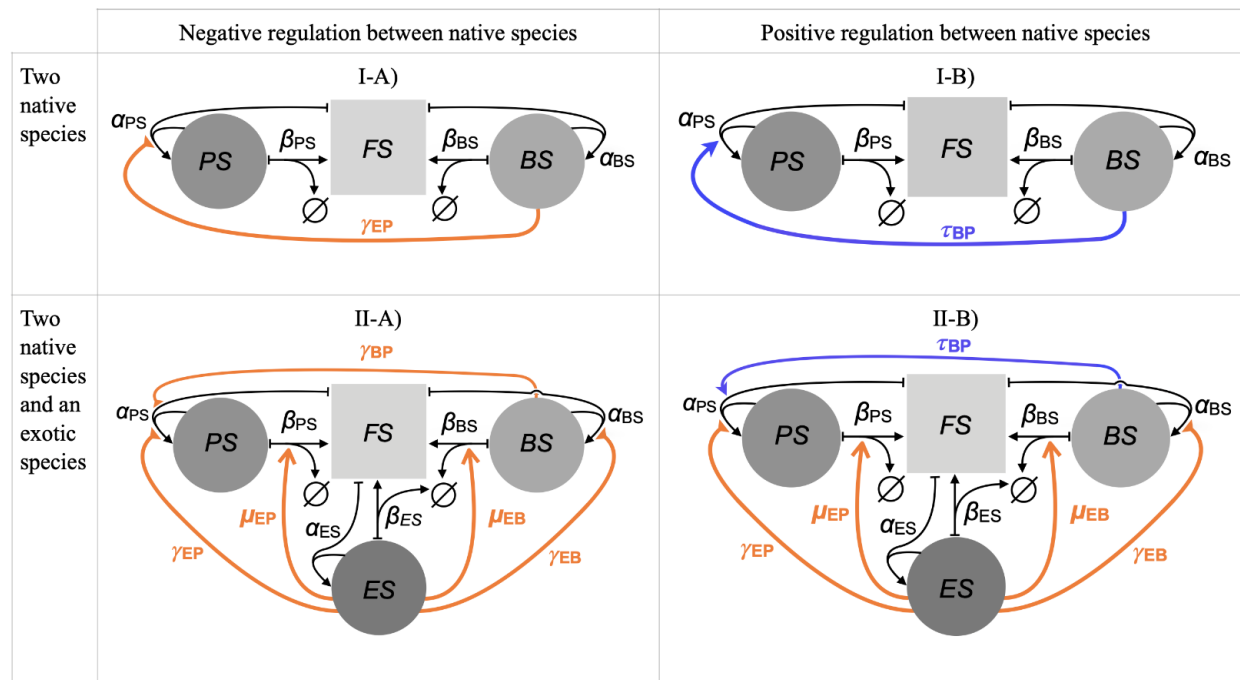


Figure 1. Mathematical models of the interplay between key ecological engineers in SAR. Type I

and type II models represent the positive (*A*) and negative (*B*) dynamic interplay between *P. praecox* (*PS*) and *Buddleja cordata* (*BS*), either in the absence (I) or presence (II) of *Eucalyptus camaldulensis* (*ES*). Circles represent the eco-dimers, the square represents free space (*FS*). Orange arrows represent negative regulations; blunt end arrows represent inhibitory effects of eco-dimer formation rates, whereas pointed arrows indicate induction of eco-dimer dissociation rates. Blue arrows represent positive regulations (induction of eco-dimer formation). The weight of the interactions is given by the parameter values (Greek letters) defined in Table 4.

Table 1. List of variables included in the models, along with their symbols, units of measurement and explanatory comments.

Symbol	Name	Units	Comments
<i>t</i>	Time (independent variable)	years	
<i>FS</i>	Free space	ha	Represented algebraically (conservation equations)
<i>PS</i>	Space occupied by <i>Pittocaulon praecox</i> (<i>Palo Loco</i>)	ha	
<i>BS</i>	Space occupied by <i>Buddleja cordata</i> (<i>Tepozán</i>)	ha	
<i>ES</i>	Space occupied by <i>Eucalyptus camaldulensis</i> (eucalypt)	ha	Models II-A and II-B only

Table 2. Model equations. Parameters in colored font represent the effects of the ecological interactions of one species on another. Parameters in orange font imply a negative effect, whereas parameters in blue font represent the facilitation of *B. cordata* on *P. praecox*.

Model	System of equations
IA	$\frac{dPS(t)}{dt} = \frac{\alpha_{PS} \cdot PS(t) \cdot FS(t)}{1 + BS(t) \cdot \gamma_{BP}} - \beta_{PS} \cdot PS(t)$ $\frac{dB(t)}{dt} = \alpha_{BS} \cdot BS(t) \cdot FS(t) - \beta_{BS} \cdot BS(t)$ $FS(t) = TS(t) - (PS(t) + BS(t))$
IB	$\frac{dPS(t)}{dt} = \alpha_{PS} \cdot PS(t) \cdot FS(t) \cdot (1 + \tau_{BP} \cdot BS(t)) - \beta_{PS} \cdot PS(t)$ $\frac{dB(t)}{dt} = \alpha_{BS} \cdot BS(t) \cdot FS(t) - \beta_{BS} \cdot BS(t)$ $FS(t) = TS(t) - (PS(t) + BS(t))$
IIA	$\frac{dPS(t)}{dt} = \frac{\alpha_{PS} \cdot PS(t) \cdot FS(t)}{1 + BS(t) \cdot \gamma_{BP} + ES(t) \cdot \gamma_{EP}} - PS(t) \cdot (\beta_{PS} + \mu_{EP} \cdot ES(t))$ $\frac{dB(t)}{dt} = \frac{\alpha_{BS} \cdot BS(t) \cdot FS(t)}{1 + (ES(t) \cdot \gamma_{EB})} - BS(t) \cdot (\beta_{BS} + \mu_{EB} \cdot ES(t))$ $\frac{dES(t)}{dt} = \alpha_{ES} \cdot ES(t) \cdot FS(t) - \beta_{ES} \cdot ES(t)$ $FS(t) = TS(t) - (PS(t) + BS(t) + ES(t))$
IIB	$\frac{dPS(t)}{dt} = \frac{\alpha_{PS} \cdot PS(t) \cdot FS(t) \cdot (1 + \tau_{BP} \cdot BS(t))}{1 + ES(t) \cdot \gamma_{EP}} - PS(t) \cdot (\beta_{PS} + \mu_{EP} \cdot ES(t))$ $\frac{dB(t)}{dt} = \left(\frac{\alpha_{BS} \cdot BS(t) \cdot FS(t)}{1 + ES(t) \cdot \gamma_{EB}} \right) - BS(t) \cdot (\beta_{BS} + \mu_{EB} \cdot ES(t))$ $\frac{dES(t)}{dt} = \alpha_{ES} \cdot ES(t) \cdot FS(t) - \beta_{ES} \cdot ES(t)$ $FS(t) = TS(t) - (PS(t) + BS(t) + ES(t))$

2.4 Construction and standardization of a database with normalized field data of eco-dimer coverage

To model growth for the three species we defined the eco-dimer formation as the association of individuals that use free space. Hence, we used units of area (ha) for the three species. Data extracted from the literature were standardized.

The first decision was to consider the size (area) of SAR as constant from 1954 until 2011. When this area was declared a nature protection area in 1983 it covered an area of 124.5 ha, but in 1990 its limits were modified to increase its area to 146.89 ha, which then remained the same until 1996 (Cano-Santana, 1994); we chose this period to represent its constant size because most records come from this time period. Although more recently its area underwent further modification until reaching its current size of 237 ha (Peralta Higuera and Prado Molina, 2009), this enlarged area was not considered for the modelling because it includes several buffer zones with potentially very different dynamics.

For the *E. camaldulensis*, the first cover data point is represented by the number of eucalypt trees planted in the early 1950s. To obtain further dynamic datapoints we searched the literature for distributional and density data and found data for three additional dates, namely 1990 (Segura-Burciaga and Martínez-Ramos, 1994; Segura-Burciaga, 1995), 1998 (Segura-Burciaga, 2009) and 2011 (Acosta-Arreola, 2015). Based on the observation that in the area of occurrence of eucalypts 25 % of the soil is free from its influence (Segura-Burciaga, 1995), we adjusted its distribution area by 75 % to determine its net cover area (Table 3).

Table 3. Total cover by species (ha) in different dates for the 1954 - 2011 period in the Pedregal de San Ángel Ecological Reserve, Mexico City.

Year	<i>B. cordata</i>	<i>P. praecox</i>	<i>E. camaldulensis</i>
1954	-	-	1.105
1990	15.467	0.078	8.932
1991	16.954	0.086	-
1992	19.187	0.096	-
1998	-	-	6.548
2011	-	-	8.251

Information for *P. praecox* and *B. cordata* was retrieved from Cano-Santana (1994). This author distinguished in the lava field two main terrain units, namely rugged sites (defined by a high abundance of cracks and depressions), and flat sites. Then, for these two species he quantified biomass storage by site type for the years 1990, 1991 and 1992. The author also recognized three vegetation strata (tree, shrub and herb strata); interestingly, despite the arborescent condition of *P. praecox*, this species was associated with the shrub stratum, which also includes a group of medium-sized young *B. cordata* individuals. For these two species and for years 1990 and 1991, there are density records for the two taller strata and for both site types. Data on total density and cover of the tree stratum were also available for 1990, and there were total biomass records for the three years by site type. Given the large substrate heterogeneity in this area (Santibáñez-Andrade et al., 2009), we transformed all records to express them in the same units (ha for area and kg for weight). Reference year for inferring 1991 and 1992 cover was 1990 (Table 3). The resulting database for dynamic eco-dimer values is given in Table 3.

2.5 Optimization of parameter values (derivation of nominal values)

Parameters were estimated through global optimization, by minimizing the cost function that measures the difference between empirical measurements of the eco-dimers and the simulated trajectories of our model variables given a set of parameters, as:

$$Cost(\bar{P}) = \sum_{i=1}^n \sum_{k=1}^m \left(x_i^{data}(t_k) - x_i^{model}(t_k) \right)^2$$

Where \bar{P} is the vector of parameters, i the index of the vector of model variables, k the time points, $x_i^{data}(t_k)$ and $x_i^{model}(t_k)$ are the measured and simulated datapoints of variable i at time k . Global optimization of the cost function was done with the `GlobalSearch` function in Matlab R2020a. We did not assess parameter interactions due to the lack of controlled field or laboratory experiments. Resulting nominal model parameters are described in Table 4.

Table 4. Model parameters.

Symbol	Description	Units	Nominal value
α_{PS}	PS reproductive rate (ha of PS)	$ha^{-1}year^{-1}$	0.00110
α_{BS}	BS reproductive rate (ha of BS)	$ha^{-1}year^{-1}$	0.00137
α_{ES}	ES reproductive rate (models II only)	$ha^{-1}year^{-1}$ (ha of ES)	0.00100
β_{PS}	PS death rate	$year^{-1}$	0.29000
β_{BS}	BS death rate	$year^{-1}$	0.07000
β_{ES}	ES death rate (models II only)	$year^{-1}$	0.01000
γ_{BP}	Inhibition of growth of PS by BS (models A only)	ha^{-1}	0.09950
γ_{EP}	Inhibition of growth of PS by ES (models II only)	ha^{-1}	0.01000
γ_{EB}	Inhibition of growth of BS by ES (models II only)	ha^{-1}	0.01000
τ_{BP}	Stimulation of growth of PS by BS (models B only)	ha^{-1}	0.09950
μ_{EP}	Stimulation of death	$ha^{-1}year^{-1}$	0.01000

	of PS by ES		
	(models II only)		
μ_{EB}	Stimulation of death	$ha^{-1}year^{-1}$	0.01000
	of BS by ES		
	(models II only)		
TS	Total size of SAR	ha	146.9

2.5 Stability analysis of the mathematical models

The derivation of steady state values and their stability conditions were derived analytically for the four models, as explained in Appendix A. Note that, since this is an analytical procedure, the results do not depend on specific parameter choices, which is very robust (they depend on equation structure only).

2.6 Constructing distributions of the stable community configurations of the two 3-species models

We used a Latin Hypercube method to randomly sample 100000 parameter sets from an 11-dimensional uniform distribution spanning seven orders of magnitude ($[10^{-5} - 10^2]$), analytically computed the steady states and assessed their stability through linearization.

2.7 Estimation of the separatrix for model II-B with nominal parameter values

Model II B (three species interactions with positive regulation between the two native species) (Figure 1), with nominal parameter values in Table 3, leads to a bistable dynamical behavior with one stable steady state (p_1) corresponding to long term extinction of the two native species with high SAR *E. camaldulensis* cover, and a second one (p_3) corresponding to the opposite scenario, with stable coexistence of the two local species and the local extinction of the invasive tree. There are other

equilibria (p_3) which are all saddle points and are contained in one or more (invariant) coordinate planes. The equilibrium point p_5 , which hereafter will be given special attention, is also a saddle point because while some of its associated eigenvalues have a negative real part (characteristic of stable steady states), one eigenvalue is positive (hence unstable). Thus, p_5 is also unstable because it is not stable.

A key question emerges here as to how to decide on the asymptotic behaviour ($t \rightarrow \infty$) of a solution if we only know the state of the system at present ($t = 0$). Will it converge towards p_1 or p_3 ? In other words, how to tell which initial conditions lead to p_1 from those that go to p_3 in the general case? The key to this answer lies on a special set of solutions associated to the equilibrium p_5 . The basins of attraction of p_1 and p_3 are separated by the stable manifold W^s of p_5 . The manifold $W^s(p_5)$ is a smooth two-dimensional invariant object which consists of all solutions that tend to p_5 in the long term. All the solutions starting on one side of $W^s(p_5)$ converge to p_1 , while all solutions on the other side of $W^s(p_5)$ converge to p_3 . This means that $W^s(p_5)$ represents the *separatrix* that divides the phase space $[Bs, Ps, Es]$ into the basin of attraction of the two stable steady states of the system, p_1 and p_3 . In general, it is not possible to derive the global stable manifold $W^s(p_5)$ in a closed formula. Here, $W^s(p_5)$ was computed numerically with the method proposed by Krauskopf and Osinga (2007) as a family of orbit segments which can be obtained as solutions of a suitable boundary value problem (BVP), implemented in the package `Auto`. The two-dimensional manifold is obtained from the output data and the respective portion of the manifold is rendered as a surface from the computed orbit segments with dedicated `Matlab` routines.

2.8 Design of optimal control strategies for *E. camaldulensis* management

We assumed a current state at the point $q90 = (0.0790; 15.4667; 8.9326)$, which corresponds to the state of the system as recorded from data in 1990. We first show that $q90$ lies above the separatrix $W^s(p_5)$ and in the basin of attraction of p_1 . In other words, the empirical data

from 1990 are on the “wrong” side of the separatrix; in the absence of interventions, the native species will go extinct locally. Hence, as $t \rightarrow \infty$ the orbit starting at $q90$ converges to $p1$. The point $qm \approx (0.0785; 16.0792; 4.2897) \in W^s(p_5)$ is the nearest point in $W^s(p_5)$ to $q90$. Such minimum distance is approximately 4.7163, which is the minimal distance from the coordinate in 1990 to the separatrix —a first measure of the strength of interventions required to avoid extinction of the local species (i.e., a catastrophe)—. The usefulness of knowing point qm lies on the fact that it indicates a possible way to establish actions aimed to eradicate the *E. camaldulensis* with minimum effort. In this context, the effort is associated with the cost of moving down the state of the system from $q90$ beyond the separatrix $W^s(p_5)$ and into the basin of attraction of $p3$. The shortest path to achieve this is by crossing $W^s(p_5)$ along a straight line from $q90$ through the threshold point qm . Since finding an analytical expression for $W^s(p_5)$ is not possible, it is also impossible to find a formula for the point qm . Therefore, we carried out numerical continuation to obtain the coordinates of qm . As a first step, we calculated an orbit segment as a solution of a two-point BVP implemented and solved in Auto. One of these boundary conditions was defined in a fundamental domain lying on the stable eigenspace of $p5$; this is a standard step in the procedure to obtain a global two-dimensional manifold (Krauskopf and Osinga, 2007; Contreras-Julio et al., 2020). The second boundary condition is located on a sphere centred at $q90$ of radius R . In this way, the computed orbit segment represents a solution in $W^s(p_5)$ whose endpoint at $t = 0$ lies at distance R from $q90$. Once the desired orbit segment in $W^s(p_5)$ was obtained, we continued this solution in terms of R (which is now a dummy parameter) until a fold is detected with respect to R , and the integration time T to trace out a locus of minima for R . This iterative process revealed the global minimum at $R \approx 4.7163$ for the orbit segment in $W^s(p_5)$ with initial conditions at qm .

For the second control strategy shown in figure 7, in which only *E. camaldulensis* is allowed to decrease, to find the other endpoint two further boundary conditions are posed, namely, to force it to lie on the planes $Ps = 0.0790 + \varphi_1$ and $Bs = 15.4667 + \varphi_2$, where φ_1 and φ_2 are dummy

parameters. Once an initial orbit segment of $W^s(p_5)$ is obtained, we continue this solution in terms of φ_1 and φ_2 until both $\varphi_1 = \varphi_2 = 0$. This iterative process reveals the coordinates of $qm \in W^s(p_5)$ as the initial point ($t = 0$) of the computed orbit segment obtained as the solution of this BVP.

2.9 Code availability

The code is written in Matlab version R2020a and in Fortran and is stored in the GitHub repository github.com/ElisaDominguezHuettinger/REPSA_Model.

3. Results

3.1 Long-term stable coexistence between two native species is more likely to occur under a positive interaction regime

The qualitative analysis of the two 2-native species models, one with positive and one with negative interaction between the native species, shows that long term stable coexistence between two native species is more likely to occur under a positive interaction regime. For both models, four steady states and their stability can be derived analytically, as shown in Appendix A. The construction of systems of equations starting from the integration of highly heterogeneous sources of information and ecological data allowed us to detect the possible scenarios in the plant community. Overall, for the two models we found analytically three possible stable states: (1) when all species become extinct; (2) when only one species survives, and (3) when two survive and coexist. In addition, in all the three models we found multi-stability under certain parameter conditions.

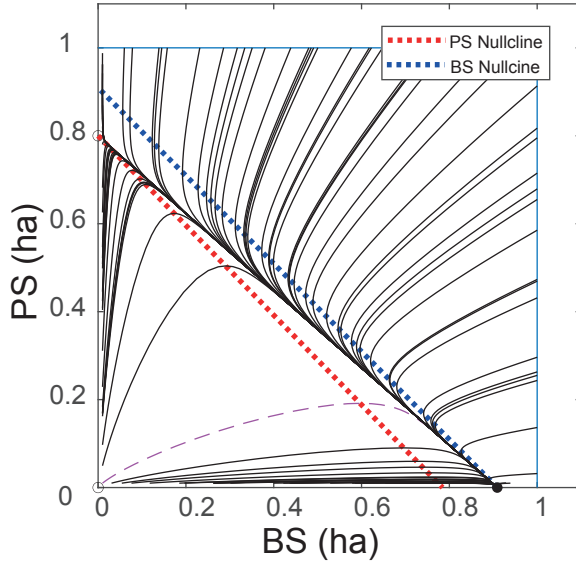
The extinction of two species occurs when the eco-dimer dissociation rate is higher than its formation rate, for both species. That is, if certain conditions change and the value of β increases or

α decreases. This may be caused by changes in one or several environmental variables, because of the arrival of a fulminating pathogen, a ravenous herbivore or an aggressive competitor.

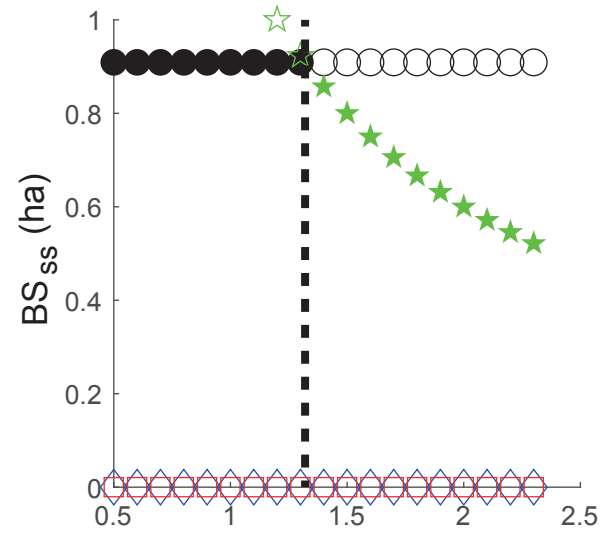
In model 1-A (two competing native species), *B. cordata* is in an advantageous position due to its ability to inhibit *P. praecox*'s growth. Therefore, parameter conditions allowing *P. praecox* to survive while leading to *B. cordata*'s extinction are more limited (it occurs if and only if $\alpha_{BS}\beta_{PS} < \alpha_{PS}\beta_{BS}$) than those necessary for the opposite to be true. This scenario is exemplified in Figure 2A.

In model I-B (two cooperating native species), *P. praecox* benefits from *B. cordata*'s growth. Hence, *Tepozan*'s survival and displacement of *P. praecox* becomes true if and only if $\alpha_{BS}\beta_{PS} < \alpha_{PS}\beta_{BS}$. This shows that stable coexistence between these two native species is more likely to occur under a positive interaction regime, since the parameter conditions for which coexistence is observed are less stringent (i.e., stable coexistence regime is more robust to perturbations in parameters). Such a scenario is exemplified in Figure 2B. This stable coexistence regime is a direct function of the strength of the positive interaction, i.e., it occurs if parameter τ_{BS} is strong enough, as shown in Figure 2C Bi-stability between the two local extension regimes in model I-B is not possible.

(A) Model I-A (negative interaction)



(C) Bifurcation diagram (I-B)



(B) Model I-B (positive interaction)

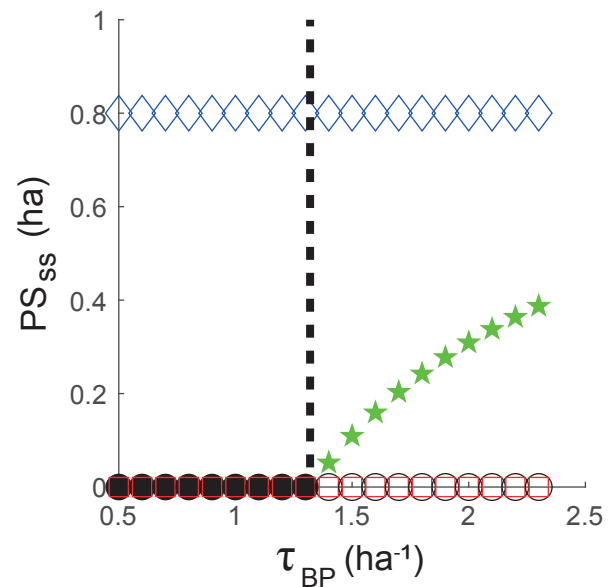
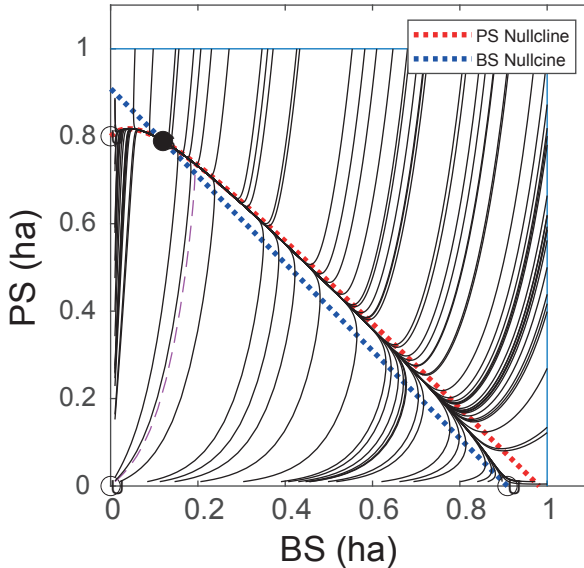


Figure 2. Qualitative analysis of the 2-native species models assuming negative or positive interactions. Representative phase planes of model I-A (negative interaction) **(A)**, and I-B (positive interaction) **(B)** showing stable local extinction of PS and stable coexistence, respectively. **(C)** shows a bifurcation diagram of model IB with the strength of the positive interaction, τ_{BP} , as a bifurcation parameter, with filled markers representing stable steady states. Strong enough positive regulatory strengths lead to a stable coexistence of both species (green solid stars). Parameter values are (A) $\alpha_{PS} = 1 \text{ ha}^{-1}\text{year}^{-1}$; $\alpha_{BS} = 0.2 \text{ ha}^{-1}\text{year}^{-1}$; $\beta_{PS} = 0.2 \text{ year}^{-1}$; $\beta_{BS} = 0.1 \text{ year}^{-1}$; $\gamma_{BP} =$

0.1 ha^{-1} ; $TS = 1 \text{ ha}$; and (*B, C*) $\alpha_{PS} = 1 \text{ ha}^{-1}\text{year}^{-1}$; $\alpha_{BS} = 1.1 \text{ ha}^{-1}\text{year}^{-1}$; $\beta_{PS} = 0.2 \text{ year}^{-1}$; $\beta_{BS} = 0.1 \text{ year}^{-1}$; $\tau_{BP} = 10 \text{ ha}^{-1}$; $TS = 1 \text{ ha}$.

3.2 Robustness of the native community to the introduction of an invasive exotic species

The symbolic analysis of the two 3-species models in Appendix A shows that both models (i.e. either with positive or negative interactions between the native species), following qualitatively different dynamic regimes (i.e. stable community configurations), are possible in the long term under certain parameter conditions (illustrated in Figure 3A): (1) all three tree species go extinct; (2-4) only one of the three species survives; or (5) the stable coexistence of *B. cordata* and *P. praecox* (case 5 in Appendix A). A stable configuration in which *E. camaldulensis* coexists with either of the other two species is not possible.

The first steady state (all extinct) is stable if $TS < \min(\beta_i/\alpha_i)$ for $i = BS, PS, ES$. A *E. camaldulensis*-only point $(0,0, ES^* > 0, \beta_3/\alpha_3)$ is stable if ES^* satisfies conditions over parameters 82-85 (II-A) / 60 (II-B) as detailed in the Appendix. A *PS*-only state $(0, PS^* > 0, 0, \beta_2/\alpha_2)$ is stable if and only if $\alpha_1\beta_2 < \alpha_2\beta_1$ AND $\alpha_3\beta_2 < \alpha_2\beta_3$. A *BS* - only state $(BS^* > 0, 0, 0, \beta_1/\alpha_1)$ is stable for model II-A if $\alpha_3\beta_1 < \alpha_1\beta_3$ and $BS^* > (\alpha_2\beta_1 - \alpha_1\beta_2)/\alpha_1\beta_2\gamma_2$, and for model II-B if $\alpha_2\beta_1 < \alpha_1\beta_2$ and $BS^* < (\alpha_1\beta_2 - \alpha_2\beta_1)/\alpha_2\beta_1\theta_3$. Finally, the *BS – PS* stable coexistence point $((\alpha_2\beta_1 - \alpha_1\beta_2)/\alpha_1\beta_2\gamma_2, PS^*, 0, \beta_1/\alpha_1)$ is stable for conditions over parameters given in eqs. (61) for model II-A and (66) for model II-B detailed in Appendix 1.

To illustrate these conditions over parameters for the two 3-species models, we numerically constructed the probability distributions of the possible community configurations under randomly varied parameter conditions (see details in Methods). We found that bi-stability is very common for both models (69.7% and 72.5% of the cases for models II-A and II-B, respectively), and that model II-A can even display tri-stability for certain parameters (1%) (figure 3A, left).

For the mono-stable scenario occurring in 29.3 and 27.5% of parameter variants for model II-

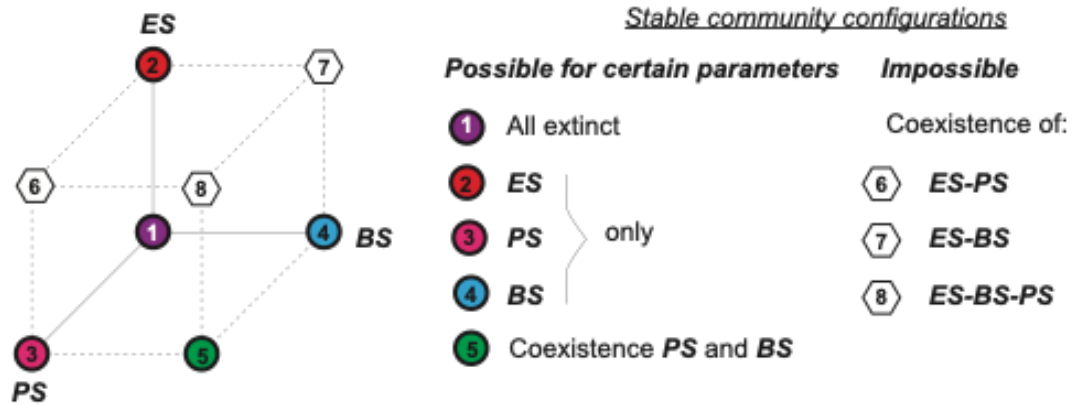
A and II-B, respectively, the proportions of parameter leading to extinction of all species is 2.7 and 2.6%; for a *E. camaldulensis*-only state, 46.8 and 45.3% (an example of this case shown in figure 3C); for a *B. cordata* -only state, 26.9 and 21.8%; for a *P. praecox* -only state, 23.6 and 26%, and, finally, and most interestingly, stable coexistence between *B. cordata* and *P. praecox* can only take place in model II-B for 4.2% of the parameter variations (Figure 3B, centre).

As shown in Figure 3B, right, for model II-A the only possible bi-stable combinations are a *E. camaldulensis*-only with a *B. cordata* -only state for 90.2% of the cases, or a *B. cordata* -only state with a *P. praecox* -only state in the remaining 9.8% of the bi-stable cases. In turn, while model II-B can also result in bi-stability between a *B. cordata* -only and a *E. camaldulensis*-only state in 43.3% of the cases, and between *B. cordata* and *P. praecox* in 50.2% of the bi-stable cases, interestingly, it can also exhibit bi-stability between a *E. camaldulensis*-only stable state and a coexistence state between *B. cordata* and *P. praecox* in the remaining 6.5% of the cases. It is this latter qualitative scenario that we analyze further in terms of intervention strategies. In addition, tri-stability between the three states in which only one of the species prevails can only be exhibited by model II-A (figure 3B down-left).

Together, these numerical results confirm the analytically derived community configurations, specifically that *E. camaldulensis* cannot stably coexist with any of the two native tree species.

3D Models (IIA and IIB)- interactions between two native and an exotic species

(A) Sketch of possible long term configurations of the community



(B) Distribution of community configurations

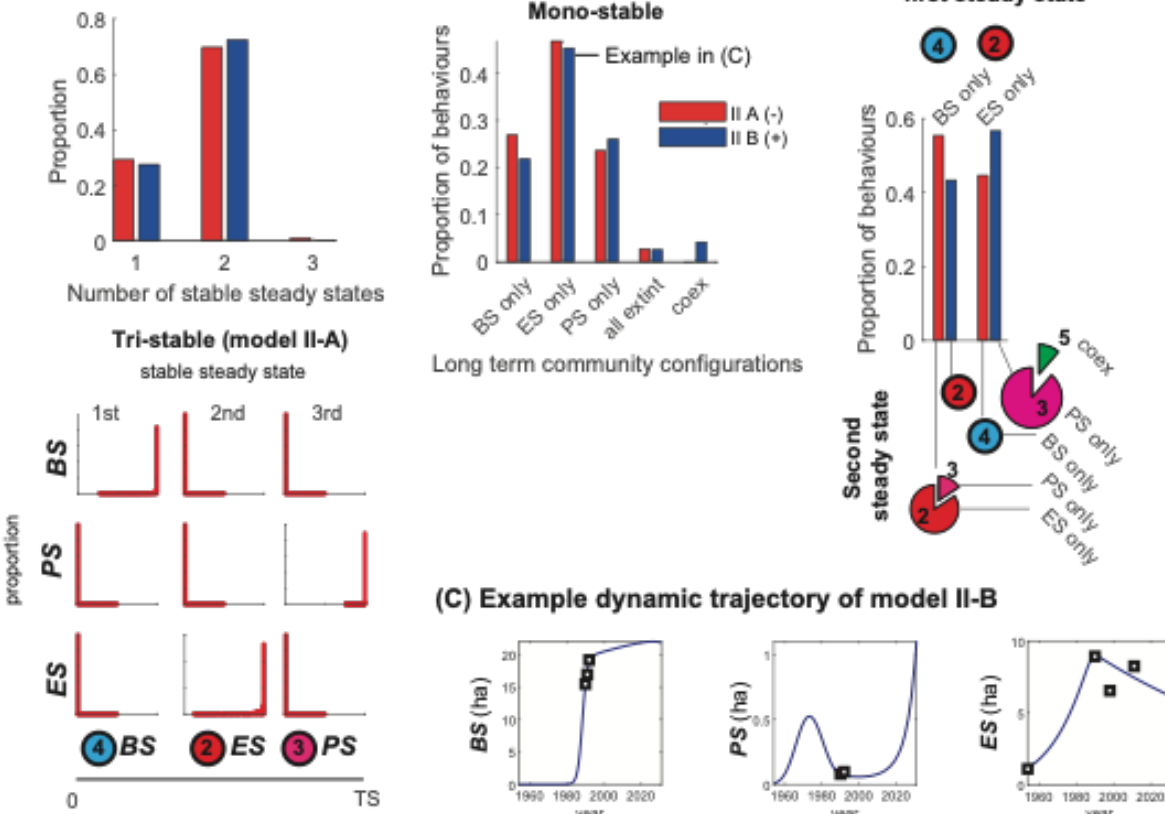


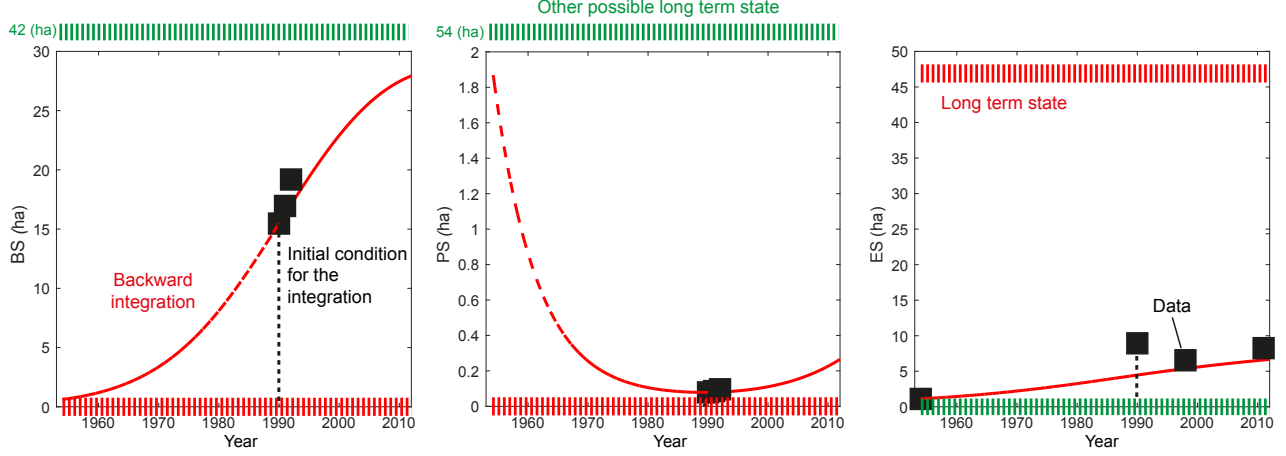
Figure 3. Possible stable long term community configurations of the two 3-species models (II-A and II-B). **(A)** Configurations sketched in the 3-species phase space. **(B)** Distribution of number of possible stable steady states and the corresponding possible community configurations for both models. In the bi-stable case, bars correspond to the proportion of community configuration of the

first steady state, with circles (pie-chart) below these denoting the corresponding configuration(s) of the second steady state. The possible community configurations of the tri-stable case in model IIA are shown by histograms of the three state variables. **(C)** Projection of the empirical data to an example dynamic trajectory for model II-B under a *E. camaldulensis*-only monostable-regime (parameters: $\alpha_{PS} = 0.021989 \text{ ha}^{-1}\text{year}^{-1}$; $\alpha_{BS} = 0.038582 \text{ ha}^{-1}\text{year}^{-1}$; $\alpha_{ES} = 0.0028517 \text{ ha}^{-1}\text{year}^{-1}$; $\beta_{PS} = 0.099878 \text{ year}^{-1}$; $\beta_{BS} = 4.5468 \text{ year}^{-1}$; $\beta_{ES} = 0.3462 \text{ year}^{-1}$; $\tau_{BP} = 0.1273 \text{ ha}^{-1}$; $\gamma_{EP} = 3.3906 \text{ ha}^{-1}$; $\gamma_{EB} = 0.0001118 \text{ ha}^{-1}$; $\mu_{EP} = 0.026769 \text{ ha}^{-1}\text{year}^{-1}$; $\mu_{EB} = 9.286e^{-05} \text{ ha}^{-1}\text{year}^{-1}$; $TS = 146.9 \text{ ha}$)

3.3 Catastrophic shifts in the SAR: in the absence of interventions, *E. camaldulensis* will lead to the local extinction of the native species

Global optimization for model IIB (tree species with positive interactions between the native species) using the field data of Cano-Santana (1994), Segura-Burciaga (1995, 2009) and Acosta-Arreola, (2015) resulted in the nominal parameter values given in Table 3 and a dynamic behaviour shown in Figure 4A. This scenario corresponds to the bi-stability of two qualitatively different regimes: in the long term, either the two native species, namely *B. cordata* and *P. praecox*, coexist and eventually displace the invasive *E. camaldulensis*, or vice versa. Further, numerical integration of our model II-B with optimal parameters shows that, without intervention, the trajectory starting at the 1990 datapoint (the only year for which we have data for all our variables) will eventually converge to the *E. camaldulensis*-only steady state, i.e., it is within the basin of attraction of the *E. camaldulensis*-only steady state (Figure 4B).

(A)



(B)

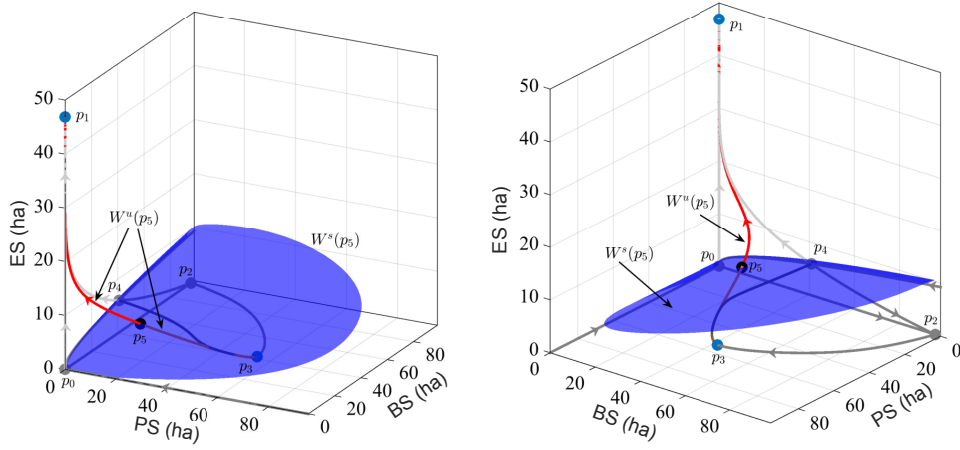


Figure 4. Model with optimal parameters. Fit of model II-B to data in Table 3 leads to a bi-stable scenario with either a *E. camaldulensis*-only regime (red) or a stable coexistence between *B. cordata* and *P. praecox* in green. The datapoint of 1990 is within the basin of attraction of the *E. camaldulensis*-only regime. Resulting optimal parameters are given in Table 4. **(A)** Dynamic trajectories. **(B)** Phase space representation of the dynamic trajectories showing the separatrix in blue.

3.4 Mathematical design of optimal strategies for SAR management

Stability and bifurcation analysis suggest that, in the absence of interventions controlling *E. camaldulensis*, the most likely long term future scenario of the ecological community is the local extinction of the native communities. Thus, here, following a similar strategy as in Contreras-Julio et al.(2020), we design two optimal intervention strategies for SAR through which the dynamical

trajectories are re-channeled to converge towards a stable coexistence between *Tepozán* and *P. praecox*. In the first strategy, we assume that the abundance of all the tree species can be modulated (e.g., by planting or felling). While this first strategy retrieves a mathematically optimal solution, it might not be realistic or plausible (in financial or practical terms) to execute. Thus, we also designed a second strategy in which we assume that only the eucalypt death rate can be reduced (e.g., through felling). In both cases, we assume that the current conditions correspond to the measured state variables in 1990, because it is the only year for which we have complete data, and computed the minimal intervention effort required to push the state trajectory from one basin of attraction (corresponding to long term death of the native species) to an other (stable coexistence of native species and local extinction of the invasive). In other words, we design an optimal control strategy for SAR, based on the available empirical information and the plausible interventions.

Figure 5 shows the results of the first design strategy. Here, we found the optimal point $qm = (0.1; 16.1; 4.3) \in W^s(p_5)$ is the nearest point to $q90$ on the separatrix; it lies at a Euclidean distance of approximately 4.7 (ha) and requires simultaneous decrease in eucalyptus from 8.9326 ha at $q90$ to 4.2897 ha and from 0.0790 at $q90$ to 0.0785 for *P. praecox*, and an increase from 15.4667 at $q90$ to 16.0792 for *B. cordata*. To illustrate the usefulness of this procedure, point qn lies directly below qm in the basin of attraction of $p3$. The corresponding trajectory (cyan curve) in panels (b1)-(b3) of Figure 5 shows that only a very small (but suitable) perturbation away from $q90$ is required to achieve long term coexistence of *Ps* and *Bs* and the elimination of *Es* (compare the cyan and magenta curves in Fig. 5).

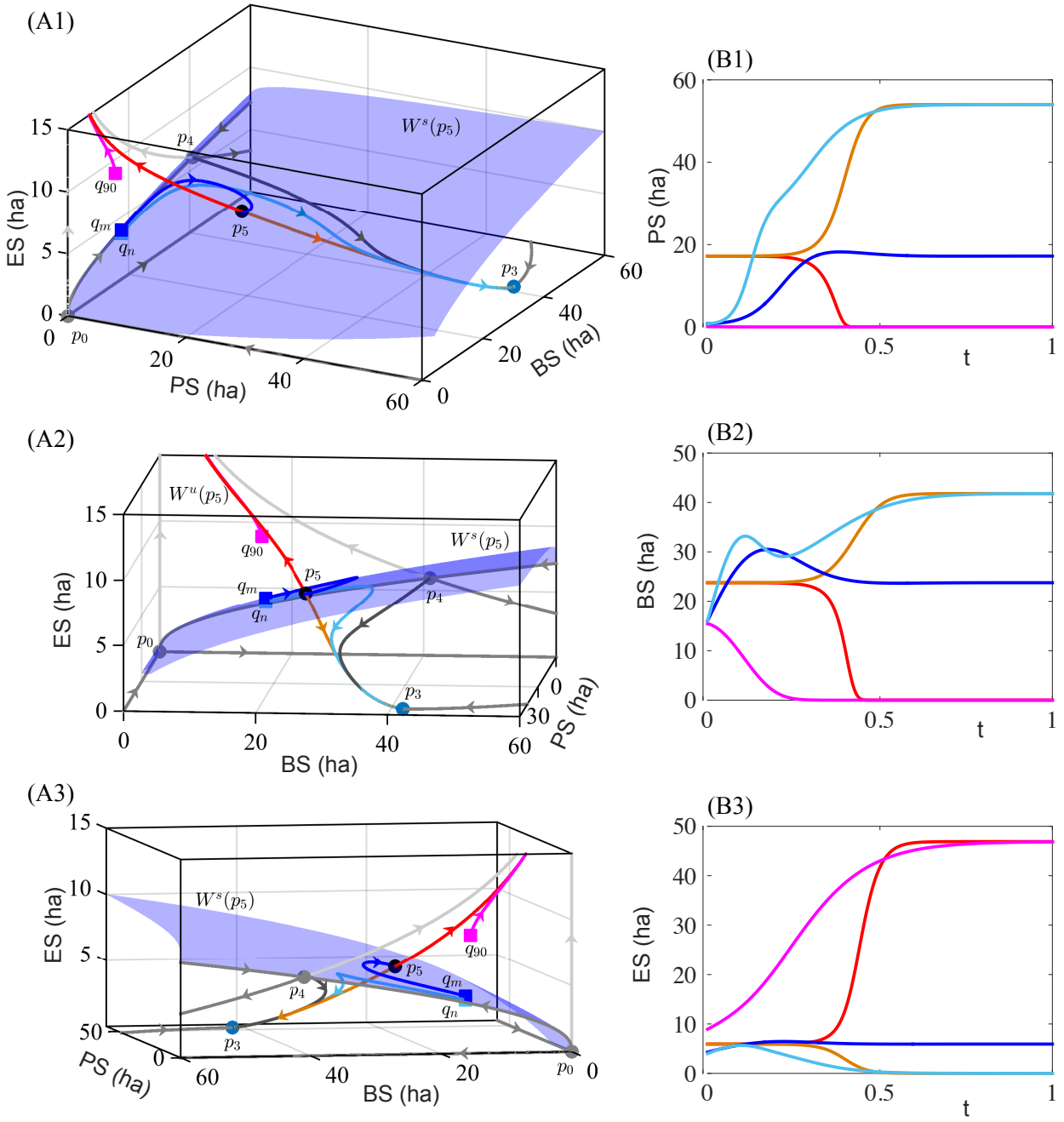


Figure 5. Optimal *E. camaldulensis* management strategies for a bistable regime, assuming the abundance of the tree species can be modulated (e.g., by planting or felling). The left panels (A1-A3) show different phase-space projections of the separatrix $W^s(p_5)$ in blue, and the right panels (B1-B3) show the dynamic evolution of our three model variables. Magenta: Trajectory from q_{90} (with $t_0=1990$) towards a *E. camaldulensis*-only state (in the absence of interventions). The point $q_m =$

$(0.1; 16.1; 4.3) \in W^s(p_5)$ is the nearest point to $q90$ at the separatrix. Trajectories starting on that point (in blue) remain in $W^s(p_5)$. Trajectories just below (cyan) converge towards the *B. cordata - P. praecox* stable steady state; trajectories starting just above (orange) still converge towards the *E. camaldulensis*-only state. The time variable t is rescaled from $t \in]-\infty; +\infty[$ to $t \in]0; 1[$ for computational purposes.

In Figure 6, we show a cross-section of the 3-species space into the 2-native species projection with constant *E. camaldulensis*. Panels (a), (b) and (c) show a cross section of Σ intersecting $W^s(p_5)$. Σ corresponds to the plane in the $(Ps; Bs; Es)$ -space where $Es = 8.2513$ is fixed; this is the recorded value of Es from data in 2011, i.e., the most recent recording. We may not know the exact value of the other two variables, Ps and Bs , in 2011. But we may still say something about the possible long-term outcome of this ecological interaction even if (at least) we have a vague idea of what were -or what were not- the possible covers of Ps and Bs back in 2011. Points on Σ can be parameterized by their projection to the $(Ps; Bs)$ -plane. Panel (d) shows such representation and how the different intersections of invariant objects and orbits lie on Σ . The set $ws = W^s(p_5) \cap \Sigma$ is a one-dimensional curve rendered in light blue color. It is bounded on one end by the intersection of the stable manifold of $p4$ with Σ which corresponds to a point in the $Ps = 0$ plane (dark grey square); the other end of ws lies outside of the plotted range. In panel (d), the region $B(p3)$ above ws corresponds to those points in Σ lying in the basin of attraction of $p3$: any orbit starting in $B(p3)$ converges to $p3$ in forward time. Hence, region $B(p3)$ is the set of all combinations of $(Ps; Bs)$ which, for the amount of Es present in 2011, would have allowed long term survival of both indigenous species, and eradication of Es .

In turn, region $B(p1)$ corresponds to those points in Σ lying in the basin of attraction of $p1$. Hence, region $B(p1)$ is the set of all pairs $(Ps; Bs)$ which evolve towards the mutual extinction of Ps and Bs and colonization by Es . Note that the unstable manifold $W^u(p_5)$ of $p5$ (red curve in panels (a), (b) and (c)) intersects Σ at a point in $B(p1)$, rendered as a red square in panel (d).

Likewise, the two orbits on the plane $Ps = 0$ coming from $p0$ and $p4$, respectively, and converging to $p1$ intersect Σ at points in $B(p1)$ (light grey squares). Note that the long-term outcome of both native species (i.e., survival or extinction) is highly sensitive to variations of Bs , but less so to changes of Ps , provided Ps is large enough. Indeed, the curve ws (i.e., the boundary between $B(p1)$ and $B(p3)$) has a small slope for $Ps > 20$ ha, so small variations of Bs near ws -that is, $40 \text{ ha} < Bs < 50$ ha approximately- may trigger the pair $(Ps; Bs)$ move to the other basin of attraction crossing ws up or down. On the other hand, if Ps is sufficiently small, say $0 < Ps < 5$ ha, and $50 \text{ ha} < Bs < 80$ ha, it is the other way around: small variations of Ps may induce the point $(Ps; Bs)$ to cross the separatrix ws from one basin to the other. On other, more colloquial words: this gives us an idea of the best strategy for interventions; planting a particular type of tree might be much more efficient (cost-effective) than planting the other.

The results of the second control strategy (manipulating Eucalypt-only) are shown in Figure 7. In mathematical terms, this strategy corresponds to follow a straight path in the $(Ps; Bs; Es)$ -space keeping Ps and Bs constant (specifically, 0.08 ha and 15.5 ha, respectively) while only Es is decreased. Once again, knowledge of $W^s(p_5)$ is useful to design an optimal management campaign. It is clear from the definition of the separatrix $W^s(p_5)$ that the minimum number of felled trees is achieved when the point $(Ps; Bs; Es)$ effectively reaches $W^s(p_5)$. This happens at the point $qm = (0.0790 \text{ ha}; 15.4667 \text{ ha}; 4.0302 \text{ ha}) \in W^s(p_5)$. The orbit starting at qm is the first in this strategy that does not converge to $p1$ but to $p5$; see the blue orbit in panels (b1)-(b3). In simple words, in this example this strategy corresponds to decreasing Es from 8.9 ha to (at least) 4.0302 ha. Any value of Es just less than 4.0302 ha will suffice, but the closer to 4.0302, the more cost-effective will be. In the special case that Es is lowered down to exactly 4.0302 ha, the system will evolve to the coexistence equilibrium $p5$. However, this asymptotic state is unstable; any generic small perturbation away from $p5$ drives the system into the basin of either $p1$ or $p3$; see the blue orbit in

panels (b1)-(b3). Therefore, to ensure success in our strategy, one must take care that $Es < 4:0302$ ha, i.e., the system is driven down to just below qm .

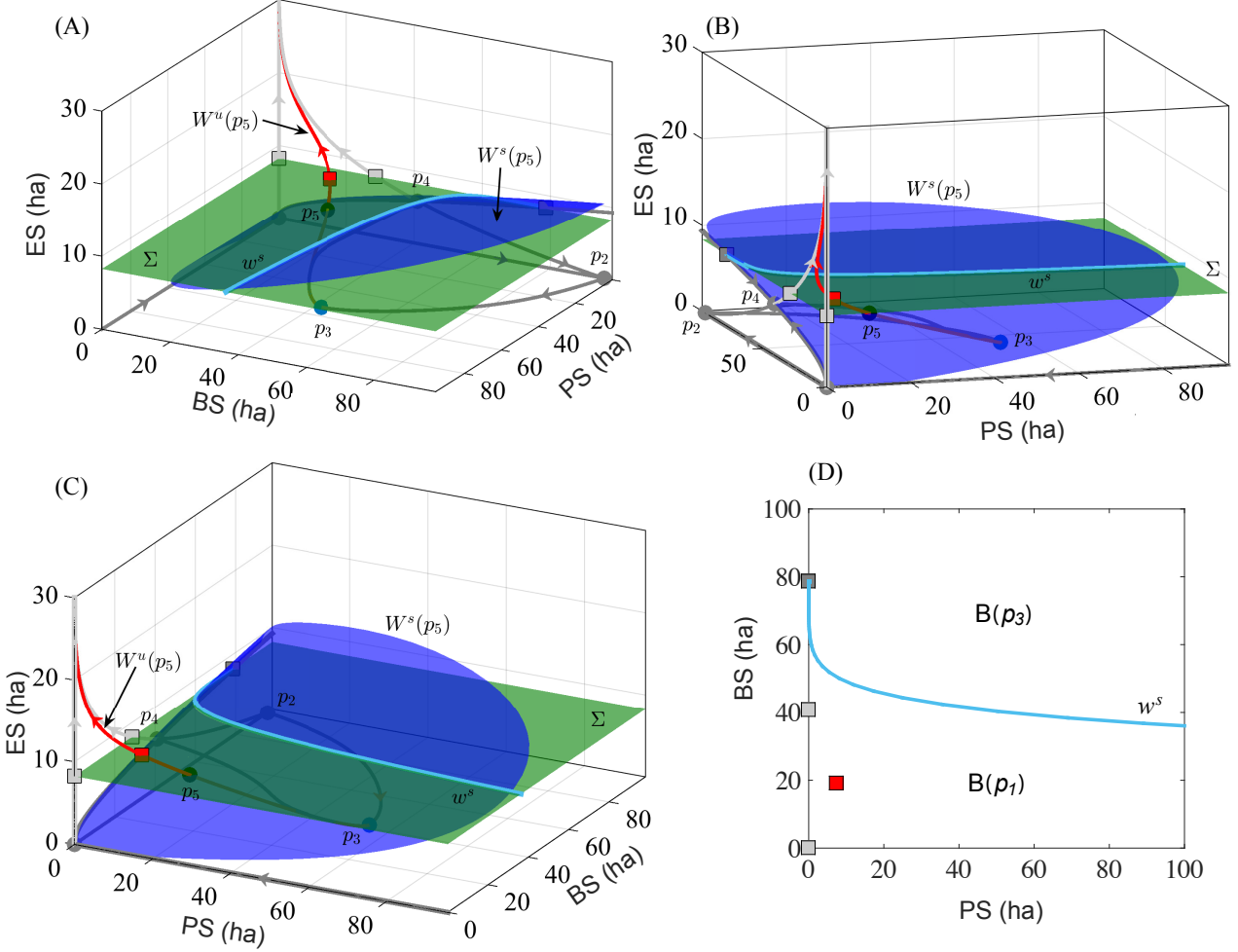


Figure 6 Cross-section of the 3-species space into the 2-native species projection with constant eucalyptus. **(a-c)** show a cross section of Σ intersecting $W^s(p_5)$, where Σ corresponds to the plane in the $(Ps; Bs; Es)$ -space where Es is fixed to its most recent recording (from 2011). **(d)** shows the projection of the points on Σ on the $(Ps; Bs)$ -plane with $w^s = W^s(p_5) \cap \Sigma$. The region $B(p_3)$ above ws corresponds to the set of all combinations of $(Ps; Bs)$ which, for the amount of Es present in 2011, would have allowed long term survival of both indigenous species, and eradication of Es and vice versa for region $B(p1)$.

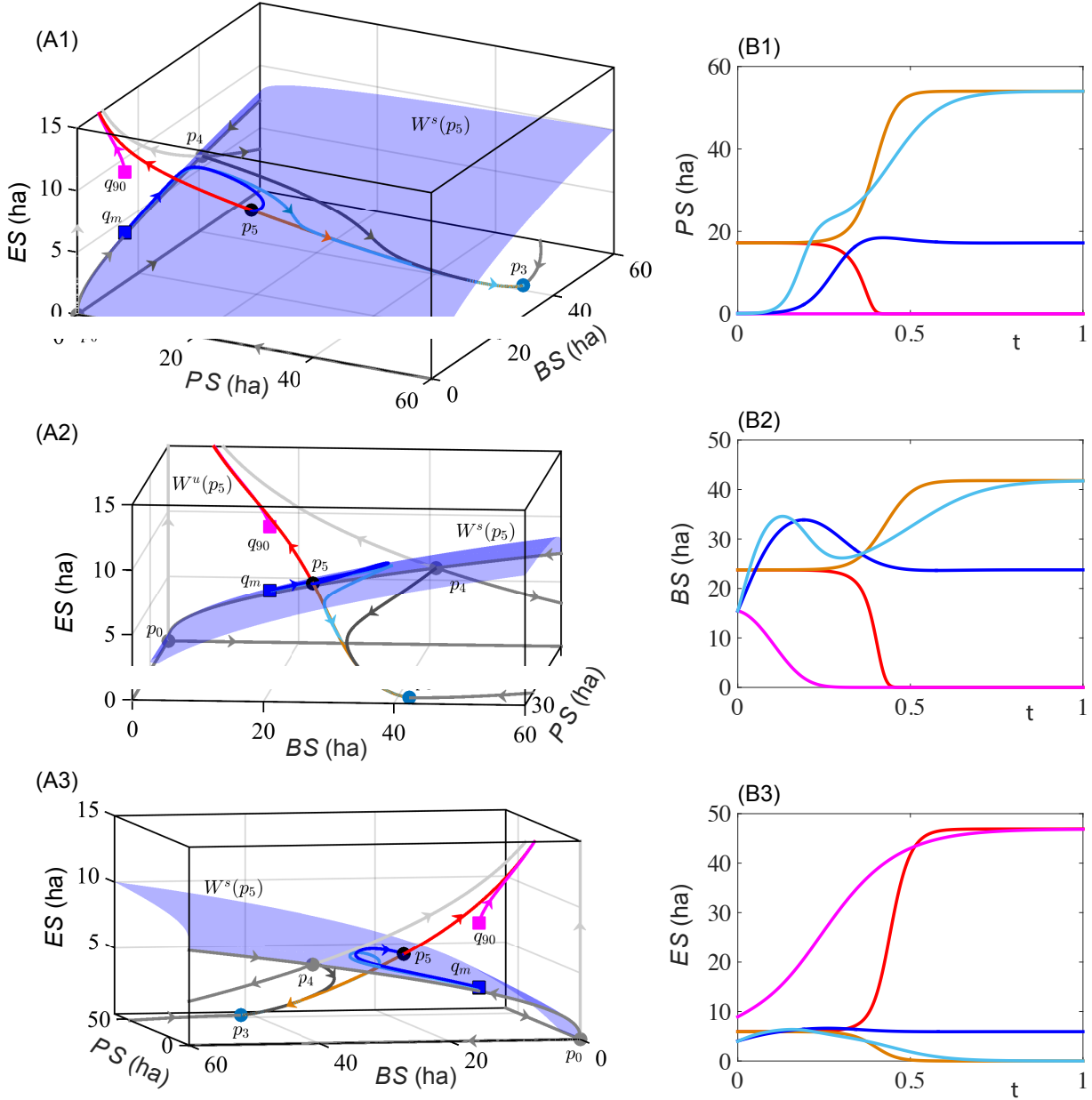


Figure 7. Optimal *E. camaldulensis* management strategies for a bistable regime, assuming that only the eucalyptus coverage can be modulated (e.g., by felling). As in figure 5, the left panels (a1-a3) show different phase-space projections of the separatrix $W^s(p_5)$ in blue and the right panels (b1-b3) the dynamic evolution of our three model variables. Magenta: Trajectory from q_{90} (with $t_0=1990$) towards a *E. camaldulensis*-only state (in the absence of interventions). The point $q_m = (0.0790; 15.4667; 4.0302) \in W^s(p_5)$ is the nearest point to q_{90} at the separatrix. The trajectory

starting at that point (in blue) remains in $W^s(p_5)$. To illustrate the usefulness of this procedure, a cyan orbit is shown in panels (B1)-(B3) whose initial point (not labeled) lies directly below qm in the basin of attraction of $p3$. It serves the purpose to show that one might only need a very small (but suitable) perturbation away from $q90$ to achieve long term coexistence of Ps and Bs and elimination of Ps ; compare the cyan and magenta curves.

4. Discussion

By using a set of mechanistic mathematical models constructed from, and calibrated with, experimental data, we evaluated the most plausible successional scenario in the Pedregal de San Ángel Ecological Reserve (PSAER or SAR); in addition, we gained insight into the effect of perturbation in the form of a invasive species (a structural perturbations) and of random parameter variation (which could be affected, for example by pollutants and pathogens acting as bifurcation parameters), in reshaping the future configuration of the tree community in this protected area. Our modeling approach was intended to gain insights into the potential consequences of implementing different management regimes with the best scientific tools currently available, as objectively as possible and recognizing both advantages and shortcomings, to ultimately make management recommendations (Schuwirth et al., 2019).

The claim that the use of mechanistic models constructed with ODEs is the most adequate approach is warranted, given the large amount of information available on this system's properties, although quantitative information on cover was rather limited (Schuwirth et al., 2019). In the case of SAR, the knowledge accumulated on the system during the last seven decades is largely derived from the location of this protected area within UNAM's main campus. Such wealth of information and ancillary observations clearly point to a “tepozanzation” process, i.e. an increase in *B. cordata* dominance combined with the concomitant reduction of the physiognomic importance of *P. praecox* over time, along with the generalized structural change in this ecosystem. However, the available

information is insufficient to unambiguously determine whether the system has reached stability. To achieve this goal, increasing information resolution would be needed, trying that the time coverage of the records last longer than the lifespan of the organisms used for the modelling and considering relevant natural cycles (Suding and Hobbs, 2009; Capon et al., 2015). Life expectancy for *B. cordata* is about 25 years (CONABIO, 2022), and thus despite the adequacy of the time window covered by the information, temporal resolution is clearly insufficient. One way to increase the temporal coverage of the study, while increasing temporal resolution, is offered by remote sensing, as will be discussed later.

Despite the limited temporal resolution of the data, the robustness of models I-B and II-B stems from their construction based on the integration of all available knowledge on this ecosystem. It is important to note that our qualitative results are not dependent on specific parameter choices, but rather on the structure of the models, derived in turn from the proposed ecosystem relationships. The two models were analysed analytically. Moreover, model II-B presented bi-stability, which is uncommon. These characteristics open several possibilities from a mathematical perspective; for example, they allow designing optimal control strategies based on the description of separatrices along with an exhaustive description of the system (independence on parameters choice or "no need for cherry-picking parameters"). Analytical approaches of this kind to detect ecological thresholds and regime shifts have become a matter of urgency because of the rapid increase of human pressure on ecosystems (Andersen et al., 2009).

The possibility to predict future successional stages has great value. In SAR, the most important limiting factor for the proper development of the plant community is soil depth (Rzedowski 1954). Being a relatively recent lava field, soil shallowness translates into physiological water deficit (Álvarez et al., 1994; Meave et al., 1994). Ecosystem engineers are organisms that regulate resource availability and the environmental conditions for the establishment and growth of other species directly or indirectly, and consequently they can trigger profound changes in the system

by modifying species abundances and the overall interspecific interactions in the habitat (Jones et al., 1994; Suding and Hobbs, 2009; Gaertner et al., 2012). In this regard, Mendoza Hernández (2002, 2003, 2013) concluded that *B. cordata* modifies the microenvironment in its close vicinity and facilitates the recruitment of late successional species by accumulating large amounts of organic matter on the soil, ultimately resulting in increased soil fertility and the creation of safe sites for seed accumulation and germination for other species, offering a larger rooting soil volume and better soil retention. If “Rzedowski hypothesis”, stating an increase in the dominance of *S. molle* instead of *B. cordata*, were correct, pedogenesis in this system would be likely slower and the probability of developing a successional more mature basin, lower.

Native species can develop a more stable coexistence if facilitation occurs in the community, especially if the dominant element has positive effects on a group of plants that will form part of the ensemble characterizing the new basin of attraction. Likewise, new microhabitats will be created for the successful establishment of late successional species. By promoting coexistence, facilitation also results in increased community resistance to exotic species compared to relationships based on competition only.

The ecological notion of a world dominated by competition has been ingrained in ecologists since Darwin’s times (Bruno et al., 2003). Therefore, the most widespread mathematical models in ecology have attempted to explain community structuring and dynamics based on competition and predation (Clements, 1916; Lotka, 1925; Volterra, 1928; Gause, 1932; Hutchinson, 1961; May and Leonard, 1975; Whittaker and Levin, 1977; Mohd, 2019). Though not necessarily incorrect, this is certainly incomplete (Bruno et al., 2003). Therefore, in model II-B we were interested in incorporating these two contrasting types of interactions occurring in nature. Positive interactions are extremely diverse and have been documented in all ecosystems of Earth (Bruno et al., 2003). Although facilitation appears to be more frequent than normally accepted, its role in community structuring has been largely neglected because it is difficult to detect (Lin et al., 2012) and due to

competition's historical influence. We believe that model II-B is more realistic and has a greater power to capture and simplify the system's complexity.

Although many coexistence models do not consider facilitation as a structuring interaction of community dynamics, we found that in PAERS it can be a fundamental mechanism to explain its high biodiversity. Facilitation intensity can vary depending on the life stage of the plants and environmental changes (Callaway, 1995). Recognizing that both competition and facilitation operate in dynamic environments can help us re-evaluate the importance of cooperation in maintaining the resilience of natural systems and, therefore, of social systems. The theoretical framework of ecology must incorporate all the research and experimentation that recognizes facilitation as a fundamental driver of ecosystem dynamics by influencing spatial patterns, allowing coexistence and high biodiversity, directing community dynamics in succession processes (Callaway, 1995; Bruno et al., 2003).

In both the 2-native species and 3-species models, we found that coexistence is more likely when a facilitative interaction occurs. The observed positive interaction between *B. cordata* and *P. praecox* could also be true for many other species inhabiting SAR. If facilitation and coexistence modify the structural and functional thresholds for changes in the basin, then their study becomes imperative in order to thoroughly understand ecosystem dynamics. Our study invites to conduct field experiments aimed at determining whether facilitative interactions occur and how they affect threshold dynamics.

Although our models allowed us to calculate structural thresholds, performing experiments is necessary to integrate the functional thresholds (Briske et al., 2005). For example, confirmation that the increase and stabilization of *B. cordata* are modifying ecosystem dynamics can be achieved through experiments to determine the effect of shade, soil and nutrient accumulation, and changes in soils humidity in *B. cordata*'s neighborhoods (Callaway, 1995), to examine whether this is creating a facilitative effect of some species of SAR. Experiments comparing species composition and abundance

both in the seed bank and in the soil microbiome would be also welcomed (Callaway, 1995; Gaertner et al., 2014) between sites with high and low *B. cordata* density, and with *E. camaldulensis*. If the significance of soil accumulation by *B. cordata* were experimentally verified, new experiments with *Quercus* seedling could be conducted to assess the possibility of an oak-dominated future basin of attraction, as also hypothesized by Rzedowski (1954). Likewise, it would be important to analyze the interactions of *B. cordata* and *E. camaldulensis* with their pollinators, since this could shed light on the effects on other species in SAR.

Evaluating coexistence and facilitation-derived resistance to native species invasions or pathogen attacks would be also very important. Our model, which incorporates *E. camaldulensis* as an exotic species, predicts that, based on its interactions with the other community components, it would become dominant, displacing the native species. Our model, which is an abstract representation of the interactions between native and exotic species, can be generalized through its qualitative or quantitative adjustment, i.e., fine-tuning the regulatory loops between native and exotic species, and adjusting the parametric values accordingly, to explicitly consider other exotic species. One of them is the African grass *Cenchrus clandestinus*, which in 2009 covered 66 of the 237 ha representing the current area of the reserve (Acosta-Arreola, 2015).

Incorporating other exotic species and their interactions into the model would require a thorough literature review to identify the existence and prevalence of three common effects of exotic species when they become established in a community (Gaertner et al., 2012): (1) reduced species richness; (2) changes in seed bank composition, and (3) the modification of interaction networks, mostly seen as decreasing interactions with pollinators or reducing the availability of beneficial soil microorganisms. Also, this often facilitates the establishment of seedlings of some species, while inhibiting other species, as is the case of *E. camaldulensis*. Changes in fire regime are also common as a result of invasive plants (Gaertner et al., 2014), thus analysing whether fire regime differs between areas with and without exotic species becomes highly relevant. The spatial structure of these

species is essential to understand their dynamics. In the case of *E. camaldulensis*, tree density decreases as one moves away from the edge (Segura-Burciaga and Martínez-Ramos, 1994), and therefore, experiments in areas close to *E. camaldulensis* dominated stands are needed to properly analyse these possible effects and their magnitude.

Based on our model, it became apparent that designing a *E. camaldulensis* removal plan for SAR and the entire UNAM campus is very important. This is so because once the structural and functional thresholds of a system have been crossed, multiple barriers to restoration emerge, making this process very difficult, if not impossible (Gaertner et al., 2012, 2014). Invasive species capable of inducing regime shifts through changes in their abundance and persistence, and suppressing native species, should be given priority in implementing management interventions (Gaertner et al., 2014).

The fact that exotic plants are also susceptible to negative effects from other species must not be overlooked. An important factor absent from our model due to lack of information on its role in SAR is the psyllid *Glycaspis brimblecombei*. This insect of Australian origin, a specific parasite of eucalyptus species, is now present in Mexico City, and there are reports of its strong effects on eucalypt trees in the Bosque de Chapultepec, the largest park in the city (GODF, 2006). Although no studies were found on its impact on SAR, its presence there has been recorded (Farfán Beltrán, 2016). This species could have a regulatory role, potentially curbing the increasing *E. camaldulensis* trajectory projected by our modelling.

All this modelling and the identification of non-linear effects of ecological interactions aims at generating knowledge that is applicable to management plans of nature protection areas. Idealizing ecosystem as they used to be in the past can result in biased decision-making, whereas explaining ecosystem dynamics without complete knowledge can produce unrealistic scenarios (Suding and Hobbs, 2009) and promote inefficient decision-making, hindering management plans for the reserve (Bruno et al., 2003). Better and more complete knowledge on a system will lead to a deeper

understanding and the possibility to interpret empirical data in a mechanistic way, ultimately leading to more robust predictions (Schuwirth et al., 2019).

In this context, incorporating tools available from dynamic ecological systems for ecosystem conservation and management becomes highly relevant. Keeping resilience as a central concept in management plans does not require great precision in predicting the future, but it needs a description of the qualitative capacity of the system to absorb and respond to future events, no matter how unexpected they might be (Holling, 1973). Due to the increasing speed of environmental changes at present, decision makers cannot afford to perform rigorous tests to determine thresholds, so many models have been used in a heuristic fashion (Suding and Hobbs, 2009). Often, the impact of a regime shift derived from a feedback involving an invasive species is identified only when it is extremely difficult to manage or reverse it (Gaertner et al., 2014). Therefore, a balance is needed between the knowledge that may be gained from modelling, on the one hand, and model accuracy on the other, while being realistic for an effective decision-making in a context of accelerated environmental change. Every model used for this purpose must be contrasted with the results of their implementation in the management plan, so that it can be adjusted, modified or discarded to build new ones.

Hence, it is crucial that our predictions and recommendations are heeded by SAR managers to control the *E. camaldulensis* population most efficiently, even under the high uncertainty of our predictions. Along with the theoretical developments, ecologists should strive to contribute qualitative ecological evidence on thresholds if we will ever be capable of effectively influencing environmental policies in the future (Andersen et al., 2009). Critical examination of these models and their constant adjustment is fundamental. In our models, the main limitation is the lack of a measure of quantifiable uncertainty of the data (Schuwirth et al., 2019). Despite this limitation, we envision several options to fill this gap.

To calibrate and validate our model, it would be necessary to make it spatially explicit by using remote sensing imagery. We have retrieved eight aerial photographs from 1943 to 1986, and 64 satellite images (Spot 5, 6 and 7) from 1992 to 2019. Increasing the spatio-temporal scale of the input variables would result in improved model robustness and increased prediction accuracy, allowing the incorporation of error measures (Schuwirth et al., 2019). Proper identification of a regime shift requires at least 100 time steps (Andersen et al., 2009); however, usually time series comprise between 20 and 40 steps at the most. Using remote sensing imagery would result in 72 time steps, which we deem sufficient to ascertain whether the “tepozanzation” process became stable already. Machine learning tools may also enable identifying the distributions and changes over time of trees and shrubs over an 80-yr period.

Incorporating the spatial scale into the models enables the design of experiments that can help calibrate the parameters, interpret the model more adequately, and make good decisions (Suding and Hobbs, 2009). The spatial scale is relevant because the dispersal dynamics of species and their spatial patterns are strongly influenced by competition and facilitation (Lin et al., 2012). The most likely expansion mode of *E. camaldulensis* is the so called “advance-front” (Segura-Burciaga, 1995); this is the case when the seeds that arrive at the edge of the distribution patch create a new fringe of individuals, and the iteration of this process leads to the expansion of the patches of this species. Having been sown at the borders of areas that became part of the ecological reserve years later, modeling the expansion dynamics across space of *E. camaldulensis* is crucial.

Through remote sensing we could use early warning signals such as autocorrelation and variance asymmetry to determine where a change occurred, or is about to occur, in the basin of attraction, whether the current community has stabilized, or if what we observe is simply a transitory state (Scheffer et al., 2009; Kéfi et al., 2013; Dakos, 2018). Models integrating autocorrelation require more precise error estimations and measure of uncertainty (Schuwirth, 2019); thus, using a much broader but at the same time more detailed time series would lead to more effective decision-

making. A further step involves the incorporation of demographic stochasticity into the model after calibrating it with the image data, for example, through including fire incidence, as fires could affect the current course of the succession (Cano-Santana and Meave, 1996). Also relevant would be the modelling of the behaviour and interaction with other species considered key to the cycles of matter and energy fluxes in SAR, such as the grass *Muhlenbergia robusta*, the shrub *Verbesina virgata*, and the grasshopper *Sphenarium purpurascens* (Cano-Santana, 1994). This approach would lead to a more robust modelling and the analysis would evolve from community to ecosystem modelling.

5. Conclusions

Our modelling approach allowed integrating complex and heterogeneous information for a plant community within an ecological reserve. By doing so, we were able to mathematize its dynamic behaviour by focusing on the trees that drive its structure. In addition, we provided evidence for the relevance of facilitation and coexistence as structuring factors of a species assemblage and made specific recommendations for the future management of an exotic species in a reserve. In this way, we opened a range of possibilities for new research that can become a methodological guideline for other reserves and other human-influenced and managed ecosystems.

Mechanistic mathematical modelling is a powerful tool potentially useful for a variety of purposes, ranging from the reconstruction of past trajectories of ecological communities to the prediction of the effects of strongly competitive invasive species and of future successional stages in the presence or absence of disturbances. Also, it may provide valuable support to decision making through *in silico* experiments to examine alternative ecosystem interventions. Finally, but not less importantly, all this may be achieved by integrating heterogeneous and scattered datasets describing individual ecological processes.

6. Acknowledgements

EDH acknowledges funding from PAPIIT UNAM IA100119, from CONACyT 319600 and from the College of Life Sciences of the *Wissenschaftskolleg zu Berlin*. JAM acknowledges funding from PAPIIT IN217620. PA thanks Proyecto basal CMM-Universidad de Chile. JAA was supported by a graduate CONACyT scholarship (No. 703449) and by PERMEA.

Competing interests

The authors declare that they have no known competing financial interests or personal relationships that could have appeared to influence the work reported in this paper.

Author contributions

Jaime Acosta-Arreola: Conceptualization, Data curation, Methodology, Writing- Original draft preparation; **Elisa Domínguez-Hüttinger:** Conceptualization, Methodology, Formal analysis, Visualization, Writing- Reviewing and Editing; **Pablo Aguirre:** Methodology, Visualization, Writing- Reviewing and Editing; **Nicolás González:** Methodology; **Jorge A. Meave:** Conceptualization, Supervision, Writing- Reviewing and Editing. All authors contributed equally to the interpretation of results and approved the final text.

References

Acosta-Arreola, J. 2015. Producción de biomasa y energía por residuos de jardinería en Ciudad Universitaria, D.F. (México). B.Sc. Thesis, Universidad Nacional Autónoma de México, Mexico City.

Álvarez, J., Carabias, J. Meave del Castillo, J.A, Moreno-Casasola, P., Nava, D., Rodríguez, F.,

- Tovar, C., Valiente, A. 1994. Proyecto para la creación de una reserva en el Pedregal de San Angel. In: Rojo, A. (ed.) Reserva Ecológica El Pedregal de San Ángel: Ecología, Historia Natural y Manejo, pp. 343–369. Universidad Nacional Autónoma de México, Mexico City.
- Andersen, T., Carstensen, J., Hernández-García, E., Duarte, C.M. 2009. Ecological thresholds and regime shifts: approaches to identification. *Trends in Ecology and Evolution* 24, 49–57. <https://doi.org/10.1016/j.tree.2008.07.014>.
- Angeler, D.G., Allen, C.R. 2016. Quantifying resilience. *Journal of Applied Ecology* 53, 617–24. <https://doi.org/10.1111/1365-2664.12649>.
- Antonio-Garcés, J., Peña, M., Cano-Santana, Z., Villeda, M., Orozco-Segovia, A. 2009. Cambios en la estructura de la vegetación derivados de acciones de restauración ecológica en las zonas de amortiguamiento Biológicas y Vivero Alto. In: Lot, A., Cano-Santana, Z. (eds.), *Biodiversidad del Ecosistema del Pedregal de San Ángel*, pp. 465–481. Universidad Nacional Autónoma de México, Mexico City.
- Borenstein, E. 2012. Computational systems biology and *in silico* modeling of the human microbiome. *Briefings in Bioinformatics* 13 (6), 769–780. <https://doi.org/10.1093/bib/bbs022>
- Briske, D.D., Fuhlendorf, S.D., Smeins, F.E. 2005. State-and-transition models, thresholds, and rangeland health: a synthesis of ecological concepts and perspectives. *Rangeland Ecology & Management*, 58, 1–10. [https://doi.org/10.2111/1551-5028\(2005\)58<1:SMTARH>2.0.CO;2](https://doi.org/10.2111/1551-5028(2005)58<1:SMTARH>2.0.CO;2)
- Bruno, J.F., Stachowicz, J.J., Bertness, M.D. 2003. Inclusion of facilitation into ecological theory. *Trends in Ecology and Evolution* 18, 119–25. [https://doi.org/10.1016/S0169-5347\(02\)00045-9](https://doi.org/10.1016/S0169-5347(02)00045-9).
- Callaway, R.M. 1995. Positive interactions among plants. *The Botanical Review* 61, 306–49. <https://doi.org/10.1007/BF02912621>.
- Camacho Altamirano, J.M. 2007. Efecto del fuego sobre la lluvia de semillas en la Reserva Ecológica del Pedregal de San Ángel, México D.F. B.Sc. Thesis, Universidad Nacional Autónoma de México, Mexico City.

Cano-Santana, Z. 1994. Flujo de energía a través de *Sphenarium purpurascens* (Orthoptera: Acrididae) y productividad primaria neta aérea en una comunidad xerófita. Ph.D. Dissertation, Universidad Nacional Autónoma de México, Mexico City.

Cano-Santana, Z., Meave, J. 1996. Sucesión secundaria en derrames volcánicos: el caso del Xitle. Ciencias 41, 58–68.

Cano-Santana, Z., Pisanty, I., Segura, S., Mendoza-Hernández, P.E., León-Rico, R., Soberón, J., Tovar, E., Martínez-Romero, E., Ruiz, L.C., Martínez-Balleste, A. 2006. Ecología, conservación, restauración y manejo de las áreas naturales y protegidas del pedregal del Xitle. In: Oyama, K., Castillo, A. (eds.) Manejo, conservación y restauración de recursos naturales en México: perspectivas desde la investigación científica, pp. 203–226. Universidad Nacional Autónoma de México/Siglo XXI, Mexico City.

Capon, S.J., Lynch, A.J.A., Bond, N., Chessman, B.C., Davis, J., Davidson, N., Finlayson, M., Gell, P.A., Hohnberg, D., Humphrey, C., Kingsford, R.T., Nielsen, D., Thomson, J.R., Ward, K., Mac Nally, R. 2015. Regime shifts, thresholds and multiple stable states in freshwater ecosystems; a critical appraisal of the evidence. *Science of the Total Environment* 534, 122–130.
<https://doi.org/10.1016/j.scitotenv.2015.02.045>

Carabias-Lillo, J., Meave del Castillo, J. 1987. La Reserva Ecológica del Pedregal de San Ángel. Potencial de investigación, docencia y difusión. *Información Científica y Tecnológica* 9, 16–19.

Castellanos Vargas, I., García Calderón, N.E., Cano Santana, Z. 2017. Procesos físicos del suelo en la Reserva Ecológica Del Pedregal de San Ángel de Ciudad Universitaria: atributos para su conservación. *Terra Latinoamericana* 35, 51–64. <https://doi.org/10.28940/terra.v35i1.241>.

Castillo-Argüero, S., Martínez-Orea, Y., Meave, J.A., Hernández-Apolinar, M., Núñez-Castillo, O., Santibáñez-Andrade, G., Guadarrama-Chávez, P. 2009. Flora: susceptibilidad de la comunidad a la invasión de malezas nativas y exóticas. In: Lot, A., Cano-Santana, Z. (eds.), *Biodiversidad del Ecosistema del Pedregal de San Ángel*, pp. 107–133. Universidad Nacional Autónoma de

México, Mexico City.

Castillo-Argüero S., Martínez-Orea, Y., Romero-Romero, M.A., Guadarrama-Chávez, P., Núñez-Castillo, O., Sánchez- Gallén, I., Meave, J.A. 2007. La reserva ecológica del Pedregal de San Ángel: aspectos florísticos y ecológicos. Universidad Nacional Autónoma de México, Mexico City.

Castillo-Argüero, S., Montes-Cartas, G., Romero-Romero, M.A., Martínez-Orea, Y., Guadarrama-Chávez, P., Sánchez-Gallén, I., Núñez-Castillo, O. 2004. Dinámica y conservación de la flora del matorral xerófilo de la Reserva Ecológica del Pedregal de San Ángel (D. F., México). *Botanical Sciences*, 74, 51–75. <https://doi.org/10.17129/botsci.1686>

Clements, F.E., 1916. Plant succession. An analysis of the development of vegetation. Carnegie Institution of Washington, Publication Number 242, Washington, D. C.

CONABIO [Mexican Biodiversity Commission]. Vecinos verdes, árboles comunes de las ciudades: Tepozán, Tepozán blanco, Axixcuáhuitl, *Buddleja cordata*. In: <https://www.biodiversidad.gob.mx/Difusion/cienciaCiudadana/aurbanos/ficha.php?item=Buddleja%20cordata> (last accessed on March 24, 2022.)

Contreras-Julio, D., Aguirre, P., Mujica, J., Vasilieva, O. 2020. Finding strategies to regulate propagation and containment of dengue via invariant manifold analysis. *SIAM Journal on Applied Dynamical Systems* 19, 1392–1437. <https://doi.org/10.1137/20M131299X>.

Corkidi, L., Cacho, S., Burquez, A. 1991. Dispersión del pirú (*Schinus molle* L., Anacardiaceae) por aves en Teotihuacán, México. *Acta Botanica Mexicana*, 15, 17–22. <https://doi.org/10.21829/abm15.1991.617>

Dakos, V. 2018. Identifying best-indicator species for abrupt transitions in multispecies communities. *Ecological Indicators* 94, 494–502. <https://doi.org/10.1016/j.ecolind.2017.10.024>.

Dakos, V., van Nes, E.H., Donangelo, R., Fort, H., Scheffer, M. 2010. Spatial correlation as leading indicator of catastrophic shifts. *Theoretical Ecology* 3, 163–74. <https://doi.org/10.1007/s12080-010-9111-0>

- Dakos, V., van Nes, E.H., D'Odorico, P., Scheffer, M. 2012. Robustness of variance and autocorrelation as indicators of critical slowing down. *Ecology* 93 264–271
<https://doi.org/10.1890/11-0889.1>
- de Bauer, M., Hernández-Tejeda, T. 2007. A review of ozone-induced effects on the forests of central Mexico. *Environmental Pollution* 147, 446–453. <https://doi.org/10.1016/j.envpol.2006.12.020>
- Espinosa-García, F.J. 1996. Revisión sobre la alelopatía de *Eucalyptus* L'Herit. *Botanical Sciences*, 58, 55–74. <https://doi.org/10.17129/botsci.1487>.
- Farfán Beltrán, M.E. 2016. Estructura de la comunidad de artrópodos en sitios conservados, perturbados y sujetos a restauración ecológica en el Pedregal de San Ángel, D.F., México. B.Sc. Thesis, Universidad Nacional Autónoma de México, Mexico City.
- Figueroa-Castro, D.M., Cano-Santana, Z., Camacho-Castillo, E. 1998. Producción de estructuras reproductivas y fenología reproductiva de cinco especies de compuestas en una comunidad xerófita. *Botanical Sciences* 63, 67–74. <https://doi.org/10.17129/botsci.1568>
- Flores Vázquez, J.C. 2004. Estudio demográfico del Tepozán (*Buddleia cordata* Kunth) en el Ajusco Medio. Universidad Nacional Autónoma de México, Mexico City.
- Gaertner, M., Biggs, R., Te Beest, M., Hui, C., Molofsky, J., Richardson, D.M. 2014. Invasive plants as drivers of regime shifts: identifying high-priority invaders that alter feedback relationships. *Diversity and Distributions* 20, 733–744. <https://doi.org/10.1111/ddi.12182>
- Gaertner, M., Holmes, P.M., Richardson, D.M. 2012. Biological invasions, resilience and Restoration. in: van Andel, J., Aronson, J. (eds.) *Restoration ecology: the new frontier*, 2nd ed., pp. 265–280. Wiley-Blackwell. <https://doi.org/10.1002/9781118223130.ch20>
- Gause, G.F. 1932. Experimental studies on the struggle for existence : I. Mixed population of two species of yeast. *Journal of Experimental Biology* 9, 389–402.
<https://doi.org/10.1242/jeb.9.4.389>

GODF [Gaceta Oficial del Distrito Federal]. 2006. Acuerdo por el que se aprueba el Programa de Manejo del Área de Valor Ambiental del Distrito Federal, con la categoría de Bosque Urbano denominada “Bosque de Chapultepec”, November 17, 2006, pp. 5–32.

Gunderson, L.H. 2000. Ecological resilience-In theory and application. *Annual Review of Ecology and Systematics*. 31, 425-439. <https://doi.org/10.1146/annurev.ecolsys.31.1.425>

Guttal, V., Jayaprakash, C. 2008. Changing skewness: an early warning signal of regime shifts in ecosystems. *Ecology Letters* 11, 450–60. <https://doi.org/10.1111/j.1461-0248.2008.01160.x>.

Hernández Islas, J.L. 1984. Variación estacional del contenido de semillas del suelo, en tres habitats de la comunidad de *Senecio praecox*, (Pedregal de San Angel, Mexico, D.F.). B.Sc. Thesis, Universidad Nacional Autónoma de México, Mexico City.

Holling, C.S. 1973. Resilience and stability of ecological systems. *Annual Review of Ecology and Systematics* 4: 1–23. <https://doi.org/10.1146/annurev.es.04.110173.000245>

Hutchinson, G.E. 1961. The paradox of the plankton. *The American Naturalist* 95, 137–145.
<https://www.jstor.org/stable/2458386>

Jones, C.G., Lawton, J.H., Shachak, M. 1994. Organisms as ecosystem engineers. *Oikos* 69, 373–386. <https://doi.org/10.2307/3545850>

Kéfi, S., Dakos, V., Scheffer, M., Van Nes, E.H., Rietkerk, M. 2013. Early warning signals also precede non-catastrophic transitions. *Oikos* 122, 641–48. <https://doi.org/10.1111/j.1600-0706.2012.20838.x>

Kéfi, S., Guttal, V., Brock, W.A., Carpenter, S.R., Ellison, A.M., Livina, V.M., Seekell, D.A., Scheffer, M., Van Nes, E.H., Dakos, V. 2014. Early warning signals of ecological transitions: methods for spatial patterns. *PLoS ONE* 9, e92097.
<https://doi.org/10.1371/journal.pone.0092097>

Krauskopf B., Osinga H.M. 2007. Computing invariant manifolds via the continuation of orbit segments. In: Krauskopf, B., Osinga, H.M., Galán-Vioque, J. (eds.) *Numerical Continuation*

Methods for Dynamical Systems. Understanding Complex Systems. Springer.

https://doi.org/10.1007/978-1-4020-6356-5_4

Lin, Y., Berger, U., Grimm, V., Ji, Q-R. 2012. Differences between symmetric and asymmetric facilitation matter: exploring the interplay between modes of positive and negative plant interactions. *Journal of Ecology* 100, 1482–1491. <https://doi.org/10.1111/j.1365-2745.2012.02019.x>

Lot, A., Cano-Santana, Z. (eds.) .2009. Biodiversidad del Ecosistema del Pedregal de San Ángel. Universidad Nacional Autónoma de México, Mexico City.

Lotka, A.J. 1925. Elements of physical biology. Williams & Wilkins.

Martínez Mateos, A.E. 2001. Regeneración natural después de un disturbio por fuego en dos microambientes contrastantes de la Reserva Ecológica “El Pedregal de San Ángel”. B.Sc. Thesis, Universidad Nacional Autónoma de México, Mexico City.

Martínez-Orea, Y., Castillo Argüero, S., Guadarrama-Chávez, M., Sánchez, I. 2010. Post-fire seed bank in a xerophytic shrubland. *Botanical Sciences* 86, 11–21.

<https://doi.org/10.17129/botsci.2316>.

Martínez-Orea, Y., Castillo-Argüero, S., Hernández-Apolinar, M., Guadarrama-Chávez, M.P., Orozco-Segovia, A. 2012. Seed rain after a fire in a xerophytic shrubland. *Revista Mexicana de Biodiversidad* 83, 447–457. <https://doi.org/10.22201/ib.20078706e.2012.2.971>.

May, R.M. 1973. Stability and Complexity in Models Systems. Princeton University Press.

May, M., Leonard, W.J. 1975. Nonlinear aspects of competition between three species. SIAM Journal on Applied Mathematics 29, 243–253. <https://doi.org/10.1137/0129022>

Meave, J., Carabias, J., Arriaga, V, Valiente-Banuet, A. 1994. Observaciones fenológicas en el Pedregal de San Ángel. In: Rojo, A. (ed.) Reserva ecológica El Pedregal de San Ángel: ecología, historia natural y manejo, pp. 91–105. Universidad Nacional Autónoma de México, Mexico City.

Meave. J.A., Ibarra-Manríquez, G., Larson-Guerra, J. 2016. Vegetación: panorama histórico, rasgos generales y patrones de pérdida. In: Moncaya Maya, J.O., López López A. (eds.). Geografía de México: una reflexión espacial contemporánea, pp. 216–234, Universidad Nacional Autónoma de México, Mexico City.

Mendoza Hernández, P.E. 2003. El Tepozán. Ciencias 70, 32-33.

Mendoza Hernández, P.E. 2002. Sobrevivencia y crecimiento de los estadios iniciales de *Buddleia cordata* (tepozán) en ambientes contrastantes del Ajusco Medio, D.F. México. M.Sc. Thesis, Universidad Nacional Autónoma de México, Mexico City.

Mendoza-Hernández, P., A. Orozco-Segovia, J. Meave, T. Valverde, M. Martinez-Ramos. 2013.

Vegetation recovery and plant facilitation in a human-disturbed lava field in a megacity: Searching tools for ecosystem restoration. Plant Ecology 2014: 153–167.

<http://doi.org/10.1007/s11258-012-0153-y>

Mohd, M.H. 2019. Diversity in interaction strength promotes rich dynamical behaviours in a three-species scological system. Applied Mathematics and Computation 353, 243–253.

<https://doi.org/10.1016/j.amc.2019.02.007>

Nazarimehr, F., Jafari, S., Golpayegani, S.M.R.H., Perc, M., Sprott, J.C. 2018. Predicting tipping points of dynamical systems during a period-doubling route to chaos. Chaos 28, 073102.
<https://doi.org/10.1063/1.5038801>.

Olvera Carrillo, Y. 2001. Estudio ecofisiológico de la germinación, sobrevivencia y crecimiento de *Opuntia tomentosa* S.D. en la Reserva del Pedregal de San Ángel. B.Sc. Thesis. Universidad Nacional Autónoma de México, Mexico City.

Peralta Higuera, A., Prado Molina J. 2009. Los límites y la cartografía. In: Lot, A., Cano-Santana, Z. (eds.), Biodiversidad del Ecosistema del Pedregal de San Ángel, pp. 27–42. Universidad Nacional Autónoma de México, Mexico City.

Pérez Ishiwarra, J.R. 2011. Reconstrucción de la historia de vida de *Pittocaulon praecox* con base en

- su morfología. M.Sc. Thesis, Universidad Nacional Autónoma de México, Mexico City.
- Peterson, G., Allen, C.R., Holling, C.S. 1998. Ecological resilience, biodiversity, and scale. *Ecosystems* 1, 6–18. <https://doi.org/10.1007/s100219900002>
- Ramírez-Albores, J.E., Badano, E.I. 2013. Perspectiva histórica, sociocultural y ecológica de una invasión biológica: el caso del Pirúl (*Schinus molle* L., Anacardiaceae) en México. *Boletín de la Red Latinoamericana para el Estudio de Especies Invasoras*, 3, 4–15.
- Rietkerk, M., Dekker, S.C., De Ruiter, P.C., Van De Koppel, J. 2004. Self-organized patchiness and catastrophic shifts in ecosystems. *Science* 305, 1926–1929.
<https://doi.org/10.1126/science.1101867>.
- Rodríguez de la Vega, H.R. 2003. Estructura poblacional y distribución espacial de *Senecio praecox* en el Ajusco Medio, D.F. Implicaciones para su reintroducción en sitios perturbados. B.Sc. Thesis. Universidad Nacional Autónoma de México, Mexico City.
- Ruiz Amaro, L.C.. 1996. Microsucesión bajo dos especies (*Sedum oxypetalum* y *Buddleia cordata*) indicadoras de distintos estadios serales en el Ajusco Medio. B.Sc. Thesis, Universidad Nacional Autónoma de México, Mexico City.
- Rzedowski, J. 1954. Vegetación del Pedregal de San Ángel. *Anales de la Escuela Nacional de Ciencias Biológicas*, Instituto Politécnico Nacional. 8, 59–129.
- Santibáñez-Andrade, G., Castillo-Argüero, S., Zavala-Hurtado, J.A., Martínez-Orea, Y., Hernández-Apolinar, M. 2009. La heterogeneidad ambiental en un matorral xerófilo. *Botanical Sciences* 85, 71–79. <https://doi.org/10.17129/botsci.2304>
- Santillán Carvantes, P. 2013. Efecto de plantas protectoras en el establecimiento clonal de *Sedum oxypetalum* en ambientes perturbados del Ajusco Medio, D. F. B.Sc. Thesis. Universidad Nacional Autónoma de México, Mexico City.
- Scheffer, M., Bascompte, J., Brock, W.A., Brovkin, V., Carpenter, S.R., Dakos, V., Held, H., van Nes, E.H., Rietkerk, M. Sugihara, G. 2009. Early-warning signals for critical transitions. *Nature*

- 461, 53–59. <https://doi.org/10.1038/nature08227>.
- Scheffer, M., Carpenter, S.R. 2003. Catastrophic regime shifts in ecosystems: linking theory to observation. *Trends in Ecology and Evolution* 18, 648–56.
<https://doi.org/10.1016/j.tree.2003.09.002>.
- Scheffer, M., Carpenter, S., Foley, J.A., Folke, C., Walker, B. 2001. Catastrophic shifts in ecosystems. *Nature* 413, 591–96. <https://doi.org/10.1038/35098000>
- Schuwirth, N., Borgwardt, F., Domisch, S., Friedrichs, M., Kattwinkel, M., Kneis, D., Kuemmerlen, M., Langhans, S.D., Martínez-López, J., Vermeiren, P. 2019. How to make ecological models useful for environmental management. *Ecological Modelling* 411, 108784.
<https://doi.org/10.1016/j.ecolmodel.2019.108784>.
- Segura-Burciaga, S. 1995. Estudio poblacional de *Eucaliptus resinifera* Smith. (Myrtaceae) en la reserva ecológica de El Pedregal de San Ángel, C.U., México D. F. B.Sc. Thesis. Universidad Nacional Autónoma de México, Mexico City.
- Segura-Burciaga, S. 2009. Introducción de especies: la invasión y el control de *Eucalyptus resinifera*. In: Lot, A., Cano-Santana, Z. (eds.), Biodiversidad del Ecosistema del Pedregal de San Ángel, pp. 533–538. Universidad Nacional Autónoma de México, Mexico City.
- Segura-Burciaga, S.G., Martínez-Ramos, M. 1994. La introducción de especies a comunidades naturales: el caso de *Eucalyptus resinifera* Smith. (Myrtaceae) en la Reserva “El Pedregal” de San Ángel. In: Rojo, A. (ed.) Reserva Ecológica El Pedregal de San Ángel: Ecología, Historia Natural y Manejo, pp. 177–186. Universidad Nacional Autónoma de México, Mexico City.
- Segura-Burciaga, S., Meave, J. 2001. Effect of the removal of individuals of the exotic species *Eucalyptus resinifera* on the floristic composition of a protected xerophytic shrubland in southern Mexico City. In: Brundu, G., Brock, J., Camarda, I., Child, L. Wade, M. (eds.). Plant invasions: species ecology and ecosystem management, pp. 319–330. Backhuys Publishers.
- Shrestha, N., Xu, X., Meng, J., Wang, Z. 2021. Vulnerabilities of protected lands in the face of

- climate and human footprint changes. *Nature Communications* 12, 1632.
<https://doi.org/10.1038/s41467-021-21914-w>.
- Siebe, C. 2009. La erupción del volcán Xitle y las lavas del Pedregal hace 1670 +/- 35 años AP y sus implicaciones. In: Lot, A., Cano-Santana, Z. (eds.), *Biodiversidad del Ecosistema del Pedregal de San Ángel*, pp. 43–49. Universidad Nacional Autónoma de México, Mexico City.
- Soberón-M., J., de la Cruz-Rosas M., Jiménez-C., G. 1991. Ecología hipotética de la Reserva del Pedregal de San Ángel. *Ciencia y Desarrollo* 99, 25–38.
- Suding, K.N., Hobbs, R.J. 2009. Threshold models in restoration and conservation: a developing framework. *Trends in Ecology & Evolution* 24, 271–79.
<https://doi.org/10.1016/j.tree.2008.11.012>
- Tansley, A.G. 1935. The use and abuse of vegetational concepts and terms. *Ecology* 16, 284–307.
<https://doi.org/10.2307/1930070>
- Valiente-Banuet, A., Verdú, M. 2007. Facilitation can increase the phylogenetic diversity of plant communities. *Ecology Letters* 10, 1029–1036. <https://doi.org/10.1111/j.1461-0248.2007.01100.x>
- Valladares, F., Zaragoza-Castells, J., Sánchez-Gómez, D., Matesanz, S., Alonso, B., Portsmuth, A., Delgado, A., Atkin, O.K. (2008). Is shade beneficial for Mediterranean shrubs experiencing periods of extreme drought and late-winter frosts? *Annals of Botany*, 102, 923–933.
<https://doi.org/10.1093/aob/mcn182>
- Valverde, T., Chávez, V.M. 2009. *Mammillaria* (Cactaceae) como indicadora del estado de conservación del ecosistema. In: Lot, A., Cano-Santana, Z. (eds.), *Biodiversidad del Ecosistema del Pedregal de San Ángel*, pp. 497–507. Universidad Nacional Autónoma de México, Mexico City.
- van Nes, E.H., Scheffer, M. 2007. Slow recovery from perturbations as a generic indicator of a nearby catastrophic shift. *American Naturalist* 169, 738–47. <https://doi.org/10.1086/516845>

- Venter, O., Sanderson, E.W., Magrach, A., Allan, J.R., Beher, J., Jones, K.R., Possingham, H.P., Laurance, W.F., Wood, P., Fekete, B.M., Levy, M.A., Watson, J.E.M. 2016. Sixteen years of change in the global terrestrial human footprint and implications for biodiversity conservation. *Nature Communications* 7, 12558. <https://doi.org/10.1038/ncomms12558>.
- Volterra, V. 1928. Variations and fluctuations of the number of individuals in animal species living together. *Conseil Permanent International Pour l'Exploration de La Mer - Journal du Conseil* 3, 3–51.
- Whittaker, R.H., Levin, S.A. 1977. The role of mosaic phenomena in natural communities. *Theoretical Population Biology* 12, 117–139. [https://doi.org/10.1016/0040-5809\(77\)90039-9](https://doi.org/10.1016/0040-5809(77)90039-9)
- Williams, B.A., Venter, O., Allan, J.R., Atkinson, S.C., Rehbein, J.A., Ward, M., Di Marco, M., Grantham, H.S., Ervin, J., Goetz, S.J., Hansen, A.J., Jantz, P., Pillay, R., Rodríguez-Buriticá, S., Supples, C., Virnig, A.L.S., Watson, J.E.M., 2020. Change in terrestrial human footprint drives continued loss of intact ecosystems. *One Earth* 3(3): 371–82.
<https://doi.org/10.1016/j.oneear.2020.08.009>.

Appendix A: Symbolic stability analysis

To simplify the notation, in this section we assume $x_1(t) = \text{BS}(t)$, $x_2(t) = \text{PS}(t)$, $x_3(t) = \text{SL}(t)$, $\alpha_1 = \alpha_{\text{BS}}$, $\alpha_2 = \alpha_{\text{PS}}$, $\beta_1 = \beta_{\text{BS}}$, $\beta_2 = \beta_{\text{PS}}$ and $\gamma = \gamma_{\text{BP}}$

Model I-A: negative interactions between native species

We start with the system of equations

$$\left\{ \begin{array}{l} \frac{d\text{BS}}{dt} = (\alpha_{\text{BS}}(\text{BS})(\text{SL})) - \beta_{\text{BS}}\text{BS} \end{array} \right. \quad (1)$$

$$\left\{ \begin{array}{l} \frac{d\text{PS}}{dt} = \frac{\alpha_{\text{PS}}(\text{PS})(\text{SL})}{1 + \gamma_{\text{BP}}(\text{BS})} - \beta_{\text{PS}}(\text{PS}) \end{array} \right. \quad (2)$$

$$\left\{ \begin{array}{l} \frac{d\text{SL}}{dt} = -\left(\alpha_{\text{BS}}(\text{BS})(\text{SL}) + \frac{\alpha_{\text{PS}}(\text{PS})(\text{SL})}{1 + \gamma_{\text{BP}}(\text{BS})} \right) + \beta_{\text{BS}}(\text{BS}) + \beta_{\text{PS}}(\text{PS}) \end{array} \right. \quad (3)$$

where $x_1(t) = \text{BS}(t)$, $x_2(t) = \text{PS}(t)$, $x_3(t) = \text{SL}(t)$, $\alpha_1 = \alpha_{\text{BS}}$, $\alpha_2 = \alpha_{\text{PS}}$, $\beta_1 = \beta_{\text{BS}}$, $\beta_2 = \beta_{\text{PS}}$ and $\gamma = \gamma_{\text{BP}}$.

Vector (x_1, x_2, x_3) is an equilibrium of system (1)-(3) if and only if it satisfies:

$$\left\{ \begin{array}{l} [\alpha_1 x_3 - \beta_1] x_1 = 0 \end{array} \right. \quad (5)$$

$$\left\{ \begin{array}{l} [\alpha_2 x_3 - \beta_2(1 + \gamma x_1)] x_2 = 0 \end{array} \right. \quad (6)$$

$$\left\{ \begin{array}{l} (1 + \gamma x_1)[\beta_1 x_1 + \beta_2 x_2] - [\alpha_1 x_1(1 + \gamma x_1) + \alpha_2 x_2] x_3 = 0 \end{array} \right. \quad (7)$$

This system has a trivial equilibrium at $(0, 0, 0)$, and three additional cases:

- If $x_1 = 0$, then $(0, x_2, x_3)$ is an equilibrium point of (1)-(3) if and only if following equations are satisfied:

$$\left\{ \begin{array}{l} [\beta_2 - \alpha_2 x_3] x_2 = 0 \end{array} \right. \quad (8)$$

$$\left\{ \begin{array}{l} [\beta_2 - \alpha_2 x_3] x_2 = 0 \end{array} \right. \quad (9)$$

Noting that (8) and (9) are the same equation, thus, any point of the form $(0, 0, x_3)$ is an equilibrium point of the system. Further, if $x_2 > 0$, then any point of the form $\left(0, x_2, \frac{\beta_2}{\alpha_2}\right)$ is an equilibrium point of the system (1)-(3).

- If $x_1 > 0$, then (x_1, x_2, x_3) is an equilibrium point of the system (1)-(3) if and only if the following equations are satisfied:

$$\left\{ \begin{array}{l} [\alpha_1 x_3 - \beta_1] x_1 = 0 \\ [\alpha_2 x_3 - \beta_2(1 + \gamma x_1)] x_2 = 0 \end{array} \right. \quad (10)$$

$$\left\{ \begin{array}{l} [\alpha_2 x_3 - \beta_2(1 + \gamma x_1)] x_2 = 0 \\ [\beta_1 x_1 + \beta_2 x_2 - \alpha_1 x_1 x_3](1 + \gamma x_1) - \alpha_2 x_2 x_3 = 0 \end{array} \right. \quad (11)$$

$$\left\{ \begin{array}{l} [\beta_1 x_1 + \beta_2 x_2 - \alpha_1 x_1 x_3](1 + \gamma x_1) - \alpha_2 x_2 x_3 = 0 \end{array} \right. \quad (12)$$

From (10) we obtain

$$x_3 = \frac{\beta_1}{\alpha_1} \quad (13)$$

Substituting (13) in (11) and (12), we obtain a new system of equations:

$$\left\{ \begin{array}{l} \left[\frac{\alpha_2 \beta_1}{\alpha_1} - \beta_2(1 + \gamma x_1) \right] x_2 = 0 \end{array} \right. \quad (14)$$

$$\left\{ \begin{array}{l} \left[\beta_2(1 + \gamma x_1) - \frac{\alpha_2 \beta_1}{\alpha_1} \right] x_2 = 0 \end{array} \right. \quad (15)$$

From (14) and (15) we get that any point of the form:

$$\left(x_1, 0, \frac{\beta_1}{\alpha_1} \right)$$

is an equilibrium point of (1)-(3). On the other hand, if $x_1 = \frac{\alpha_2 \beta_1 - \alpha_1 \beta_2}{\alpha_1 \beta_2 \gamma}$, then (1)-(3) has an infinite number of equilibrium points, of the form:

$$\left(\frac{\alpha_2 \beta_1 - \alpha_1 \beta_2}{\alpha_1 \beta_2 \gamma}, x_2, \frac{\beta_1}{\alpha_1} \right)$$

Summary of the equilibrium points of model 1-A

The dynamical system (1)-(3) has the following equilibrium solutions:

1. Equilibrium sets of the form $(0, 0, x_3)$, $x_3 \geq 0$.

2. Equilibrium sets of the form $\left(0, x_2, \frac{\beta_2}{\alpha_2} \right)$, $x_2 > 0$.

3. Equilibrium sets of the form $\left(x_1, 0, \frac{\beta_1}{\alpha_1} \right)$, $x_1 > 0$.

$$4. \text{ Equilibrium sets of the form } \left(\frac{\alpha_2\beta_1 - \alpha_1\beta_2}{\alpha_1\beta_2\gamma}, x_2, \frac{\beta_1}{\alpha_1} \right), x_2 > 0.$$

Note that, in general, the equilibrium sets of cases 1, 2 and 3 are always non-negative, while case 4 is negative if and only if $\alpha_2\beta_1 > \alpha_1\beta_2$. Note also that case 1 corresponds to an "extinction" case, while case 4 corresponds to "coexistence", if condition $\alpha_2\beta_1 > \alpha_1\beta_2$ is satisfied. In case 2 only x_2 survives, while in case 3 only x_1 survives. In the following section we will study the stability of these equilibrium points.

Stability of equilibrium points of model I-A

Given the conservation equations in (4), we showed that one of the equations (1)-(3) can always be written as a function of the other two - in which case, however, the determinant of the Jacobian Matrix would always be 0, and therefore we would not be able to use the typical stability criteria. However, note that in each case we have a vector space of dimension 1 with equilibrium solutions. Thus, if the equilibrium point is stable in the orthogonal coordinates to that line, then the close orbits will converge to a point in this vector space. Thus, we do not have stable equilibria, but instead whole line segments that can be either attracting or repelling. Therefore, instead of focusing on the equilibrium points, we will focus on those segments.

For system (1)-(3) we have the Jacobian matrix

$$J(x_1, x_2, x_3) = \begin{pmatrix} \alpha_1x_3 - \beta_1 & 0 & \alpha_1x_1 \\ -\frac{\alpha_2\gamma x_2 x_3}{(1 + \gamma x_1)^2} & \frac{\alpha_2 x_3}{1 + \gamma x_1} - \beta_2 & \frac{\alpha_2 x_2}{1 + \gamma x_1} \\ \frac{\alpha_2\gamma x_2 x_3}{(1 + \gamma x_1)^2} + \beta_1 - \alpha_1 x_3 & \beta_2 - \frac{\alpha_2 x_3}{1 + \gamma x_1} & -\left(\alpha_1 x_1 + \frac{\alpha_2 x_2}{1 + \gamma x_1}\right) \end{pmatrix}$$

We will proceed now to a case-by-case analysis.

Case 1

We have:

$$J(0, 0, x_3) = \begin{pmatrix} \alpha_1 x_3 - \beta_1 & 0 & 0 \\ 0 & \alpha_2 x_3 - \beta_2 & 0 \\ \beta_1 - \alpha_1 x_3 & \beta_2 - \alpha_2 x_3 & 0 \end{pmatrix}$$

This matrix has eigenvalues of the form $\lambda_1 = \alpha_1 x_3 - \beta_1$, $\lambda_2 = \alpha_2 x_3 - \beta_2$ and $\lambda_3 = 0$. The corresponding eigenspaces are

$$E_1 = \text{Span}\langle(1, 0, -1)\rangle, \quad E_2 = \text{Span}\langle(0, 1, -1)\rangle, \quad E_3 = \text{Span}\langle(0, 0, 1)\rangle$$

Note that $\lambda_1 < 0$ if and only if $\alpha_1 x_3 < \beta_1$, while $\lambda_2 < 0$ if and only if $\alpha_2 x_3 < \beta_2$. Thus, we have the attracting object

$$W_1 = W^s = \left\{ (0, 0, x_3) : 0 \leq x_3 < \min \left\{ \frac{\beta_1}{\alpha_1}, \frac{\beta_2}{\alpha_2} \right\} \right\}$$

and the repelling object

$$W^u = \left\{ (0, 0, x_3) : x_3 > \max \left\{ \frac{\beta_1}{\alpha_1}, \frac{\beta_2}{\alpha_2} \right\} \right\}$$

Case 2

In this case we have:

$$J\left(0, x_2, \frac{\beta_2}{\alpha_2}\right) = \begin{pmatrix} \frac{\alpha_1\beta_2 - \alpha_2\beta_1}{\alpha_2} & 0 & 0 \\ -\gamma\beta_2 x_2 & 0 & \alpha_2 x_2 \\ \beta_2\gamma x_2 + \frac{\alpha_2\beta_1 - \alpha_1\beta_2}{\alpha_2} & 0 & -\alpha_2 x_2 \end{pmatrix}$$

The eigenvalues of this matrix are $\lambda_1 = \frac{\alpha_1\beta_2 - \alpha_2\beta_1}{\alpha_2}$, $\lambda_2 = 0$ and $\lambda_3 = -\alpha_2 x_2$, with the corresponding eigenspaces

$$E_1 = \text{Span} \left\langle \left(\frac{\alpha_2^2 x_2 + \alpha_1\beta_2 - \alpha_2\beta_1}{\alpha_2}, -(\gamma\beta_2 + \alpha_2), -\left[\frac{\alpha_2^2 x_2 + \alpha_1\beta_2 - \alpha_2\beta_1}{\alpha_2} - \gamma\beta_2 - \alpha_2 \right] \right) \right\rangle, \quad E_2 = \text{Span} \langle 0, 1, 0 \rangle, \quad E_3 = \text{Span} \langle (0, 1, -1) \rangle$$

Note that $\lambda_3 < 0$ for any $x_2 > 0$. On the other hand, λ_1 does not depend on x_2 , and therefore in this case we have the attracting object:

$$W_2 = \left\{ \left(0, x_2, \frac{\beta_2}{\alpha_2} \right) : x_2 > 0 \right\}$$

if and only if $\alpha_1\beta_2 < \alpha_2\beta_1$.

Case 3

Here we have:

$$J\left(x_1, 0, \frac{\beta_1}{\alpha_1}\right) = \begin{pmatrix} 0 & 0 & \alpha_1 x_1 \\ 0 & \frac{\alpha_2 \beta_1}{\alpha_1(1 + \gamma x_1)} - \beta_1 & 0 \\ 0 & \beta_2 - \frac{\alpha_2 \beta_1}{\alpha_1(1 + \gamma x_1)} & -\alpha_1 x_1 \end{pmatrix}$$

This matrix has eigenvalues $\lambda_1 = 0$, $\lambda_2 = \frac{\alpha_2 \beta_1}{\alpha_1(1 + \gamma x_1)} - \beta_1$, $\lambda_3 = -\alpha_1 x_1$, with

$$E_1 = \text{Span}\langle(1, 0, 0)\rangle, \quad E_2 = \text{Span}\left\langle\left(\alpha_1 x_1, \frac{\alpha_2 \beta_1}{\alpha_1(1 + \gamma x_1)} - \beta_1 - \alpha_1 x_1, \frac{\alpha_2 \beta_1}{\alpha_1(1 + \gamma x_1)} - \beta_1\right)\right\rangle, \quad E_3 = \text{Span}\langle(1, 0, -1)\rangle$$

respectively. Note that $\lambda_3 < 0$ for any $x_1 > 0$. On the other hand, $\lambda_2 < 0$ if and only if $x_1 > \frac{\alpha_2 - \alpha_1}{\alpha_1 \gamma}$. Thus, the object

$$W_3 = \left\{ \left(x_1, 0, \frac{\beta_1}{\alpha_1}\right) : x_1 > \max \left\{ 0, \frac{\alpha_2 - \alpha_1}{\alpha_1 \gamma} \right\} \right\}$$

is always an attractor.

Case 4

For this case we have:

$$J\left(\frac{\alpha_2 \beta_1 - \alpha_1 \beta_2}{\alpha_1 \beta_2 \gamma}, x_2, \frac{\beta_1}{\alpha_1}\right) = \begin{pmatrix} 0 & 0 & \frac{\alpha_2 \beta_1 - \alpha_1 \beta_2}{\beta_2 \gamma} \\ \frac{\alpha_1 \beta_2^2 \gamma x_2}{\alpha_2 \beta_1} & 0 & \frac{\alpha_1 \beta_2 x_2}{\beta_1} \\ -\frac{\alpha_1 \beta_2^2 \gamma x_2}{\alpha_2 \beta_1} & 0 & -\left(\frac{\alpha_2 \beta_1 - \alpha_1 \beta_2}{\beta_2 \gamma} + \frac{\alpha_1 \beta_2 x_2}{\beta_1}\right) \end{pmatrix}$$

Here, one of the eigenvalues is $\lambda_2 = 0$. Defining

$$A = \frac{\alpha_1 \beta_2 x_2}{\beta_1}, \quad B = \frac{\alpha_2 \beta_1 - \alpha_1 \beta_2}{\beta_2 \gamma}$$

we obtain the other two eigenvalues as:

$$\lambda_{1/3} = \frac{-(B+A) \pm \sqrt{(B+A)^2 - \frac{4AB\beta_2\gamma}{\alpha_2}}}{2}$$

Note that in this case the eigenvalues can be complex whenever

$$(B+A)^2 < \frac{4AB\beta_2\gamma}{\alpha_2}$$

Defining

$$C = \frac{\alpha_1\beta_1}{\beta_2} B \left[1 - \frac{2\beta_2\gamma}{\alpha_2} \right]$$

is equivalent to

$$\frac{\alpha_1^2\beta_2^2}{\beta_1^2} x_2^2 - 2Cx_2 + B^2 < 0 \quad (16)$$

This is only possible if

$$\frac{\beta_2^2}{\beta_1^2} + \frac{2\beta_2\gamma}{\alpha_2} < 1 \quad (17)$$

Thus, if (17) and (16) are satisfied then

$$E_- = \left[C - \sqrt{C^2 - \frac{\alpha_1^2\beta_2^2}{\beta_1^2} B^2} \right] \frac{\beta_1^2}{\alpha_1^2\beta_2^2} < x_2 < \left[C + \sqrt{C^2 - \frac{\alpha_1^2\beta_2^2}{\beta_1^2} B^2} \right] \frac{\beta_1^2}{\alpha_1^2\beta_2^2} = E_+ \quad (18)$$

Thus, if (18), $\operatorname{Re}(\lambda_1) < 0$ and $\operatorname{Re}(\lambda_3) < 0$ simultaneously if and only if $B > -A$, i.e., if

$$x_2 > \frac{(\alpha_1\beta_2 - \alpha_2\beta_1)\beta_1}{\alpha_1\beta_2^2\gamma} \quad (19)$$

Note that for the equilibrium points to be non-negative, we require that $\alpha_1\beta_2 \leq \alpha_2\beta_1$ is satisfied, and therefore, verification of (19) is trivial.

On the other hand, if λ_1, λ_3 are real values, i.e., (17) or $x_2 < I_-$ or $x_2 > I_+$ are not satisfied, then $\lambda_1 < 0$ and $\lambda_2 < 0$ simultaneously if and only if

$$-(B + A) + \sqrt{(B + A)^2 - \frac{4AB\beta_2\gamma}{\alpha_2}} < 0$$

This implies that $(B + A) > 0$. Thus, algebraically re-arranging the expression above, we obtain the equivalent expression

$$\frac{4AB\beta_2\gamma}{\alpha_2} > 0$$

Given that $A > 0$, it follows that $\lambda_1 < 0$ and $\lambda_3 < 0$ simultaneously if and only if $B > 0$, which is equivalent to $\alpha_2\beta_1 > \alpha_1\beta_2$, which is not in conflict with the non-negativity of the equilibrium points.

Using a similar reasoning, it can be shown that both eigenvalues cannot be simultaneously positive.

Recall that these equilibrium points are non-negative if and only if $\alpha_2\beta_1 > \alpha_1\beta_2$, and therefore

$$\frac{\beta_1(\alpha_1\beta_2 - \alpha_2\beta_1)}{\alpha_1\beta_2^2\gamma} < 0. \text{ Thus, defining}$$

$$W_c^s = \begin{cases} \left\{ \left(\frac{\alpha_2\beta_1 - \alpha_1\beta_2}{\alpha_1\beta_2\gamma}, x_2, \frac{\beta_1}{\alpha_1} \right) : \max \{0, E_- \} < x_2 < E_+ \right\} & \text{if (17) holds} \\ \emptyset & \text{otherwise} \end{cases}$$

and

$$W_r^s = \begin{cases} \left\{ \left(\frac{\alpha_2\beta_1 - \alpha_1\beta_2}{\alpha_1\beta_2\gamma}, x_2, \frac{\beta_1}{\alpha_1} \right) : \max \{E_+, 0 \} < x_2 \quad \text{or} \quad 0 < x_2 < E_- \right\} & \text{if (17) holds and } \alpha_2\beta_1 > \alpha_1\beta_2 \\ \left\{ \left(\frac{\alpha_2\beta_1 - \alpha_1\beta_2}{\alpha_1\beta_2\gamma}, x_2, \frac{\beta_1}{\alpha_1} \right) : 0 < x_2 \right\} & \text{if (17) is false and } \alpha_2\beta_1 > \alpha_1\beta_2 \\ \emptyset & \text{if } \alpha_2\beta_1 = \alpha_1\beta_2 \end{cases}$$

then:

$$W_4 = W_c^s \cup W_r^s = \begin{cases} \left\{ \left(\frac{\alpha_2\beta_1 - \alpha_1\beta_2}{\alpha_1\beta_2\gamma}, x_2, \frac{\beta_1}{\alpha_1} \right) : x_2 > 0 \quad \text{and} \quad x_2 \neq E_- \quad \text{and} \quad x_2 \neq E_+ \right\} & \text{if (17) holds} \\ \left\{ \left(\frac{\alpha_2\beta_1 - \alpha_1\beta_2}{\alpha_1\beta_2\gamma}, x_2, \frac{\beta_1}{\alpha_1} \right) : x_2 > 0 \right\} & \text{otherwise} \end{cases}$$

is an attractor if and only if $\alpha_2\beta_1 > \alpha_1\beta_2$, while there are no repelling objects.

Summary of stability of model I-A

The conditions for stability can be summarized as follows:

1. In case 1, object $W_1 = \left\{ (0, 0, x_3) : 0 \leq x_3 < \min \left\{ \frac{\beta_1}{\alpha_1}, \frac{\beta_2}{\alpha_2} \right\} \right\}$ is always an attractor, while

$W^u = \left\{ (0, 0, x_3) : x_3 > \max \left\{ \frac{\beta_1}{\alpha_1}, \frac{\beta_2}{\alpha_2} \right\} \right\}$ is a repeller.

2. In case 2, object $W_2 = \left\{ \left(0, x_2, \frac{\beta_2}{\alpha_2} \right) : x_2 > 0 \right\}$ is an attractor if and only if $\alpha_1\beta_2 < \alpha_2\beta_1$. There are no repelling objects.

3. In case 3, object $W_3 = \left\{ \left(x_1, 0, \frac{\beta_1}{\alpha_1} \right) : x_1 > \max \left\{ 0, \frac{\alpha_2 - \alpha_1}{\alpha_1\gamma} \right\} \right\}$ is always an attractor. There are no repelling objects.

4. In case 4, object $W_4 = W_c^s \cup W_r^s$ is an attractor, while there are no repelling objects. Furthermore, W_4 is non-empty in most of the cases in which the equilibrium points are non-negative.

As we can see, there is always multi-stability in this model. In particular, W_1 and W_3 are always attractors. If population sizes of x_1 and x_2 are sufficiently small, at least one of them will converge towards local extinction, but because W_2 and W_3 are infinitely close to the origin, it is not possible to know a priori which one(s) will go extinct, except perhaps studying x_3 . However, if $\alpha_2\beta_1 > \alpha_1\beta_2$, and (x_1, x_2, x_3) are sufficiently close to W_4 , then there will be coexistence between both species.

Last, note that the fact that W_2 is an attractor implies that W_4 is non-empty, and thus, in this case we have a tri-stable scenario.

In general, any behaviour (coexistence, survival of one of the species and extinction) is possible.

Model I-B

Now let us consider the 2-species model with positive interactions given by:

$$\left\{ \begin{array}{l} \frac{dBS}{dt} = \alpha_{BS}(BS)(SL) - \beta_{BS}(BS) \\ \frac{dPS}{dt} = \alpha_{PS}(PS)(SL)(1 + \theta_{BP}(BS)) - \beta_{PS}(PS) \end{array} \right. \quad (20)$$

$$\left\{ \begin{array}{l} \frac{dPS}{dt} = \alpha_{PS}(PS)(SL)(1 + \theta_{BP}(BS)) - \beta_{PS}(PS) \\ \frac{dSL}{dt} = -(\alpha_{BS}(BS)(SL) + \alpha_{PS}(PS)(SL)(1 + \theta_{BP}(BS))) + (\beta_{BS}(BS) + \beta_{PS}(PS)) \end{array} \right. \quad (21)$$

$$\left\{ \begin{array}{l} \frac{dPS}{dt} = \alpha_{PS}(PS)(SL)(1 + \theta_{BP}(BS)) - \beta_{PS}(PS) \\ \frac{dSL}{dt} = -(\alpha_{BS}(BS)(SL) + \alpha_{PS}(PS)(SL)(1 + \theta_{BP}(BS))) + (\beta_{BS}(BS) + \beta_{PS}(PS)) \end{array} \right. \quad (22)$$

We will introduce the same notation as with model I-A, and additionally, we denote $\theta = \theta_{BP}$. This model can also be reduced to a 2D model, considering that also these the variables satisfy relation (4). Again,

we will omit this reduction to work with the 3-dimensional model. A point (x_1, x_2, x_3) is an equilibrium point of the system (20)-(22) if and only if:

$$\left\{ \begin{array}{l} [\alpha_1 x_3 - \beta_1] x_1 = 0 \end{array} \right. \quad (23)$$

$$\left\{ \begin{array}{l} [\alpha_2 x_3 (1 + \theta x_1) - \beta_2] x_2 = 0 \end{array} \right. \quad (24)$$

$$\left\{ \begin{array}{l} \beta_1 x_1 + \beta_2 x_2 - [\alpha_1 x_1 + \alpha_2 x_2 (1 + \theta x_1)] x_3 = 0 \end{array} \right. \quad (25)$$

which has a trivial solution $(0, 0, 0)$. Analogously to model I-A, we will consider two cases.

- If $x_1 = 0$, then we get the system of equations

$$\left\{ \begin{array}{l} [\alpha_2 x_3 - \beta_2] x_2 = 0 \\ [\beta_2 - \alpha_2 x_3] x_2 = 0 \end{array} \right.$$

which are, in fact, one single equation. Thus, if $x_2 = 0$, we obtain equilibrium points of the form $(0, 0, x_3)$, while if $x_2 > 0$, they are of the form $\left(0, x_2, \frac{\beta_2}{\alpha_2}\right)$.

- If $x_1 > 0$, then from equation (23) we obtain that $x_3 = \frac{\beta_1}{\alpha_1}$. Substituting this into equations (24) and (25), we obtain

$$\left[\frac{\alpha_2 \beta_1}{\alpha_1} (1 + \theta x_1) - \beta_2 \right] x_2 = 0$$

Thus, if $x_2 = 0$, then we obtain equilibrium points of the form $\left(x_1, 0, \frac{\beta_1}{\alpha_1}\right)$, while if $x_2 > 0$, the equilibrium points are of the form $\left(\frac{\alpha_1 \beta_2 - \alpha_2 \beta_1}{\alpha_2 \beta_1 \theta}, x_2, \frac{\beta_1}{\alpha_1}\right)$.

Summary of equilibrium points of model I-B

In conclusion, the equilibrium points of system (16)-(18) can have following forms:

1. Extinction $(0, 0, x_3)$, $x_3 \geq 0$.

2. Survival of *Palo loco* only $\left(0, x_2, \frac{\beta_2}{\alpha_2}\right)$, $x_2 > 0$.

3. Survival of *Tepozán* only $\left(x_1, 0, \frac{\beta_1}{\alpha_1}\right)$, $x_1 > 0$.

4. Stable coexistence $\left(\frac{\alpha_1\beta_2 - \alpha_2\beta_1}{\alpha_2\beta_1\theta}, x_2, \frac{\beta_1}{\alpha_1}\right)$, $x_2 > 0$.

In general, in cases 1, 2 and 3, the equilibrium points are always non-negative, while in case 4 the equilibrium point is non-negative if and only if $\alpha_1\beta_2 \geq \alpha_2\beta_1$.

Stability analysis

As with model I-A, we have neither stable or unstable equilibrium points, but instead attracting or repelling objects.

The Jacobian matrix of model I-A is given by

$$J(x_1, x_2, x_3) = \begin{pmatrix} \alpha_1x_3 - \beta_1 & 0 & \alpha_1x_1 \\ \alpha_2\theta x_2 x_3 & \alpha_2x_3(1 + \theta x_1) - \beta_2 & \alpha_2x_2(1 + \theta x_1) \\ \beta_1 - [\alpha_1 + \alpha_2\theta x_2]x_3 & \beta_2 - \alpha_2x_3(1 + \theta x_1) & -[\alpha_1x_1 + \alpha_2x_2(1 + \theta x_1)] \end{pmatrix}$$

Again, we will analyse the stability by cases.

Case 1

In this case we have:

$$J(0, 0, x_3) = \begin{pmatrix} \alpha_1x_3 - \beta_1 & 0 & 0 \\ 0 & \alpha_2x_3 - \beta_2 & 0 \\ \beta_1 - \alpha_1x_3 & \beta_2 - \alpha_2x_3 & 0 \end{pmatrix}$$

This matrix has eigenvalues $\lambda_1 = \alpha_1x_3 - \beta_1$, $\lambda_2 = \alpha_2x_3 - \beta_2$, $\lambda_3 = 0$, with eigenspaces

$$E_1 = \text{Span}\langle(1, 0, -1)\rangle, \quad E_2 = \text{Span}\langle(0, 1, -1)\rangle, \quad E_3 = \text{Span}\langle(0, 0, 1)\rangle$$

respectively. Note that $\lambda_1 < 0$ if and only if $x_3 < \frac{\beta_1}{\alpha_1}$, while $\lambda_2 < 0$ if and only if $x_3 < \frac{\beta_2}{\alpha_2}$. Analogously, $\lambda_1 > 0$ if and only if $x_3 > \frac{\beta_1}{\alpha_1}$, while $\lambda_2 > 0$ if and only if $x_3 < \frac{\beta_2}{\alpha_2}$. This, we have an attracting object given by

$$U_1 = U^s = \left\{ (0, 0, x_3) : 0 \leq x_3 < \min \left\{ \frac{\beta_1}{\alpha_1}, \frac{\beta_2}{\alpha_2} \right\} \right\}$$

and a repelling object

$$U^u = \left\{ (0, 0, x_3) : x_3 > \max \left\{ \frac{\beta_1}{\alpha_1}, \frac{\beta_2}{\alpha_2} \right\} \right\}$$

Case 2

We have:

$$J\left(0, x_2, \frac{\beta_2}{\alpha_2}\right) = \begin{pmatrix} \frac{\alpha_1\beta_2 - \alpha_2\beta_1}{\alpha_2} & 0 & 0 \\ \beta_2\theta x_2 & 0 & \alpha_2 x_2 \\ \frac{\alpha_2\beta_1 - \alpha_1\beta_2}{\alpha_2} - \beta_2\theta x_2 & 0 & -\alpha_2 x_2 \end{pmatrix}$$

With eigenvalues $\lambda_1 = \frac{\alpha_1\beta_2 - \alpha_2\beta_1}{\alpha_2}$, $\lambda_2 = 0$, $\lambda_3 = -\alpha_2 x_2$, and eigenspace

$$E_1 = \text{Span} \left\langle \left(\alpha_2 x_2 + \frac{\alpha_1\beta_2 - \alpha_2\beta_1}{\alpha_2}, \beta_2\theta x_2 - \alpha_2 x_2, \frac{\alpha_2\beta_1 - \alpha_1\beta_2}{\alpha_2} - \beta_2\theta x_2 \right) \right\rangle, \quad E_2 = \text{Span} \langle (0, 1, 0) \rangle, \quad E_3 = \text{Span} \langle (0, 1, -1) \rangle$$

respectively. Note that $\lambda_3 < 0$ for all $x_2 > 0$. On the other hand, $\lambda_1 < 0$ if and only if $\alpha_1\beta_2 < \alpha_2\beta_1$, and therefore as long as this condition holds, the object

$$U_2 = \left\{ \left(0, x_2, \frac{\beta_2}{\alpha_2} \right) : x_2 > 0 \right\}$$

is an attractor.

Case 3

For this case we have:

$$J\left(x_1, 0, \frac{\beta_1}{\alpha_1}\right) = \begin{pmatrix} 0 & 0 & \alpha_1 x_1 \\ 0 & \frac{\alpha_2 \beta_1}{\alpha_1} (1 + \theta x_1) - \beta_2 & 0 \\ 0 & \beta_2 - \frac{\alpha_2 \beta_1}{\alpha_1} (1 + \theta x_1) & -\alpha_1 x_1 \end{pmatrix}$$

With eigenvalues $\lambda_1 = 0$, $\lambda_2 = \frac{\alpha_2 \beta_1}{\alpha_1} (1 + \theta x_1) - \beta_2$, $\lambda_3 = -\alpha_1 x_1$, and eigenspaces

$$E_1 = \text{Span}\langle(1, 0, 0)\rangle, \quad E_2 = \text{Span}\left\langle\left(-\alpha_1 x_1, \alpha_1 x_1 - \beta_2 + \frac{\alpha_2 \beta_1}{\alpha_1} (1 + \theta x_1), \beta_2 - \frac{\alpha_2 \beta_1}{\alpha_1} (1 + \theta x_1)\right)\right\rangle, \quad E_3 = \text{Span}\langle(0, 1, -1)\rangle$$

respectively. Note that $\lambda_3 < 0$ for all $x_1 > 0$, while $\lambda_2 < 0$ if and only if $x_1 < \frac{\alpha_1 \beta_2 - \alpha_2 \beta_1}{\theta \alpha_1}$, and therefore as long as the object

$$U_3 = \left\{ \left(x_1, 0, \frac{\beta_1}{\alpha_1}\right) : 0 < x_1 < \frac{\alpha_1 \beta_2 - \alpha_2 \beta_1}{\alpha_1 \theta} \right\}$$

exists, it is an attractor.

Case 4

We obtain:

$$J\left(\frac{\alpha_1 \beta_2 - \alpha_2 \beta_1}{\alpha_2 \beta_1 \theta}, x_2, \frac{\beta_1}{\alpha_1}\right) = \begin{pmatrix} 0 & 0 & \frac{\alpha_1 (\alpha_1 \beta_2 - \alpha_2 \beta_1)}{\alpha_2 \beta_1 \theta} \\ \frac{\alpha_2 \beta_1 \theta x_2}{\alpha_1} & 0 & \frac{\alpha_1 \beta_2 x_2}{\beta_1} \\ -\frac{\alpha_2 \beta_1 \theta x_2}{\alpha_1} & 0 & \frac{\alpha_1 (\alpha_2 \beta_1 - \alpha_1 \beta_2)}{\alpha_2 \beta_1 \theta} - \frac{\alpha_1 \beta_2 x_2}{\beta_1} \end{pmatrix}$$

This matrix has an eigenvalue $\lambda_2 = 0$. Further, defining

$$F = \frac{\alpha_1 \beta_2 x_2}{\beta_1} - \frac{\alpha_1 (\alpha_2 \beta_1 - \alpha_1 \beta_2)}{\alpha_2 \beta_1 \theta}$$

The remaining eigenvalues are given by

$$\lambda_{1/3} = \frac{-F \pm \sqrt{F^2 - 4x_2(\alpha_2\beta_1 - \alpha_1\beta_2)}}{2}$$

Where $\lambda_{1/3}$ are complex if and only if

$$F^2 < 4x_2(\alpha_2\beta_1 - \alpha_1\beta_2)$$

Denoting

$$G = (\alpha_2\beta_1 - \alpha_1\beta_2) \left[2 + \frac{\alpha_1^2\beta_2}{\alpha_2\beta_1^2\theta} \right], \quad H = \frac{\alpha_1^2(\alpha_2\beta_1 - \alpha_1\beta_2)}{\alpha_2^2\beta_1^2\theta^2}$$

The latter is equivalent to

$$\frac{\alpha_1^2\beta_2^2}{\beta_1^2} x_2^2 - 2Gx_2 + H < 0$$

This is possible if

$$G^2 > \frac{\alpha_1^2\beta_2^2}{\beta_1^2} H \quad (26)$$

where (26) always holds. Thus, $\lambda_1, \lambda_3 \notin \mathbb{R}$ if and only if

$$I_- = \left[G - \sqrt{G^2 - \frac{\alpha_1^2\beta_2^2}{\beta_1^2} H} \right] \frac{\beta_1^2}{\alpha_1^2\beta_2^2} < x_2 < \left[G + \sqrt{G^2 - \frac{\alpha_1^2\beta_2^2}{\beta_1^2} H} \right] \frac{\beta_1^2}{\alpha_1^2\beta_2^2} = I_+ \quad (27)$$

Note that, given that $\alpha_1\beta_2 - \alpha_2\beta_1 \geq 0$, then $H \leq 0$, and therefore $I_- \leq 0$, and thus $x_2 > I_-$ is trivial.

In this case, $\operatorname{Re}(\lambda_1) < 0$ and $\operatorname{Re}(\lambda_3) < 0$ simultaneously if and only if

$$x_2 > \frac{\alpha_2\beta_1 - \alpha_1\beta_2}{\alpha_2\beta_2\theta} \quad (28)$$

Given that our equilibrium points are non-negative if and only if $\alpha_1\beta_2 > \alpha_2\beta_1$, condition (28) is always true.

On the other hand, if (26) is not held or $x_2 > I_+$ or $x_2 < I_-$, then $\lambda_1, \lambda_3 \in \mathbb{R}$. In this case, $\lambda_1 < 0$ and $\lambda_3 < 0$ simultaneously if and only if

$$-F + \sqrt{F^2 - 4x_2(\alpha_2\beta_1 - \alpha_1\beta_2)} < 0$$

This is only possible if $F > 0$, or, equivalently, if

$$x_2 > \frac{\alpha_2\beta_1 - \alpha_1\beta_2}{\alpha_2\beta_2\theta} \quad (29)$$

If (29) holds, then $\lambda_1 < 0$ and $\lambda_3 < 0$ simultaneously if and only if $\alpha_2\beta_1 > \alpha_1\beta_2$. However, note that in this case the equilibrium points have negative components and therefore this condition is not possible.

Analogously, if (26) cannot be verified or $x_2 > I_+$ or $x_2 < I_-$, then $\lambda_1 > 0$ and $\lambda_3 > 0$ simultaneously if and only if

$$\alpha_2\beta_1 > \alpha_1\beta_2 \quad \text{and} \quad x_2 < \frac{\alpha_2\beta_1 - \alpha_1\beta_2}{\alpha_2\beta_2\theta} \quad (30)$$

which again is not valid in our case. Thus, the set

$$U_4 = U_c^s = \left\{ \left(\frac{\alpha_1\beta_2 - \alpha_2\beta_1}{\alpha_2\beta_1\theta}, x_2, \frac{\beta_1}{\alpha_1} \right) : 0 < x_2 < I_+ \right\}$$

is an attractor, and this case cannot have repelling objects.

Summary of stability conditions for model I-B

1. In case 1, the object $U_1 = \left\{ (0, 0, x_3) : 0 \leq x_3 < \min \left\{ \frac{\beta_1}{\alpha_1}, \frac{\beta_2}{\alpha_2} \right\} \right\}$ is an attractor, while the object $U^u = \left\{ (0, 0, x_3) : x_3 > \max \left\{ \frac{\beta_1}{\alpha_1}, \frac{\beta_2}{\alpha_2} \right\} \right\}$ is repeller.
2. In case 2, the object $U_2 = \left\{ \left(0, x_2, \frac{\beta_2}{\alpha_2} \right) : x_2 > 0 \right\}$ is attractor if and only if $\alpha_1\beta_2 < \alpha_2\beta_1$. There are no repelling objects.

3. In case 3, the object $U_3 = \left\{ \left(x_1, 0, \frac{\beta_1}{\alpha_1} \right) : 0 < x_1 < \frac{\alpha_1 \beta_2 - \alpha_2 \beta_1}{\alpha_1 \theta} \right\}$ is always an attractor. Further, this set is nonempty if and only if $\alpha_1 \beta_2 > \alpha_2 \beta_1$. There are no repelling objects.

4. In case 4, the object U_4 is always attractor. There are no repelling sets.

Note that cases 2 and 3 cannot happen simultaneously. Nonetheless, there is multi-stability between the attracting object of case 1 with any other of cases 2 or 3. For this, it suffices if $\alpha_1 \beta_2 \neq \alpha_2 \beta_1$. Given that, in practice, the probability that two parameter combinations are exactly the same is 0, we conclude that this stability is guaranteed.

On the other hand, a multi-stable scenario involving the object U_4 is also possible. In fact, for this to happen it suffices if condition (26) is met and if $I_+ > 0$. Condition $I_+ > 0$ holds if and only if $G \geq 0$ or $H < 0$. In particular, if $H < 0$, condition (26) can be satisfied trivially. Furthermore, $H < 0$ is equivalent to $\alpha_2 \beta_1 < \alpha_1 \beta_2$, i.e., $H < 0$ is equivalent to U_2 being an attractor.

From this, we can determine U_2 being an attractor implies (but is not necessarily equivalent to) $I_+ > 0$, and therefore, that U_4 is a non-empty attractor.

Last, note that in models I-A and I-B the component x_3 can be used to predict towards which object the orbits will converge. In general, if x_3 is sufficiently small, both species go locally extinct.

In general, any of the behaviours (coexistence, survival of one of the species and local extinction) is possible.

Model II-A

Now let us consider the 3D model with negative interactions given by

$$\left\{ \begin{array}{l} \frac{dBS}{dt} = \frac{\alpha_{BS}(BS)(SL)}{1 + \gamma_{EB}(ES)} - (BS)(\beta_{BS} + \mu_{EB}(ES)) \end{array} \right. \quad (67)$$

$$\left\{ \begin{array}{l} \frac{dPS}{dt} = \frac{\alpha_{PS}(PS)(SL)}{1 + \gamma_{BP}(BS) + \gamma_{EP}(ES)} - (PS)(\beta_{PS} + \mu_{EP}(ES)) \end{array} \right. \quad (68)$$

$$\left\{ \begin{array}{l} \frac{dES}{dt} = \alpha_{ES}(ES)(SL) - \beta_{ES}(ES) \end{array} \right. \quad (69)$$

$$\left\{ \begin{array}{l} \frac{dSL}{dt} = \beta_{ES}(ES) + (PS)(\beta_{PS} + \mu_{EP}(ES)) + (BS)(\beta_{BS} + \mu_{EP}(ES)) - \alpha_{ES}(ES)(SL) - \frac{\alpha_{PS}(PS)(SL)}{1 + \gamma_{BP}(BS) + \gamma_{EP}(ES)} - \frac{\alpha_{BS}(BS)(SL)}{1 + \gamma_{EB}(ES)} \end{array} \right. \quad (70)$$

This system of equations, as in model II-B, can be reduced to a 3D system using the conservation equations given by (35). Here we will denote $BS(t) = x_1(t)$, $PS(t) = x_2(t)$, $ES(t) = x_3(t)$, $SL(t) = x_4(t)$, $\alpha_{BS} = \alpha_1$, $\alpha_{PS} = \alpha_2$, $\alpha_{ES} = \alpha_3$, $\beta_{BS} = \beta_1$, $\beta_{PS} = \beta_2$, $\beta_{ES} = \beta_3$, $\gamma_{EB} = \gamma_1$, $\gamma_{BP} = \gamma_2$, $\gamma_{EP} = \gamma_3$, $\mu_{EB} = \mu_1$, $\mu_{EP} = \mu_2$.

Equilibrium points of model II-A

Given the linear dependency of the system, a point of the form (x_1, x_2, x_3, x_4) will be an equilibrium of the system (67)-(70) if and only if it is a solution of the system of equations

$$\left\{ \begin{array}{l} [\alpha_1 x_4 - (\beta_1 + \mu_1 x_3)(1 + \gamma_1 x_3)]x_1 = 0 \\ [\alpha_2 x_4 - (\beta_2 + \mu_2 x_3)(1 + \gamma_2 x_1 + \gamma_3 x_3)]x_2 = 0 \end{array} \right. \quad (71)$$

$$\left\{ \begin{array}{l} [\alpha_2 x_4 - (\beta_2 + \mu_2 x_3)(1 + \gamma_2 x_1 + \gamma_3 x_3)]x_2 = 0 \\ [\alpha_3 x_4 - \beta_3]x_3 = 0 \end{array} \right. \quad (72)$$

$$[\alpha_3 x_4 - \beta_3]x_3 = 0 \quad (73)$$

We will study this system case by case.

1. If $x_1 = 0$, then solving system (71)-(73) is equivalent to solving

$$\left\{ \begin{array}{l} [\alpha_2 x_4 - (\beta_2 + \mu x_3)(1 + \gamma_3 x_3)]x_2 = 0 \\ [\alpha_3 x_4 - \beta_3]x_3 = 0 \end{array} \right. \quad (74)$$

$$\left\{ \begin{array}{l} [\alpha_2 x_4 - (\beta_2 + \mu x_3)(1 + \gamma_3 x_3)]x_2 = 0 \\ [\alpha_3 x_4 - \beta_3]x_3 = 0 \end{array} \right. \quad (75)$$

1.1. If $x_2 = 0$, then we obtain equilibrium points of the form $(0, 0, 0, x_4)$, $x_4 \geq 0$ and of the form

$$\left(0, 0, x_3, \frac{\beta_3}{\alpha_3} \right), \quad x_3 > 0.$$

1.2. If $x_2 > 0$, then we have two subcases:

1.2.1. If $x_3 = 0$, then we have equilibrium points of the form $\left(0, x_2, 0, \frac{\beta_2}{\alpha_2} \right)$, $x_2 > 0$.

1.2.2. If $x_3 > 0$, then $x_4 = \frac{\beta_3}{\alpha_3}$ and x_3 are solutions to the quadratic equation

$$\mu_2 \gamma_3 x_3^2 + [\mu_2 + \beta_2 \gamma_3]x_3 + \beta_2 - \frac{\alpha_2 \beta_3}{\alpha_3} = 0 \quad (76)$$

i.e.,

$$x_3 = x_3^\pm = \frac{1}{2\mu_2 \gamma_3} \left[-(\mu_2 + \beta_2 \gamma_3) \pm \sqrt{(\mu_2 + \beta_2 \gamma_3)^2 + \frac{4\alpha_2 \beta_3 \mu_2 \gamma_3}{\alpha_3}} \right]$$

Note that the solutions of (76) are real. Further, note that $x_3^- < 0$, and therefore we will only consider the solution $x_3 = x_3^+$. With this in mind, we obtain that $x_3 > 0$ if and only if $\alpha_3 \beta_2 < \alpha_2 \beta_3$. Thus, we get equilibrium points of the form

$$\left(0, x_2, \frac{1}{2\mu_2\gamma_3} \left[-(\mu_2 + \beta_2\gamma_3) + \sqrt{(\mu_2 - \beta_2\gamma_3)^2 + \frac{4\alpha_2\beta_3\mu_2\gamma_3}{\alpha_3}} \right], \frac{\beta_3}{\alpha_3} \right), \quad x_2 > 0$$

2. If $x_1 > 0$, then solving (71)-(73) is equivalent to solving

$$\left\{ \begin{array}{l} \alpha_1x_4 - (\beta_1 + \mu_1x_3)(1 + \gamma_1x_3) = 0 \end{array} \right. \quad (77)$$

$$[\alpha_2x_4 - (\beta_2 + \mu_2x_3)(1 + \gamma_2x_1 + \gamma_3x_3)]x_2 = 0 \quad (78)$$

$$[\alpha_3x_4 - \beta_3]x_3 = 0 \quad (79)$$

2.1. If $x_2 = 0$, then we distinguish between two cases.

2.1.1. If $x_3 = 0$, then we get equilibrium points of the form $\left(x_1, 0, 0, \frac{\beta_1}{\alpha_1}\right)$, $x_1 > 0$

2.1.2. If $x_3 > 0$, then $x_4 = \frac{\beta_3}{\alpha_3}$ and x_3 is a solution to the quadratic equation

$$\mu_1\gamma_1x_3^2 + [\mu_1 + \beta_1\gamma_1]x_3 + \beta_1 - \frac{\alpha_1\beta_3}{\alpha_3} = 0 \quad (80)$$

i.e.,

$$x_3 = x_3^\pm = \frac{1}{2\mu_1\gamma_1} \left[-(\mu_1 + \beta_1\gamma_1) \pm \sqrt{(\mu_1 - \beta_1\gamma_1)^2 + \frac{4\alpha_1\beta_3\mu_1\gamma_1}{\alpha_3}} \right]$$

Again, these solutions are real. On the other hand, $x_3^- < 0$, and thus we do not consider this case, and keep only $x_3 = x_3^+$. Further, in this case $x_3 > 0$ if and only if $\alpha_3\beta_1 < \alpha_1\beta_3$. In this case, we determine the existence of equilibrium points of the form

$$\left(x_1, 0, \frac{1}{2\mu_1\gamma_1} \left[-(\mu_1 + \beta_1\gamma_1) + \sqrt{(\mu_1 - \beta_1\gamma_1)^2 + \frac{4\alpha_1\beta_3\mu_1\gamma_1}{\alpha_3}} \right], \frac{\beta_3}{\alpha_3} \right), \quad x_1 > 0$$

2.2. If $x_2 > 0$, we, again, distinguish between two cases.

2.2.1. If $x_3 = 0$, then we obtain equilibrium points of the form $\left(\frac{\alpha_2\beta_1 - \alpha_1\beta_2}{\alpha_1\beta_2\gamma_2}, x_2, 0, \frac{\beta_1}{\alpha_1}\right)$, $x_2 > 0$, if and only if $\alpha_2\beta_1 > \alpha_1\beta_2$.

2.2.2. If $x_3 > 0$, then $x_4 = \frac{\beta_3}{\alpha_3}$, x_3 is solution to (80) and x_1 is solution to

$$\gamma_2(\beta_2 + \mu_2 x_3)x_1 = \frac{\alpha_2 \beta_3}{\alpha_3} - (\beta_2 + \mu_2 x_3)(1 + \gamma_3 x_3) \quad (81)$$

From this, (80) implies that

$$x_3 = \frac{1}{2\mu_1\gamma_1} \left[-(\mu_1 + \beta_1\gamma_1) + \sqrt{(\mu_1 - \beta_1\gamma_1)^2 + \frac{4\alpha_1\beta_3\mu_1\gamma_1}{\alpha_3}} \right] = M_1$$

which is true if and only if $\alpha_3\beta_1 < \alpha_1\beta_3$. Further, the previous expression combined with (81) implies that

$$x_1 = \frac{\alpha_2\beta_3 - \alpha_3(\beta_2 + \mu_2 M_1)(1 + \gamma_3 M_1)}{\alpha_3\gamma_2(\beta_2 + \mu_2 M_1)}$$

where $x_1 > 0$ if and only if $\alpha_2\beta_3 > \alpha_3(\beta_2 + \mu_2 M_1)(1 + \gamma_3 M_1)$. Thus, we get equilibrium points of the form

$$\left(\frac{\alpha_2\beta_3 - \alpha_3(\beta_2 + \mu_2 M_1)(1 + \gamma_3 M_1)}{\alpha_3\gamma_2(\beta_2 + \mu_2 M_1)}, x_2, \frac{1}{2\mu_1\gamma_1} \left[-(\mu_1 + \beta_1\gamma_1) + \sqrt{(\mu_1 - \beta_1\gamma_1)^2 + \frac{4\alpha_1\beta_3\mu_1\gamma_1}{\alpha_3}} \right], \frac{\beta_3}{\alpha_3} \right), \quad x_2 > 0$$

Summary of equilibrium points of model II-A

In total, model II-A can display at most eight sets of non-negative equilibrium points:

1. Points of the form $(0, 0, 0, x_4)$, $x_4 \geq 0$.

2. Points of the form $\left(0, 0, x_3, \frac{\beta_3}{\alpha_3} \right)$, $x_3 > 0$.

3. Points of the form $\left(0, x_2, 0, \frac{\beta_2}{\alpha_2} \right)$, $x_2 > 0$.

4. Points of the form $\left(0, x_2, \frac{1}{2\mu_2\gamma_3} \left[-(\mu_2 + \beta_2\gamma_3) + \sqrt{(\mu_2 - \beta_2\gamma_3)^2 + \frac{4\alpha_2\beta_3\mu_2\gamma_3}{\alpha_3}} \right], \frac{\beta_3}{\alpha_3} \right)$, $x_2 > 0$, if and only if $\alpha_3\beta_2 < \alpha_2\beta_3$.

5. Points of the form $\left(x_1, 0, 0, \frac{\beta_1}{\alpha_1}\right)$, $x_1 > 0$.

6. Points of the form $\left(x_1, 0, \frac{1}{2\mu_1\gamma_1} \left[-(\mu_1 + \beta_1\gamma_1) + \sqrt{(\mu_1 - \beta_1\gamma_1)^2 + \frac{4\alpha_1\beta_3\mu_1\gamma_1}{\alpha_3}} \right], \frac{\beta_3}{\alpha_3}\right)$, $x_1 > 0$, if and only if $\alpha_3\beta_1 < \alpha_1\beta_3$.

7. Points of the form $\left(\frac{\alpha_2\beta_1 - \alpha_1\beta_2}{\alpha_1\beta_2\gamma_2}, x_2, 0, \frac{\beta_1}{\alpha_1}\right)$, $x_2 > 0$, if and only if $\alpha_2\beta_1 > \alpha_1\beta_2$.

8. Points of the form

$$\left(\frac{\alpha_2\beta_3 - \alpha_3(\beta_2 + \mu_2M_1)(1 + \gamma_3M_1)}{\alpha_3\gamma_2(\beta_2 + \mu_2M_1)}, x_2, \frac{1}{2\mu_1\gamma_1} \left[-(\mu_1 + \beta_1\gamma_1) + \sqrt{(\mu_1 - \beta_1\gamma_1)^2 + \frac{4\alpha_1\beta_3\mu_1\gamma_1}{\alpha_3}} \right], \frac{\beta_3}{\alpha_3}\right), x_2 > 0$$

if and only if $\alpha_3\beta_1 < \alpha_1\beta_3$ and $\alpha_2\beta_3 > \alpha_3(\beta_2 + \mu_2M_1)(1 + \gamma_3M_1)$.

Note that in principle all 8 equilibrium points can exist simultaneously. Specifically, the existence of points of the form described in case 8 also implies the existence of points described in case 6.

Stability analysis of model II-A

The system has following Jacobian matrix:

$$J(x_1, x_2, x_3, x_4) = \begin{pmatrix} \frac{\alpha_1x_4}{1 + \gamma_1x_3} - \beta_1 - \mu_1x_3 & 0 & -\frac{\alpha_1\gamma_1x_1x_4}{(1 + \gamma_1x_3)^2} - \mu_1x_1 \\ -\frac{\alpha_2\gamma_2x_2x_4}{(1 + \gamma_2x_1 + \gamma_3x_3)^2} & \frac{\alpha_2x_4}{1 + \gamma_2x_1 + \gamma_3x_3} - \beta_2 - \mu_2x_3 & -\frac{\alpha_2\gamma_3x_2x_4}{(1 + \gamma_2x_1 + \gamma_3x_3)^2} - \mu_2x_2 \\ 0 & 0 & \alpha_3x_4 - \beta_3 \\ \beta_1 + \mu_1x_3 + \frac{\alpha_2\gamma_2x_2x_4}{(1 + \gamma_2x_1 + \gamma_3x_3)^2} - \frac{\alpha_1x_4}{1 + \gamma_1x_3} & \beta_2 + \mu_2x_3 - \frac{\alpha_2x_4}{1 + \gamma_2x_1 + \gamma_3x_3} & \beta_3 + \mu_1x_1 + \mu_2x_2 + \frac{\alpha_1\gamma_1x_1x_4}{(1 + \gamma_1x_3)^2} + \frac{\alpha_2\gamma_3x_2x_4}{(1 + \gamma_2x_1 + \gamma_3x_3)^2} - \alpha_3x_4 - \alpha_3x_3 - \frac{1}{1 + \gamma_3x_3} \end{pmatrix}$$

We will examine this matrix case by case.

Case 1

Here we have:

$$J(0, 0, 0, x_4) = \begin{pmatrix} \alpha_1 x_4 - \beta_1 & 0 & 0 & 0 \\ 0 & \alpha_2 x_4 - \beta_2 & 0 & 0 \\ 0 & 0 & \alpha_3 x_4 - \beta_3 & 0 \\ \beta_1 - \alpha_1 x_4 & \beta_2 - \alpha_2 x_4 & \beta_3 - \alpha_3 x_4 & 0 \end{pmatrix}$$

This matrix has eigenvalues $\lambda_1 = \alpha_1 x_4 - \beta_1$, $\lambda_2 = \alpha_2 x_4 - \beta_2$, $\lambda_3 = \alpha_3 x_4 - \beta_3$, $\lambda_4 = 0$. Thus, these points are attractors if and only if

$$x_4 < \min \left\{ \frac{\beta_1}{\alpha_1}, \frac{\beta_2}{\alpha_2}, \frac{\beta_3}{\alpha_3} \right\}$$

and repellers if and only if

$$x_4 > \max \left\{ \frac{\beta_1}{\alpha_1}, \frac{\beta_2}{\alpha_2}, \frac{\beta_3}{\alpha_3} \right\}$$

Thus, the object

$$W_1 = W_1^s = \left\{ (0, 0, 0, x_4) : x_4 < \min \left\{ \frac{\beta_1}{\alpha_1}, \frac{\beta_2}{\alpha_2}, \frac{\beta_3}{\alpha_3} \right\} \right\}$$

is an attractor, while

$$W_1^u = \left\{ (0, 0, 0, x_4) : x_4 > \max \left\{ \frac{\beta_1}{\alpha_1}, \frac{\beta_2}{\alpha_2}, \frac{\beta_3}{\alpha_3} \right\} \right\}$$

is a repeller.

Case 2

In this case we have:

$$J\left(0, 0, x_3, \frac{\beta_3}{\alpha_3}\right) = \begin{pmatrix} \frac{\alpha_1 \beta_3}{\alpha_3(1 + \gamma_1 x_3)} - \beta_1 - \mu_1 x_3 & 0 & 0 & 0 \\ 0 & \frac{\alpha_2 \beta_3}{\alpha_3(1 + \gamma_3 x_3)} - \beta_2 - \mu_2 x_3 & 0 & 0 \\ 0 & 0 & 0 & \alpha_3 x_3 \\ \beta_1 + \mu_1 x_3 - \frac{\alpha_1 \beta_3}{\alpha_3(1 + \gamma_1 x_3)} & \beta_2 + \mu_2 x_3 - \frac{\alpha_2 \beta_3}{\alpha_3(1 + \gamma_3 x_3)} & 0 & -\alpha_3 x_3 \end{pmatrix}$$

with eigenvalues $\lambda_1 = \frac{\alpha_1\beta_3}{\alpha_3(1 + \gamma_1x_3)} - \beta_1 - \mu_1x_3$, $\lambda_2 = \frac{\alpha_2\beta_3}{\alpha_3(1 + \gamma_3x_3)} - \beta_2 - \mu_2x_3$, $\lambda_3 = 0$, $\lambda_4 = -\alpha_3x_3$. Note that λ_4 is always negative. In this case, if and only if

$$\gamma_1\mu_1x_3^2 + [\beta_1\gamma_1 + \mu_1]x_3 + \beta_1 - \frac{\alpha_1\beta_3}{\alpha_3} > 0$$

which happens if and only if any of the following conditions are met:

$$\alpha_3\beta_1 \geq \alpha_1\beta_3 \quad (82)$$

$$\alpha_3\beta_1 < \alpha_1\beta_3 \quad \text{y} \quad x_3 > M_1 \quad (83)$$

Analogously, we obtain that $\lambda_2 < 0$ if and only if any of the following conditions are met:

$$\alpha_3\beta_2 \geq \alpha_2\beta_3 \quad (84)$$

$$\alpha_3\beta_2 < \alpha_2\beta_3 \quad \text{y} \quad x_3 > M_2 \quad (85)$$

where

$$M_2 = \frac{1}{2\mu_2\gamma_3} \left[-(\mu_2 + \beta_2\gamma_3) + \sqrt{(\mu_2 - \beta_2\gamma_3)^2 + \frac{4\alpha_2\beta_3\mu_2\gamma_3}{\alpha_3}} \right]$$

In general, the object

$$W_2 = \left\{ \left(0, 0, x_3, \frac{\beta_3}{\alpha_3} \right) : x_3 > \max \{ 0, M_1, M_2 \} \right\}$$

is an attractor, with $M_1 \leq 0$ if and only if (82) can be verified, while $M_2 \leq 0$ if and only if (84) holds. In this case there are no repellers.

Case 3

For this case we have:

$$J\left(0, x_2, 0, \frac{\beta_2}{\alpha_2}\right) = \begin{pmatrix} \frac{\alpha_1\beta_2 - \alpha_2\beta_1}{\alpha_2} & 0 & 0 & 0 \\ -\beta_2\gamma_2x_2 & 0 & -[\beta_2\gamma_3 - \mu_2]x_2 & \alpha_2x_2 \\ 0 & 0 & \frac{\alpha_3\beta_2 - \alpha_2\beta_3}{\alpha_2} & 0 \\ \beta_2\gamma_2x_2 + \frac{\alpha_2\beta_1 - \alpha_1\beta_2}{\alpha_2} & 0 & [\beta_2\gamma_3 + \mu_2]x_2 - \frac{\alpha_3\beta_2 - \alpha_2\beta_3}{\alpha_2} & -\alpha_2x_2 \end{pmatrix}$$

with eigenvalues $\lambda_1 = \frac{\alpha_1\beta_2 - \alpha_2\beta_1}{\alpha_2}$, $\lambda_2 = 0$, $\lambda_3 = \frac{\alpha_3\beta_2 - \alpha_2\beta_3}{\alpha_2}$, $\lambda_4 = -\alpha_2x_2$. Again, $\lambda_4 < 0$. Thus, the object

$$W_3 = \left\{ \left(0, x_2, 0, \frac{\beta_2}{\alpha_2}\right) : x_2 > 0 \right\}$$

is an attractor if and only if $\alpha_1\beta_2 < \alpha_2\beta_1$ and $\alpha_3\beta_2 < \alpha_2\beta_3$. There are no repelling objects.

Case 4

In this case we have the matrix:

$$J\left(0, x_2, M_2, \frac{\beta_3}{\alpha_3}\right) = \begin{pmatrix} \frac{\alpha_1\beta_3}{\alpha_3(1 + \gamma_1M_2)} - \beta_1 - \mu_1M_2 & 0 & 0 & 0 \\ -\frac{(\beta_2 + \mu_2M_2)\gamma_2x_2}{1 + \gamma_3M_2} & 0 & -\left[\frac{(\beta_2 + \mu_2M_2)\gamma_3}{1 + \gamma_3M_2} + \mu_2\right]x_2 & \frac{\alpha_2x_2}{1 + \gamma_3M_2} \\ 0 & 0 & 0 & \alpha_3M_2 \\ \beta_1 + \mu_1M_2 - \frac{\alpha_1\beta_3}{\alpha_3(1 + \gamma_1M_2)} + \frac{(\beta_2 + \mu_2M_2)\gamma_2x_2}{1 + \gamma_3M_2} & 0 & \left[\frac{(\beta_2 + \mu_2M_2)\gamma_3}{1 + \gamma_3M_2} + \mu_2\right]x_2 & -\alpha_3M_2 - \frac{\alpha_2x_2}{1 + \gamma_3M_2} \end{pmatrix}$$

with eigenvalues $\lambda_1 = \frac{\alpha_1\beta_3}{\alpha_3(1 + \gamma_1M_2)} - \beta_1 - \mu_1M_2$, $\lambda_2 = 0$ and the other two eigenvalues corresponding to the roots of the quadratic polynomial

$$p(\lambda) = \lambda^2 + \left[\alpha_3M_2 + \frac{\alpha_2x_2}{1 + \gamma_3M_2}\right]\lambda - \alpha_3M_2\left[\frac{(\beta_2 + \mu_2M_2)\gamma_3}{1 + \gamma_3M_2} + \mu_2\right]x_2$$

i.e.,

$$\lambda_{3/4} = \frac{1}{2} \left[-\left(\alpha_3M_2 + \frac{\alpha_2x_2}{1 + \gamma_3M_2}\right) \pm \sqrt{\left(\alpha_3M_2 + \frac{\alpha_2x_2}{1 + \gamma_3M_2}\right)^2 + 4\alpha_3M_2\left(\mu_2 + \frac{(\beta_2 + \mu_2M_2)\gamma_3}{1 + \gamma_3M_2}\right)x_2} \right]$$

Note that all eigenvalues are real. On the other hand, note that

$$\lambda_3 = \frac{1}{2} \left[-\left(\alpha_3 M_2 + \frac{\alpha_2 x_2}{1 + \gamma_3 M_2} \right) - \sqrt{\left(\alpha_3 M_2 + \frac{\alpha_2 x_2}{1 + \gamma_3 M_2} \right)^2 + 4\alpha_3 M_2 \left(\mu_2 + \frac{(\beta_2 + \mu_2 M_2)\gamma_3}{1 + \gamma_3 M_2} \right) x_2} \right] < 0$$

while

$$\lambda_4 = \frac{1}{2} \left[-\left(\alpha_3 M_2 + \frac{\alpha_2 x_2}{1 + \gamma_3 M_2} \right) + \sqrt{\left(\alpha_3 M_2 + \frac{\alpha_2 x_2}{1 + \gamma_3 M_2} \right)^2 + 4\alpha_3 M_2 \left(\mu_2 + \frac{(\beta_2 + \mu_2 M_2)\gamma_3}{1 + \gamma_3 M_2} \right) x_2} \right] > 0$$

and therefore, in this case, there are neither attractors nor repellers.

Case 5

In this case, the Jacobian matrix is given by

$$J\left(x_1, 0, 0, \frac{\beta_1}{\alpha_1}\right) = \begin{pmatrix} 0 & 0 & -[\beta_1\gamma_1 + \mu_1]x_1 & \alpha_1 x_1 \\ 0 & \frac{\alpha_2\beta_1}{\alpha_1(1 + \gamma_2 x_1)} - \beta_2 & 0 & 0 \\ 0 & 0 & \frac{\alpha_3\beta_1 - \alpha_1\beta_3}{\alpha_1} & 0 \\ 0 & \beta_2 - \frac{\alpha_2\beta_1}{\alpha_1(1 + \gamma_2 x_1)} & [\beta_1\gamma_1 + \mu_1]x_1 + \frac{\alpha_1\beta_3 - \alpha_3\beta_1}{\alpha_1} & -\alpha_1 x_1 \end{pmatrix}$$

with eigenvalues $\lambda_1 = 0$, $\lambda_2 = \frac{\alpha_2\beta_1}{\alpha_1(1 + \gamma_2 x_1)} - \beta_2$, $\lambda_3 = \frac{\alpha_3\beta_1 - \alpha_1\beta_3}{\alpha_1}$, $\lambda_4 = -\alpha_1 x_1$. Note that $\lambda_4 < 0$. On the other hand, $\lambda_2 < 0$ if and only if

$$x_1 > \frac{\alpha_2\beta_1 - \alpha_1\beta_2}{\alpha_1\beta_2\gamma_2}$$

Finally, given that $\lambda_3 < 0$ if and only if $\alpha_3\beta_1 < \alpha_1\beta_3$, it follows that the object

$$W_5 = \left\{ \left(x_1, 0, 0, \frac{\beta_1}{\alpha_1} \right) : x_1 > \max \left\{ 0, \frac{\alpha_2\beta_1 - \alpha_1\beta_2}{\alpha_1\beta_2\gamma_2} \right\} \right\}$$

is an attractor if and only if $\alpha_3\beta_1 < \alpha_1\beta_3$. In this case there are no repellers.

Case 6

In this case we have:

$$J\left(x_1, 0, M_1, \frac{\beta_3}{\alpha_3}\right) = \begin{pmatrix} 0 & 0 & -\frac{\alpha_3}{\alpha_1\beta_3}(\beta_1 + \mu_1M_1)^2\gamma_1x_1 - \mu_1x_1 & \frac{\alpha_3}{\beta_3}(\beta_1 + \mu_1M_1)x_1 \\ 0 & \frac{\alpha_2\beta_3}{\alpha_3(1 + \gamma_2x_1 + \gamma_3M_1)} - \beta_2 - \mu_2M_1 & 0 & 0 \\ 0 & 0 & 0 & \alpha_3M_1 \\ 0 & \beta_2 + \mu_2M_1 - \frac{\alpha_2\beta_3}{\alpha_3(1 + \gamma_2x_1 + \gamma_3M_1)} & \mu_1x_1 + \frac{\alpha_3}{\alpha_1\beta_3}(\beta_1 + \mu_1M_1)^2\gamma_1x_1 & -\alpha_3M_1 - \frac{\alpha_3}{\beta_3}(\beta_1 + \mu_1M_1)x_1 \end{pmatrix}$$

with eigenvalues $\lambda_1 = 0$, $\lambda_2 = \frac{\alpha_2\beta_3}{\alpha_3(1 + \gamma_2x_1 + \gamma_3M_1)} - \beta_2 - \mu_2M_1$, and the other two eigenvalues correspond to the roots of the second order polynomial

$$p(\lambda) = \lambda^2 + \left[\alpha_3M_1 + \frac{\alpha_3}{\beta_3}(\beta_1 + \mu_1M_1)x_1\right]\lambda - \alpha_3M_1\left[\mu_1 + \frac{(\beta_1 + \mu_1M_1)\gamma_1}{1 + \gamma_1M_1}\right]x_1$$

i.e.

$$\lambda_{3/4} = \frac{1}{2} \left[-\left(\alpha_3M_1 + \frac{\alpha_3}{\beta_3}(\beta_1 + \mu_1M_1)x_1\right) \pm \sqrt{\left(\alpha_3M_1 + \frac{\alpha_3}{\beta_3}(\beta_1 + \mu_1M_1)x_1\right)^2 + 4\alpha_3M_1\left(\mu_1 + \frac{(\beta_1 + \mu_1M_1)\gamma_1}{1 + \gamma_1M_1}\right)x_1} \right]$$

Note that all eigenvalues are real. Additionally, note that

$$\lambda_3 = \frac{1}{2} \left[-\left(\alpha_3M_1 + \frac{\alpha_3}{\beta_3}(\beta_1 + \mu_1M_1)x_1\right) - \sqrt{\left(\alpha_3M_1 + \frac{\alpha_3}{\beta_3}(\beta_1 + \mu_1M_1)x_1\right)^2 + 4\alpha_3M_1\left(\mu_1 + \frac{(\beta_1 + \mu_1M_1)\gamma_1}{1 + \gamma_1M_1}\right)x_1} \right] < 0$$

while

$$\lambda_4 = \frac{1}{2} \left[-\left(\alpha_3M_1 + \frac{\alpha_3}{\beta_3}(\beta_1 + \mu_1M_1)x_1\right) + \sqrt{\left(\alpha_3M_1 + \frac{\alpha_3}{\beta_3}(\beta_1 + \mu_1M_1)x_1\right)^2 + 4\alpha_3M_1\left(\mu_1 + \frac{(\beta_1 + \mu_1M_1)\gamma_1}{1 + \gamma_1M_1}\right)x_1} \right] > 0$$

and therefore, in this case there are neither attractors nor repellers.

Case 7

For this case we have:

$$J\left(\frac{\alpha_2\beta_1 - \alpha_1\beta_2}{\alpha_1\beta_2\gamma_2}, x_2, 0, \frac{\beta_1}{\alpha_1}\right) = \begin{pmatrix} 0 & 0 & -[\beta_1\gamma_1 + \mu_1]\frac{\alpha_2\beta_1 - \alpha_1\beta_2}{\alpha_1\beta_2\gamma_2} & \frac{\alpha_2\beta_1 - \alpha_1\beta_2}{\beta_2\gamma_2} \\ \beta_2\gamma_2x_2 & 0 & \frac{\alpha_1^2\alpha_2\beta_1\beta_2^2\gamma_3x_2}{\alpha_2\beta_1} & \frac{\alpha_1\beta_2x_2}{\beta_1} \\ 0 & 0 & \frac{\alpha_3(\alpha_2\beta_1 - \alpha_1\beta_2)}{\alpha_1\beta_2\gamma_2} - \beta_3 & 0 \\ -\beta_2\gamma_2x_2 & 0 & \beta_3 + [\beta_1\gamma_1 + \mu_1]\frac{\alpha_2\beta_1 - \alpha_1\beta_2}{\alpha_1\beta_2\gamma_2} - \frac{\alpha_1^2\alpha_2\beta_1\beta_2^2\gamma_3x_2}{\alpha_2\beta_1} - \frac{\alpha_3(\alpha_2\beta_1 - \alpha_1\beta_2)}{\alpha_1\beta_2\gamma_2} & \frac{\alpha_1\beta_2 - \alpha_2\beta_1}{\beta_2\gamma_2} - \frac{\alpha_1\beta_2x_2}{\beta_1} \end{pmatrix}$$

with eigenvalues $\lambda_2 = 0$, $\lambda_3 = \frac{\alpha_3(\alpha_2\beta_1 - \alpha_1\beta_2)}{\alpha_1\beta_2\gamma_2} - \beta_3$, and the other two eigenvalues corresponding to the roots of the quadratic polynomial

$$p(\lambda) = \lambda^2 + \left[\frac{\alpha_1\beta_2x_2}{\beta_1} + \frac{\alpha_2\beta_1 - \alpha_1\beta_2}{\beta_2\gamma_2} \right] \lambda + (\alpha_2\beta_1 - \alpha_1\beta_2)x_2$$

i.e.,

$$\lambda_{1/4} = \frac{1}{2} \left[-\left(\frac{\alpha_1\beta_2x_2}{\beta_1} + \frac{\alpha_2\beta_1 - \alpha_1\beta_2}{\beta_2\gamma_2} \right) \pm \sqrt{\left(\frac{\alpha_1\beta_2x_2}{\beta_1} + \frac{\alpha_2\beta_1 - \alpha_1\beta_2}{\beta_2\gamma_2} \right)^2 - 4(\alpha_2\beta_1 - \alpha_1\beta_2)x_2} \right]$$

In this case, $\lambda_{1/4} \notin \mathbb{R}$ if and only if

$$\frac{\alpha_1^2\beta_2^2}{\beta_1^2}x_2^2 + 2\left[\frac{\alpha_1}{\beta_1\gamma_2} - 2\right](\alpha_2\beta_1 - \alpha_1\beta_2)x_2 + \left(\frac{\alpha_2\beta_1 - \alpha_1\beta_2}{\beta_2\gamma_2}\right) < 0$$

This happens if and only if the following two conditions are met simultaneously

$$\frac{\alpha_1}{\beta_1\gamma_2} < 1 \quad (86)$$

$$K_- = \frac{\beta_1^2}{\alpha_1^2\beta_2^2} \left[2 - \frac{\alpha_1}{\beta_1\gamma_2} - 2\sqrt{1 - \frac{\alpha_1}{\beta_1\gamma_2}} \right] (\alpha_2\beta_1 - \alpha_1\beta_2) < x_2 < \frac{\beta_1^2}{\alpha_1^2\beta_2^2} \left[2 - \frac{\alpha_1}{\beta_1\gamma_2} + 2\sqrt{1 - \frac{\alpha_1}{\beta_1\gamma_2}} \right] (\alpha_2\beta_1 - \alpha_1\beta_2) = K_+ \quad (87)$$

Under these conditions $Re(\lambda_{1/4}) < 0$.

On the other hand, if $\lambda_{1/4} \in \mathbb{R}$, i.e., if conditions (86) or (87) are not met, given that $\alpha_2\beta_1 > \alpha_1\beta_2$, then $\lambda_{1/4} < 0$. Thus, given that $\lambda_3 < 0$ if and only if $\alpha_2\beta_1 > \alpha_1\beta_2 + \frac{\alpha_1\beta_2\beta_3\gamma_2}{\alpha_3}$, then the object

$$W_7 = \left\{ \left(\frac{\alpha_2\beta_1 - \alpha_1\beta_2}{\alpha_1\beta_2\gamma_2}, x_2, 0, \frac{\beta_1}{\alpha_1} \right) : x_2 > 0 \right\}$$

is an attractor if and only if $\alpha_2\beta_1 > \alpha_1\beta_2 + \frac{\alpha_1\beta_2\beta_3\gamma_2}{\alpha_3}$, while there are no repelling objects.

Case 8

Defining

$$Q = \frac{\alpha_2\beta_3 - \alpha_3(\beta_2 + \mu_2M_1)(1 + \gamma_3M_1)}{\alpha_3\gamma_2(\beta_2 + \mu_2M_1)}$$

We have

$$J\left(Q, x_2, M_1, \frac{\beta_3}{\alpha_3}\right) = \begin{pmatrix} 0 & 0 & -\frac{\alpha_3\gamma_1(\beta_1 + \mu_1M_1)Q}{\alpha_1\beta_3} - \mu_1Q & \frac{\alpha_3(\beta_1 + \mu_1M_1)Q}{\beta_3} \\ -\frac{\alpha_3\gamma_2(\beta_2 + \mu_2M_1)^2x_2}{\alpha_2\beta_3} & 0 & -\frac{\alpha_3\gamma_3(\beta_2 + \mu_2M_1)^2x_2}{\alpha_2\beta_3} - \mu_2x_2 & \frac{\alpha_3(\beta_2 + \mu_2M_1)x_2}{\beta_3} \\ 0 & 0 & 0 & \alpha_3M_1 \\ \frac{\alpha_3\gamma_2(\beta_2 + \mu_2M_1)^2x_2}{\alpha_2\beta_3} & 0 & \mu_1Q + \mu_2x_2 + \frac{\alpha_3\gamma_1(\beta_1 + \mu_1M_1)Q}{\alpha_1\beta_3} + \frac{\alpha_3\gamma_3(\beta_2 + \mu_2M_1)^2x_2}{\alpha_2\beta_3} & -\alpha_3M_1 - \frac{\alpha_3(\beta_1 + \mu_1M_1)Q}{\beta_3} - \frac{\alpha_3(\beta_2 + \mu_2M_1)x_2}{\beta_3} \end{pmatrix}$$

with eigenvalues $\lambda_2 = 0$, and the other eigenvalues corresponding to the roots of the cubic polynomial

$$p(\lambda) = \lambda^3 - J_{44}\lambda^2 - [J_{14}J_{41} + \alpha_3M_1J_{43}]\lambda - \alpha_3M_1J_{13}J_{41}$$

where

$$J_{13} = -\frac{\alpha_3\gamma_1(\beta_1 + \mu_1M_1)Q}{\alpha_1\beta_3} - \mu_1Q$$

$$J_{14} = \frac{\alpha_3(\beta_1 + \mu_1M_1)Q}{\beta_3}$$

$$J_{41} = \frac{\alpha_3\gamma_2(\beta_2 + \mu_2M_1)^2x_2}{\alpha_2\beta_3}$$

$$J_{43} = \mu_1Q + \mu_2x_2 + \frac{\alpha_3\gamma_1(\beta_1 + \mu_1M_1)Q}{\alpha_1\beta_3} + \frac{\alpha_3\gamma_3(\beta_2 + \mu_2M_1)^2x_2}{\alpha_2\beta_3}$$

$$J_{44} = -\alpha_3M_1 - \frac{\alpha_3(\beta_1 + \mu_1M_1)Q}{\beta_3} - \frac{\alpha_3(\beta_2 + \mu_2M_1)x_2}{\beta_3}$$

Summary of stability conditions for model II-A

1. The object $W_1 = W_1^s = \left\{ (0, 0, 0, x_4) : x_4 < \min \left\{ \frac{\beta_1}{\alpha_1}, \frac{\beta_2}{\alpha_2}, \frac{\beta_3}{\alpha_3} \right\} \right\}$ is an attractor, while the object $W_1^u = \left\{ (0, 0, 0, x_4) : x_4 > \max \left\{ \frac{\beta_1}{\alpha_1}, \frac{\beta_2}{\alpha_2}, \frac{\beta_3}{\alpha_3} \right\} \right\}$ is a repeller.
2. The object $W_2 = \left\{ \left(0, 0, x_3, \frac{\beta_3}{\alpha_3} \right) : x_3 > \max \{0, M_1, M_2\} \right\}$ is an attractor, where $M_1 \leq 0$ if and only if condition (82) is satisfied, while $M_2 \leq 0$ if and only if (84) is satisfied. There are no repellers.
3. The object $W_3 = \left\{ \left(0, x_2, 0, \frac{\beta_2}{\alpha_2} \right) : x_2 > 0 \right\}$ is an attractor if and only if $\alpha_1\beta_2 < \alpha_2\beta_1$ and $\alpha_3\beta_2 < \alpha_2\beta_3$. There are no repellers.
4. Points of the form $\left(0, x_2, M_2, \frac{\beta_3}{\alpha_3} \right)$ are neither attractors nor repellers.
5. $W_5 = \left\{ \left(x_1, 0, 0, \frac{\beta_1}{\alpha_1} \right) : x_1 > \max \left\{ 0, \frac{\alpha_2\beta_1 - \alpha_1\beta_2}{\alpha_1\beta_2\gamma_2} \right\} \right\}$ is an attractor if and only if $\alpha_3\beta_1 < \alpha_1\beta_3$. There are no repellers.
6. Points of the form $\left(x_1, 0, M_1, \frac{\beta_3}{\alpha_3} \right)$ are neither attractors nor repellers.
7. $W_7 = \left\{ \left(\frac{\alpha_2\beta_1 - \alpha_1\beta_2}{\alpha_1\beta_2\gamma_2}, x_2, 0, \frac{\beta_1}{\alpha_1} \right) : x_2 > 0 \right\}$ is an attractor if and only if $\alpha_2\beta_1 > \alpha_1\beta_2 + \frac{\alpha_1\beta_2\beta_3\gamma_2}{\alpha_3}$. There are no repellers.
8. Deriving the stability conditions for points of the form $\left(Q, x_2, M_1, \frac{\beta_3}{\alpha_3} \right)$ requires solving a cubic polynomial.

Note that, in general, there is multi-stability. Specifically, for adequately chosen parameter values the system can converge to a stable coexistence between species x_1 and x_2 , stably displacing species x_3 .

Note further that, in general, the stable coexistence between species x_3 with any of the native species is not possible.

In general, the system can converge to the local extinction of all species (case 1), to the survival of one of the species only (cases 2, 3 and 5) or to the coexistence between x_1 and x_2 (case 7).

Model II-B: 3D with positive interactions between natives

$$\left\{ \begin{array}{l} \frac{dBS}{dt} = \frac{\alpha_{BS}(BS)(SL)}{1 + \gamma_{EB}(ES)} - (BS)(\beta_{BS} + \mu_{EB}(ES)) \end{array} \right. \quad (31)$$

$$\left\{ \begin{array}{l} \frac{dPS}{dt} = \frac{\alpha_{PS}(PS)(SL)(1 + \theta_{BP}(BS))}{1 + \gamma_{EP}(ES)} - (PS)(\beta_{PS} + \mu_{EP}(ES)) \end{array} \right. \quad (32)$$

$$\left\{ \begin{array}{l} \frac{dES}{dt} = \alpha_{ES}(ES)(SL) - \beta_{ES}(ES) \end{array} \right. \quad (33)$$

$$\left\{ \begin{array}{l} \frac{dSL}{dt} = \beta_{ES}(ES) + (PS)(\beta_{PS} + \mu_{EP}(ES)) + (BS)(\beta_{BS} + \mu_{EB}(ES)) - \alpha_{ES}(ES)(SL) - \frac{\alpha_{PS}(PS)(SL)(1 + \theta_{BP}(BS))}{1 + \gamma_{EP}(ES)} - \frac{\alpha_{BS}(BS)(SL)}{1 + \gamma_{EB}(ES)} \end{array} \right. \quad (34)$$

To simplify notations, we denote $BS(t) = x_1(t)$, $PS(t) = x_2(t)$, $ES(t) = x_3(t)$, $SL(t) = x_4(t)$, $\alpha_{BS} = \alpha_1$, $\alpha_{PS} = \alpha_2$, $\alpha_{ES} = \alpha_3$, $\beta_{BS} = \beta_1$, $\beta_{PS} = \beta_2$, $\beta_{ES} = \beta_3$, $\gamma_{EB} = \gamma_1$, $\gamma_{EP} = \gamma_2$, $\theta_{BP} = \theta$, $\mu_{EB} = \mu_1$, $\mu_{EP} = \mu_2$.

Also, this model satisfies the conservation equations and can hence be reduced to 3D:

$$\frac{dx_1}{dt} + \frac{dx_2}{dt} + \frac{dx_3}{dt} + \frac{dx_4}{dt} = 0 \quad (35)$$

Equilibrium points of the model

Given the linear dependency of equations (31)-(34), we may consider only 3 of them. Thus, a point of the form (x_1, x_2, x_3, x_4) is an equilibrium point of the system (31)-(34) if and only if following system of equations is satisfied:

$$\left\{ \begin{array}{l} [\alpha_1 x_4 - (1 + \gamma_1 x_3)(\beta_1 + \mu_1 x_3)]x_1 = 0 \end{array} \right. \quad (36)$$

$$\left\{ \begin{array}{l} [\alpha_2 x_4(1 + \theta x_1) - (1 + \gamma_2 x_3)(\beta_2 + \mu_2 x_3)]x_2 = 0 \end{array} \right. \quad (37)$$

$$\left\{ \begin{array}{l} [\alpha_3 x_4 - \beta_3]x_3 = 0 \end{array} \right. \quad (38)$$

We will consider the equilibrium points by cases:

1. If $x_1 = 0$, then $(0, x_2, x_3, x_4)$ is an equilibrium point of (31)-(34) if and only if it satisfies following system of equations:

$$\left\{ \begin{array}{l} [\alpha_2 x_4 - (1 + \gamma_2 x_3)(\beta_2 + \mu_2 x_3)]x_2 = 0 \end{array} \right. \quad (39)$$

$$\left\{ \begin{array}{l} [\alpha_3 x_4 - \beta_3]x_3 = 0 \end{array} \right. \quad (40)$$

1.1. If $x_2 = 0$, then $[\alpha_3 x_4 - \beta_3]x_3 = 0$. We have two types of equilibrium points: Those with the form

$(0, 0, 0, x_4)$, $x_4 \geq 0$ and those with the form $\left(0, 0, x_3, \frac{\beta_3}{\alpha_3}\right)$, $x_3 \geq 0$.

1.2. If $x_2 > 0$, then we can identify two new cases:

1.2.1. If $x_3 = 0$, then the equilibrium points are of the form $\left(0, x_2, 0, \frac{\beta_2}{\alpha_2}\right)$, $x_2 > 0$.

1.2.2. If $x_3 > 0$, then $x_4 = \frac{\beta_3}{\alpha_3}$ and x_3 is solution to

$$\gamma_2\mu_2x_3^2 + [\beta_2\gamma_2 + \mu_2]x_3 + \beta_2 - \frac{\alpha_2\beta_3}{\alpha_3} = 0 \quad (41)$$

with which we obtain following solutions:

$$x_3^\pm = \frac{1}{2\beta_2\gamma_2} \left[-(\beta_2\gamma_2 + \mu_2) \pm \sqrt{(\beta_2\gamma_2 - \mu_2)^2 + \frac{4\alpha_2\beta_3\gamma_2\mu_2}{\alpha_3}} \right] \quad (42)$$

Note that solution x_3^\pm is always real. However, x_3^- is always negative, and thus we can discard this case and consider only $x_3 = x_3^+$. On the other hand, given that all the parameters are positive, $x_3^+ > 0$ if and only if $\beta_2\alpha_3 < \beta_3\alpha_2$.

2. If $x_1 > 0$, then solving (36)-(38) is equivalent to solving

$$\left\{ \begin{array}{l} \alpha_1x_4 - (1 + \gamma_1x_3)(\beta_1 + \mu_1x_3) = 0 \\ [\alpha_2x_4(1 + \theta x_1) - (1 + \gamma_2x_3)(\beta_2 + \mu_2x_3)]x_2 = 0 \end{array} \right. \quad (43)$$

$$\left\{ \begin{array}{l} \alpha_1x_4 - (1 + \gamma_1x_3)(\beta_1 + \mu_1x_3) = 0 \\ [\alpha_3x_4 - \beta_3]x_3 = 0 \end{array} \right. \quad (44)$$

$$\left\{ \begin{array}{l} \alpha_1x_4 - (1 + \gamma_1x_3)(\beta_1 + \mu_1x_3) = 0 \\ [\alpha_3x_4 - \beta_3]x_3 = 0 \end{array} \right. \quad (45)$$

2.1. If $x_2 = 0$, then solving (43)-(45) is in turn equivalent to solving

$$\left\{ \begin{array}{l} \alpha_1x_4 - (1 + \gamma_1x_3)(\beta_1 + \mu_1x_3) = 0 \\ [\alpha_3x_4 - \beta_3]x_3 = 0 \end{array} \right. \quad (43)$$

$$\left\{ \begin{array}{l} \alpha_1x_4 - (1 + \gamma_1x_3)(\beta_1 + \mu_1x_3) = 0 \\ [\alpha_3x_4 - \beta_3]x_3 = 0 \end{array} \right. \quad (45)$$

2.1.1. If $x_3 = 0$, then $x_4 = \frac{\beta_1}{\alpha_1}$, through which we obtain equilibrium points of the form $\left(x_1, 0, 0, \frac{\beta_1}{\alpha_1}\right)$, $x_1 > 0$.

2.1.2. If $x_3 > 0$, then $x_4 = \frac{\beta_3}{\alpha_3}$ and x_3 solve

$$\gamma_1\mu_1x_3^2 + [\beta_1\gamma_1 + \mu_1]x_3 + \beta_1 - \frac{\alpha_1\beta_3}{\alpha_3} = 0$$

with which

$$x_3^\pm = \frac{1}{2\gamma_1\mu_1} \left[-(\beta_1\gamma_1 + \mu_1) \pm \sqrt{(\beta_1\gamma_1 - \mu_1)^2 + \frac{4\alpha_1\beta_3\gamma_1\mu_1}{\alpha_3}} \right] \quad (46)$$

As in case 1.2.2, $x_3^\pm \in \mathbb{R}$ and $x_3^- < 0$, and therefore in this case we can discard the second solution, keeping only $x_3 = x_3^+$. Analogously to case 1.2.2, $x_3^+ > 0$ if and only if $\beta_1\alpha_3 < \alpha_1\beta_3$.

2.2. If $x_2 > 0$, then solving (43)-(45) is equivalent to solving

$$\left\{ \begin{array}{l} \alpha_1x_4 - (1 + \gamma_1x_3)(\beta_1 + \mu_1x_3) = 0 \\ \alpha_2x_4(1 + \theta x_1) - (1 + \gamma_2x_3)(\beta_2 + \mu_2x_3) = 0 \end{array} \right. \quad (47)$$

$$\left\{ \begin{array}{l} \alpha_2x_4(1 + \theta x_1) - (1 + \gamma_2x_3)(\beta_2 + \mu_2x_3) = 0 \\ [\alpha_3x_4 - \beta_3]x_3 = 0 \end{array} \right. \quad (48)$$

$$\left\{ \begin{array}{l} [\alpha_3x_4 - \beta_3]x_3 = 0 \end{array} \right. \quad (49)$$

2.2.1. If $x_3 = 0$, then $x_4 = \frac{\beta_1}{\alpha_1}$ and

$$\frac{\alpha_2\beta_1}{\alpha_1}(1 + \theta x_1) - \beta_2 = 0 \quad (50)$$

with which $x_1 = \frac{\alpha_1\beta_2 - \alpha_2\beta_1}{\alpha_2\beta_1\theta}$, where $x_1 > 0$ if and only if $\alpha_1\beta_2 > \alpha_2\beta_1$, obtaining in this case equilibrium points of the form $\left(\frac{\alpha_1\beta_2 - \alpha_2\beta_1}{\alpha_2\beta_1\theta}, x_2, 0, \frac{\beta_1}{\alpha_1} \right)$, $x_2 > 0$.

2.2.2. If $x_3 > 0$, then $x_4 = \frac{\beta_3}{\alpha_3}$ and x_1, x_3 solve

$$\left\{ \begin{array}{l} \gamma_1\mu_1x_3^2 + [\beta_1\gamma_1 + \mu_1]x_3 + \frac{\alpha_3\beta_1 - \alpha_1\beta_3}{\alpha_3} = 0 \end{array} \right. \quad (51)$$

$$\left\{ \begin{array}{l} \gamma_2\mu_2x_3^2 + [\beta_2\gamma_2 + \mu_2]x_3 + \frac{\alpha_3\beta_2 - \alpha_2\beta_3}{\alpha_3} - \frac{\alpha_2\beta_3\theta}{\alpha_3}x_1 = 0 \end{array} \right. \quad (52)$$

From (51) we obtain that

$$x_3^\pm = \frac{1}{2\gamma_1\mu_1} \left[-(\beta_1\gamma_1 + \mu_1) \pm \sqrt{(\beta_1\gamma_1 - \mu_1)^2 + \frac{4\alpha_1\beta_3\gamma_1\mu_1}{\alpha_3}} \right] \quad (53)$$

As with previous cases, $x_3^\pm \in \mathbb{R}$ and $x_3^- < 0$, and therefore we only consider case $x_3 = x_3^+$. Further, $x_3^+ > 0$ if and only if $\alpha_3\beta_1 < \alpha_1\beta_3$.

Thus, writing

$$K = \frac{\alpha_3\beta_2 - \alpha_2\beta_3 + 4\alpha_1\beta_3\gamma_1\mu_1}{\alpha_3} + 2(\beta_1^2\gamma_1^2 + \mu_1^2)$$

$$M = \beta_2\gamma_2 + \mu_2 - 2\gamma_2\mu_2(\beta_1\gamma_1 + \mu_1), \quad N = (\beta_1\gamma_1 - \mu_1)^2 + \frac{4\alpha_1\beta_3\gamma_1\mu_1}{\alpha_3}$$

substituting $x_3 = x_3^+$ in (52), we obtain that

$$x_1 = K + M \sqrt{N} \quad (54)$$

where $x_1 > 0$ if and only if one of the following conditions is satisfied:

$$K > 0 \geq -M \quad \text{or} \quad K \geq 0 > -M \quad (55)$$

$$K \geq 0 \quad \text{and} \quad M \leq 0 \quad \text{and} \quad K^2 > M^2N \quad (56)$$

$$K \leq 0 \quad \text{and} \quad M \geq 0 \quad \text{and} \quad K^2 < M^2N \quad (57)$$

Note that these conditions don't exclude each other.

Summary of equilibrium points of model II-B

Model II-B can display following equilibrium points:

1. Equilibrium points of the form $(0, 0, 0, x_4)$, $x_4 \geq 0$.

2. Equilibrium points of the form $\left(0, 0, x_3, \frac{\beta_3}{\alpha_3}\right)$, $x_3 \geq 0$.

3. Points of the form $\left(0, x_2, 0, \frac{\beta_2}{\alpha_2}\right)$, $x_2 > 0$.

4. Points of the form $\left(0, x_2, \frac{1}{2\gamma_2\mu_2} \left[-(\beta_2\gamma_2 + \mu_2) + \sqrt{(\beta_2\gamma_2 - \mu_2)^2 + \frac{4\alpha_2\beta_3\gamma_2\mu_2}{\alpha_3}} \right], \frac{\beta_3}{\alpha_3}\right)$, $x_2 > 0$, as long as $\alpha_3\beta_2 < \beta_3\alpha_2$.

5. Points of the form $\left(x_1, 0, 0, \frac{\beta_1}{\alpha_1}\right)$, $x_1 > 0$.

6. Points of the form $\left(x_1, 0, \frac{1}{2\gamma_1\mu_1} \left[-(\beta_1\gamma_1 + \mu_1) + \sqrt{(\beta_1\gamma_1 - \mu_1)^2 + \frac{4\alpha_1\beta_3\gamma_1\mu_1}{\alpha_3}} \right], \frac{\beta_3}{\alpha_3}\right)$, $x_1 > 0$, as long as $\alpha_3\beta_1 < \alpha_1\beta_3$.

7. Points of the form $\left(\frac{\alpha_1\beta_2 - \alpha_2\beta_1}{\alpha_2\beta_1\theta}, x_2, 0, \frac{\beta_1}{\alpha_1}\right)$, $x_2 > 0$, as long as $\alpha_1\beta_2 > \alpha_2\beta_1$.

8. Points of the form $\left(K + M\sqrt{N}, x_2, \frac{1}{2\gamma_1\mu_1} \left[-(\beta_1\gamma_1 + \mu_1) + \sqrt{(\beta_1\gamma_1 - \mu_1)^2 + \frac{4\alpha_1\beta_3\gamma_1\mu_1}{\alpha_3}} \right], \frac{\beta_3}{\alpha_3}\right)$, $x_2 > 0$, as long as $\alpha_3\beta_1 < \alpha_1\beta_3$ and at least one of the conditions (55)-(57) are satisfied.

Note that it is possible to have the 8 types of equilibrium points simultaneously. Further, as with previous models, instead of isolated equilibrium points, we have "equilibrium sets", corresponding to line segments of infinite length.

Stability analysis of model II-B

As with previous models, given that there is a linear dependency between equations, our Jacobian matrices have a 0 determinant. Therefore, we proceed our analysis as with the previous cases: we look at the sign of the eigenvalues of the equilibrium objects. Additionally, we study the equilibrium points case by case.

For this model we have the Jacobian matrix

$$J(x_1, x_2, x_3, x_4) = \begin{pmatrix} \frac{\alpha_1x_4}{1+\gamma_1x_3} - (\beta_1 + \mu_1x_3) & 0 & -\mu_1x_1 - \frac{\alpha_1\gamma_1x_1x_4}{(1+\gamma_1x_3)^2} & \frac{\alpha_1x_1}{1+\gamma_1x_3} \\ \frac{\alpha_2\theta x_2x_4}{1+\gamma_2x_3} & \frac{\alpha_2x_4(1+\theta x_1)}{1+\gamma_2x_3} - (\beta_2 + \mu_2x_3) & -\mu_2x_1 - \frac{\alpha_2\gamma_2x_2x_4(1+\theta x_1)}{(1+\gamma_2x_3)^2} & \frac{\alpha_2x_2(1+\theta x_1)}{1+\gamma_2x_3} \\ 0 & 0 & \alpha_3x_4 - \beta_3 & \alpha_3x_3 \\ \beta_1 + \mu_1x_3 - \frac{\alpha_1x_4}{1+\gamma_1x_3} - \frac{\alpha_2\theta x_2x_4}{1+\gamma_2x_3} & \beta_2 + \mu_2x_3 - \frac{\alpha_2x_4(1+\theta x_1)}{1+\gamma_2x_3} & \beta_3 + \mu_2x_1 + \mu_1x_1 - \alpha_3x_4 + \frac{\alpha_1\gamma_1x_1x_4}{(1+\gamma_1x_3)^2} + \frac{\alpha_2\gamma_2x_2x_4(1+\theta x_1)}{(1+\gamma_2x_3)^2} & -\alpha_3x_3 - \frac{\alpha_2x_2(1+\theta x_1)}{1+\gamma_2x_3} \end{pmatrix}$$

Case 1

For the first type of equilibrium point we have:

$$J(0, 0, 0, x_4) = \begin{pmatrix} \alpha_1 x_4 - \beta_1 & 0 & 0 & 0 \\ 0 & \alpha_2 x_4 - \beta_2 & 0 & 0 \\ 0 & 0 & \alpha_3 x_4 - \beta_3 & 0 \\ \beta_1 - \alpha_1 x_4 & \beta_2 - \alpha_2 x_4 & \beta_3 - \alpha_3 x_4 & 0 \end{pmatrix}$$

this matrix has eigenvalues $\lambda_1 = \alpha_1 x_4 - \beta_1$, $\lambda_2 = \alpha_2 x_4 - \beta_2$, $\lambda_3 = \alpha_3 x_4 - \beta_3$, $\lambda_4 = 0$. Thus, $\lambda_1, \lambda_2, \lambda_3$ are simultaneously negative if and only if

$$x_4 < \min \left\{ \frac{\beta_1}{\alpha_1}, \frac{\beta_2}{\alpha_2}, \frac{\beta_3}{\alpha_3} \right\}$$

and they are simultaneously positive if and only if

$$x_4 > \max \left\{ \frac{\beta_1}{\alpha_1}, \frac{\beta_2}{\alpha_2}, \frac{\beta_3}{\alpha_3} \right\}$$

Thus, we have the attracting object

$$W_1 = W_1^s = \left\{ (0, 0, 0, x_4) : 0 < x_4 < \min \left\{ \frac{\beta_1}{\alpha_1}, \frac{\beta_2}{\alpha_2}, \frac{\beta_3}{\alpha_3} \right\} \right\}$$

and the object repeller

$$W_1^u = \left\{ (0, 0, 0, x_4) : x_4 > \max \left\{ \frac{\beta_1}{\alpha_1}, \frac{\beta_2}{\alpha_2}, \frac{\beta_3}{\alpha_3} \right\} \right\}$$

Case 2

We have that:

$$J\left(0, 0, x_3, \frac{\beta_3}{\alpha_3}\right) = \begin{pmatrix} \frac{\alpha_1\beta_3}{\alpha_3(1+\gamma_1x_3)} - (\beta_1 + \mu_1x_3) & 0 & 0 & 0 \\ 0 & \frac{\alpha_2\beta_3}{\alpha_3(1+\gamma_2x_3)} - (\beta_2 + \mu_2x_3) & 0 & 0 \\ 0 & 0 & 0 & \alpha_3x_3 \\ \beta_1 + \mu_1x_3 - \frac{\alpha_1\beta_3}{\alpha_3(1+\gamma_1x_3)} & \beta_2 + \mu_2x_3 - \frac{\alpha_2\beta_3}{\alpha_3(1+\gamma_2x_3)} & 0 & -\alpha_3x_3 \end{pmatrix}$$

has eigenvalues $\lambda_1 = \frac{\alpha_1\beta_3}{\alpha_3(1+\gamma_1x_3)} - (\beta_1 + \mu_1x_3)$, $\lambda_2 = \frac{\alpha_2\beta_3}{\alpha_3(1+\gamma_2x_3)} - (\beta_2 + \mu_2x_3)$, $\lambda_3 = 0$, $\lambda_4 = -\alpha_3x_3$. On the one hand, $\lambda_1 < 0$ if and only if

$$\gamma_1\mu_1x_3^2 + [\beta_1\gamma_1 + \mu_1]x_3 + \beta_1 - \frac{\alpha_1\beta_3}{\alpha_3} > 0 \quad (58)$$

Condition (58) is equivalent to

$$x_3 > \left[-(\beta_1\gamma_1 + \mu_1) + \sqrt{(\beta_1\gamma_1 - \mu_1)^2 + \frac{4\alpha_1\beta_3\gamma_1\mu_1}{\alpha_3}} \right] \frac{1}{2\gamma_1\mu_1} \quad (59)$$

Specifically, defining for each $i = 1, 2$ the magnitudes

$$N_i = \left[-(\beta_i\gamma_i + \mu_i) + \sqrt{(\beta_i\gamma_i - \mu_i)^2 + \frac{4\alpha_i\beta_3\gamma_i\mu_i}{\alpha_3}} \right] \frac{1}{2\gamma_i\mu_i} \quad (60)$$

we obtain that $\lambda_1 < 0$ and $\lambda_2 < 0$ simultaneously if and only if

$$x_3 > \max \{N_1, N_2\}$$

because $\lambda_4 < 0$ for all $x_3 > 0$, we that an attracting object of the form:

$$W_2 = \left\{ \left(0, 0, x_3, \frac{\beta_3}{\alpha_3}\right) : x_3 > \max \{N_1, N_2\} \right\}$$

exists, while there no repellers in this case.

Case 3

We have that

$$J\left(0, x_2, 0, \frac{\beta_2}{\alpha_2}\right) = \begin{pmatrix} \frac{\alpha_1\beta_2 - \alpha_2\beta_1}{\alpha_2} & 0 & 0 & 0 \\ \beta_2\theta x_2 & 0 & \beta_2\gamma_2 x_2 & \alpha_2 x_2 \\ 0 & 0 & \frac{\alpha_3\beta_2 - \alpha_2\beta_3}{\alpha_2} & 0 \\ \frac{\alpha_2\beta_1 - \alpha_1\beta_2}{\alpha_2} - \beta_2\theta x_2 & 0 & \frac{\alpha_2\beta_3 - \alpha_3\beta_2}{\alpha_2} - \beta_2\gamma_2 x_2 & -\alpha_2 x_2 \end{pmatrix}$$

has eigenvalues $\lambda_1 = \frac{\alpha_1\beta_2 - \alpha_2\beta_1}{\alpha_2}$, $\lambda_2 = 0$, $\lambda_3 = \frac{\alpha_3\beta_2 - \alpha_2\beta_3}{\alpha_2}$, $\lambda_4 = -\alpha_2 x_2$. Note that λ_4 is always negative.

Thus, if $\alpha_1\beta_2 < \alpha_2\beta_1$ and $\alpha_3\beta_2 < \alpha_2\beta_3$ simultaneously, we get that the object

$$W_3 = \left\{ \left(0, x_2, 0, \frac{\beta_2}{\alpha_2}\right) : 0 < x_2 \right\}$$

is an attractor. There are no repelling objects.

Case 4

In this case, using that, per definition, N_2 is such that

$$\frac{\alpha_2\beta_3}{\alpha_3(1 + \gamma_2 N_2)} - (\beta_2 + \mu_2 N_2) = 0$$

We get the Jacobian matrix

$$J\left(0, x_2, N_2, \frac{\beta_3}{\alpha_3}\right) = \begin{pmatrix} \frac{\alpha_1\beta_3}{\alpha_3(1 + \gamma_1 N_2)} - (\beta_1 + \mu_1 N_2) & 0 & 0 & 0 \\ \frac{\alpha_2\beta_3\theta x_2}{\alpha_3(1 + \gamma_2 N_2)} & 0 & -\frac{\alpha_2\beta_3\gamma_2 x_2}{\alpha_3(1 + \gamma_2 N_2)^2} & \frac{\alpha_2 x_2}{1 + \gamma_2 N_2} \\ 0 & 0 & 0 & \alpha_3 N_2 \\ \beta_1 + \mu_1 N_2 - \frac{\alpha_1\beta_3}{\alpha_3(1 + \gamma_1 N_2)} - \frac{\alpha_2\beta_3\theta x_2}{\alpha_3(1 + \gamma_2 N_2)} & 0 & \frac{\alpha_2\beta_3\gamma_2 x_2}{\alpha_3(1 + \gamma_2 N_2)^2} & -\alpha_3 N_2 - \frac{\alpha_2 x_2}{1 + \gamma_2 N_2} \end{pmatrix}$$

with eigenvalues $\lambda_1 = \frac{\alpha_1\beta_3}{\alpha_3(1 + \gamma_1N_2)} - (\beta_1 + \mu_1N_2)$, $\lambda_2 = 0$,

$$\lambda_{3/4} = \frac{1}{2} \left[-\left(\alpha_3N_2 + \frac{\alpha_2x_2}{1 + \gamma_2N_2} \right) \pm \sqrt{\left(\alpha_3N_2 + \frac{\alpha_2x_2}{1 + \gamma_2N_2} \right)^2 + \frac{4\alpha_2\beta_3\gamma_2N_2x_2}{(1 + \gamma_2N_2)^2}} \right]$$

Note that $\lambda_{3/4} \in \mathbb{R}$. Further, note that

$$\frac{1}{2} \left[-\left(\alpha_3N_2 + \frac{\alpha_2x_2}{1 + \gamma_2N_2} \right) - \sqrt{\left(\alpha_3N_2 + \frac{\alpha_2x_2}{1 + \gamma_2N_2} \right)^2 + \frac{4\alpha_2\beta_3\gamma_2N_2x_2}{(1 + \gamma_2N_2)^2}} \right] < 0$$

While

$$\frac{1}{2} \left[-\left(\alpha_3N_2 + \frac{\alpha_2x_2}{1 + \gamma_2N_2} \right) + \sqrt{\left(\alpha_3N_2 + \frac{\alpha_2x_2}{1 + \gamma_2N_2} \right)^2 + \frac{4\alpha_2\beta_3\gamma_2N_2x_2}{(1 + \gamma_2N_2)^2}} \right] > 0$$

Then, there are neither attractors nor repellers in this case.

Case 5

In this case we have that

$$J\left(x_1, 0, 0, \frac{\beta_1}{\alpha_1}\right) = \begin{pmatrix} 0 & 0 & -[\mu_1 + \beta_1\gamma_1]x_1 & \alpha_1x_1 \\ 0 & \frac{\alpha_2\beta_1 - \alpha_1\beta_2 + \alpha_2\beta_1\theta x_1}{\alpha_1} & -\mu_2x_1 & 0 \\ 0 & 0 & \frac{\alpha_2\beta_1 - \alpha_1\beta_2}{\alpha_1} & 0 \\ 0 & \frac{\alpha_1\beta_2 - \alpha_2\beta_1 - \alpha_2\beta_1\theta x_1}{\alpha_1} & [\mu_1 + \beta_1\gamma_1 + \mu_2]x_1 + \frac{\alpha_1\beta_2 - \alpha_2\beta_1}{\alpha_1} & -\alpha_1x_1 \end{pmatrix}$$

has eigenvalues $\lambda_1 = 0$, $\lambda_2 = \frac{\alpha_2\beta_1 - \alpha_1\beta_2 + \alpha_2\beta_1\theta x_1}{\alpha_1}$, $\lambda_3 = \frac{\alpha_2\beta_1 - \alpha_1\beta_2}{\alpha_1}$, $\lambda_4 = -\alpha_1x_1$. Note that λ_4 is always negative. On the other hand, $\lambda_3 < 0$ if and only if $\alpha_2\beta_1 < \alpha_1\beta_2$. Lastly, $\lambda_2 < 0$ if and only if

$$x_1 < \frac{\alpha_1\beta_2 - \alpha_2\beta_1}{\alpha_2\beta_1\theta}$$

Thus, if $\alpha_2\beta_1 < \alpha_1\beta_2$, we get that the object

$$W_5 = \left\{ \left(x_1, 0, 0, \frac{\beta_1}{\alpha_1} \right) : x_1 < \frac{\alpha_1\beta_2 - \alpha_2\beta_1}{\alpha_2\beta_1\theta} \right\}$$

is an attractor. There are no repellers in this case.

Case 6

In this case, using that, per definition, N_1 is such that

$$\frac{\alpha_1\beta_3}{\alpha_3(1 + \gamma_1N_1)} - (\beta_1 + \mu_1N_1) = 0$$

We obtain the Jacobian matrix:

$$J \left(x_1, 0, N_1, \frac{\beta_3}{\alpha_3} \right) = \begin{pmatrix} 0 & 0 & -\mu_1x_1 - \frac{\alpha_1\beta_3\gamma_1x_1}{\alpha_3(1 + \gamma_1N_1)^2} & \frac{\alpha_1x_1}{1 + \gamma_1N_1} \\ 0 & \frac{\alpha_2\beta_3(1 + \theta x_1)}{\alpha_3(1 + \gamma_2N_1)} - (\beta_2 + \mu_2N_1) & -\mu_2x_1 & 0 \\ 0 & 0 & 0 & \alpha_3N_1 \\ 0 & \beta_2 + \mu_2N_1 - \frac{\alpha_2\beta_3(1 + \theta x_1)}{\alpha_3(1 + \gamma_2N_1)} & [\mu_2 + \mu_1]x_1 + \frac{\alpha_1\beta_3\gamma_1x_1}{\alpha_3(1 + \gamma_1N_1)^2} & -\alpha_3N_1 - \frac{\alpha_1x_1}{1 + \gamma_1N_1} \end{pmatrix}$$

with eigenvalues $\lambda_1 = 0$. Its other 3 eigenvalues correspond to the roots of the cubic polynomial

$$p(\lambda) = \lambda^3 - [J_{22} + J_{44}]\lambda^2 + [J_{22}J_{44} - \alpha_3N_1J_{43}]\lambda + \alpha_3N_1[J_{22}J_{43} + \mu_2x_1J_{42}]$$

where

$$J_{22} = \frac{\alpha_2\beta_3(1 + \theta x_1)}{\alpha_3(1 + \gamma_2N_1)} - (\beta_2 + \mu_2N_1)$$

$$J_{44} = -\alpha_3N_1 - \frac{\alpha_1x_1}{1 + \gamma_1N_1}$$

$$J_{42} = \beta_2 + \mu_2N_1 - \frac{\alpha_2\beta_3(1 + \theta x_1)}{\alpha_3(1 + \gamma_2N_1)}$$

$$J_{43} = \left[\mu_2 + \mu_1 + \frac{\alpha_1 \beta_3 \gamma_1}{\alpha_3 (1 + \gamma_1 N_1)^2} \right] x_1$$

Writing

$$b = -[J_{22} + J_{44}], \quad c = J_{22}J_{44} - \alpha_3 N_1 J_{43}, \quad d = \alpha_3 N_1 [J_{22}J_{43} + \mu_2 x_1 J_{42}]$$

we can write a polynomial p of the form

$$p(\lambda) = \lambda^3 + b\lambda^2 + c\lambda + d$$

Case 7

We have that:

$$J\left(\frac{\alpha_1 \beta_2 - \alpha_2 \beta_1}{\alpha_2 \beta_1 \theta}, x_2, 0, \frac{\beta_1}{\alpha_1}\right) = \begin{pmatrix} 0 & 0 & -[\mu_1 + \beta_1 \gamma_1] \frac{\alpha_1 \beta_2 - \alpha_2 \beta_1}{\alpha_2 \beta_1 \theta} & \frac{\alpha_1 (\alpha_1 \beta_2 - \alpha_2 \beta_1)}{\alpha_2 \beta_1 \theta} \\ \frac{\alpha_2 \beta_1 \theta x_2}{\alpha_1} & 0 & -\beta_2 \gamma_2 x_2 - \frac{\mu_2 (\alpha_1 \beta_2 - \alpha_2 \beta_1)}{\alpha_2 \beta_1 \theta} & \frac{\alpha_1 \beta_2 x_2}{\beta_1} \\ 0 & 0 & \frac{\alpha_3 \beta_1 - \alpha_1 \beta_3}{\alpha_1} & 0 \\ -\frac{\alpha_2 \beta_1 \theta x_2}{\alpha_1} & 0 & [\mu_1 + \beta_1 \gamma_1] \frac{\alpha_1 \beta_2 - \alpha_2 \beta_1}{\alpha_2 \beta_1 \theta} + \beta_2 \gamma_2 x_2 + \frac{\mu_2 (\alpha_1 \beta_2 - \alpha_2 \beta_1)}{\alpha_2 \beta_1 \theta} + \frac{\alpha_1 \beta_3 - \alpha_3 \beta_1}{\alpha_1} & \frac{\alpha_1 (\alpha_2 \beta_1 - \alpha_1 \beta_2)}{\alpha_2 \beta_1 \theta} - \frac{\alpha_1 \beta_2 x_2}{\beta_1} \end{pmatrix}$$

has eigenvalues $\lambda_2 = 0$, $\lambda_3 = \frac{\alpha_3 \beta_1 - \alpha_1 \beta_3}{\alpha_1}$ and

$$\lambda_{1/4} = \frac{1}{2} \left[\frac{\alpha_1 (\alpha_2 \beta_1 - \alpha_1 \beta_2)}{\alpha_2 \beta_1 \theta} - \frac{\alpha_1 \beta_2 x_2}{\beta_1} \pm \sqrt{\frac{\alpha_1^2 \beta_2^2}{\beta_1^2} x_2^2 + 2 \left[\frac{\alpha_1^2 \beta_2 (\alpha_2 \beta_1 - \alpha_1 \beta_2)}{\alpha_2 \beta_1^2 \theta} + 2(\alpha_2 \beta_1 - \alpha_1 \beta_2) \right] x_2 + \frac{\alpha_1^2 (\alpha_2 \beta_1 - \alpha_1 \beta_2)^2}{\alpha_2^2 \beta_1^2 \theta^2}} \right]$$

Writing

$$P_{\pm} = \frac{\beta_1^2}{\alpha_1^2 \beta_2^2} \left[-\left(\frac{\alpha_1^2 \beta_2}{\alpha_2 \beta_1^2 \theta} + 2 \right) (\alpha_2 \beta_1 - \alpha_1 \beta_2) \pm 2 \sqrt{\left[\frac{\alpha_1^2 \beta_2}{\alpha_2 \beta_1^2 \theta} + 1 \right] (\alpha_2 \beta_1 - \alpha_1 \beta_2)^2} \right]$$

we have that if

$$\alpha_2 \beta_1 < \alpha_1 \beta_2 \quad (61)$$

or alternatively, if

$$\alpha_2\beta_1 > \alpha_1\beta_2 \quad \text{and} \quad \frac{\alpha_1^2\beta_2}{\alpha_2\beta_1^2\theta} < 1 \quad (62)$$

Then $\lambda_{1/4} \notin \mathbb{R}$ if and only if

$$0 < x_2 < P_+ \quad (63)$$

In this case, $\operatorname{Re}(\lambda_{1/4}) < 0$ as long as condition (61) is met, while $\operatorname{Re}(\lambda_{1/4}) > 0$ whenever condition (62) is met.

In case that $\lambda_{1/4} \in \mathbb{R}$, i.e., if neither (61) nor (62) can be verified, or if

$$x_2 > P_+$$

then $\lambda_{1/4} < 0$ if following conditions are met simultaneously:

$$\alpha_2\beta_1 < \alpha_1\beta_2 \quad (64)$$

$$x_2 > \frac{\alpha_1^2(\alpha_1\beta_2 - \alpha_2\beta_1)}{\alpha_2\theta(\alpha_1^2\beta_2 + \alpha_2\beta_1^2\theta)} \quad (65)$$

while it is not possible that $\lambda_1 > 0$ and $\lambda_4 > 0$ simultaneously. Note that condition (64) is the same as condition (61), which means that if (61) is satisfied, then for $x_2 > 0$ sufficiently large the system has complex eigenvalues.

Finally, given that $\lambda_3 < 0$ if and only if

$$\alpha_3\beta_1 < \alpha_1\beta_3 \quad (66)$$

Defining the sets

$$W_{7c}^s = \begin{cases} \left\{ \left(\frac{\alpha_1\beta_2 - \alpha_2\beta_1}{\alpha_2\beta_1\theta}, x_2, 0, \frac{\beta_1}{\alpha_1} \right) : 0 < x_2 < P_+ \right\} & \text{if both (61) and (66) are satisfied} \\ \emptyset & \text{otherwise} \end{cases}$$

and

$$W_{7r}^s = \begin{cases} \left\{ \left(\frac{\alpha_1\beta_2 - \alpha_2\beta_1}{\alpha_2\beta_1\theta}, x_2, 0, \frac{\beta_1}{\alpha_1} \right) : \max \left\{ P_+, \frac{\alpha_1^2(\alpha_1\beta_2 - \alpha_2\beta_1)}{\alpha_2\theta(\alpha_1^2\beta_2 + \alpha_2\beta_1^2\theta)} \right\} < x_2 \right\} & \text{if both (61) and (66) are satisfied} \\ \emptyset & \text{otherwise} \end{cases}$$

we obtain that the object

$$W_7 = W_{7c}^s \cup W_{7r}^s$$

is an attractor, while there are no repelling objects.

Case 8

Given that N_1 is such that

$$\frac{\alpha_1\beta_3}{\alpha_3(1 + \gamma_1 N_1)} = \beta_1 + \mu_1 N_1$$

and K, M, N are such that

$$\frac{\alpha_2\beta_3(1 + \theta(K + M\sqrt{N}))}{\alpha_3(1 + \gamma_2 N_1)} = \mu_2 N_1 + \beta_2$$

We get the Jacobian matrix:

$$J\left(K + M\sqrt{N}, x_2, N_1, \frac{\beta_3}{\alpha_3}\right) = \begin{pmatrix} 0 & 0 & -\left[\mu_1 + \frac{\gamma_1(\beta_1 + \mu_1 N_1)}{1 + \gamma_1 N_1}\right](K + M\sqrt{N}) & \frac{\alpha_3}{\beta_3}(\beta_1 + \mu_1 N_1)(K + M\sqrt{N}) \\ \frac{\alpha_2\beta_3\theta x_2}{\alpha_3(1 + \gamma_2 N_1)} & 0 & -\mu_2(K + M\sqrt{N}) - \frac{(\beta_2 + \mu_2 N_1)\gamma_2 x_2}{1 + \gamma_2 N_1} & (\beta_2 + \mu_2 N_1)\frac{\alpha_3}{\beta_2} \\ 0 & 0 & 0 & \alpha_3 N_1 \\ -\frac{\alpha_2\beta_3\theta x_2}{\alpha_3(1 + \gamma_2 N_1)} & 0 & \left[\mu_1 + \frac{\gamma_1(\beta_1 + \mu_1 N_1)}{1 + \gamma_1 N_1}\right](K + M\sqrt{N}) + \mu_2(K + M\sqrt{N}) + \frac{(\beta_2 + \mu_2 N_1)\gamma_2 x_2}{1 + \gamma_2 N_1} & -\frac{\alpha_3}{\beta_3}(\beta_1 + \mu_1 N_1)(K + M\sqrt{N}) - (\beta_2 + \mu_2 N_1)\frac{\alpha_3}{\beta_2} \end{pmatrix}$$

where this matrix anterior has an eigenvalue $\lambda_2 = 0$, while its other eigenvalues correspond to the roots of the cubic polynomial

$$p(\lambda) = \lambda^3 - J_{44}\lambda^2 - [\alpha_3 N_1 J - 43 - J_{14}J_{21}]\lambda + \alpha_3 N_1 J_{13}J_{21}$$

where

$$J_{13} = - \left[\mu_1 + \frac{\gamma_1(\beta_1 + \mu_1 N_1)}{1 + \gamma_1 N_1} \right] (K + M \sqrt{N})$$

$$J_{14} = \frac{\alpha_3}{\beta_3} (\beta_1 + \mu_1 N_1) (K + M \sqrt{N})$$

$$J_{21} = \frac{\alpha_2 \beta_3 \theta x_2}{\alpha_3 (1 + \gamma_2 N_1)}$$

$$J_{43} = \left[\mu_1 + \frac{\gamma_1(\beta_1 + \mu_1 N_1)}{1 + \gamma_1 N_1} \right] (K + M \sqrt{N}) + \mu_2 (K + M \sqrt{N}) + \frac{(\beta_2 + \mu_2 N_1) \gamma_2 x_2}{1 + \gamma_2 N_1}$$

$$J_{44} = - \frac{\alpha_3}{\beta_3} (\beta_1 + \mu_1 N_1) (K + M \sqrt{N}) - (\beta_2 + \mu_2 N_1) \frac{\alpha_3 x_2}{\beta_2} - \alpha_3 N_1$$

Summary of stability for model II-B

1. The object $W_1 = W_1^s = \left\{ (0, 0, 0, x_4) : 0 < x_4 < \min \left\{ \frac{\beta_1}{\alpha_1}, \frac{\beta_2}{\alpha_2}, \frac{\beta_3}{\alpha_3} \right\} \right\}$ is an attractor, while the object $W_1^u = \left\{ (0, 0, 0, x_4) : x_4 > \max \left\{ \frac{\beta_1}{\alpha_1}, \frac{\beta_2}{\alpha_2}, \frac{\beta_3}{\alpha_3} \right\} \right\}$ is a repeller.
2. The object $W_2 = \left\{ \left(0, 0, x_3, \frac{\beta_3}{\alpha_3} \right) : x_3 > \max \{ N_1, N_2 \} \right\}$ is an attractor. In this case there are no repellers.
3. The object $W_3 = \left\{ \left(0, x_2, 0, \frac{\beta_2}{\alpha_2} \right) : 0 < x_2 \right\}$ is an attractor if and only if $\alpha_1 \beta_2 < \alpha_2 \beta_1$ and $\alpha_3 \beta_2 < \alpha_2 \beta_3$. There are no repelling objects.
4. In this case, we have equilibrium points of the form $\left(0, x_2, N_2, \frac{\beta_3}{\alpha_3} \right)$, $x_2 > 0$. There are neither attractors nor repellers.
5. The object $W_5 = \left\{ \left(x_1, 0, 0, \frac{\beta_1}{\alpha_1} \right) : x_1 < \frac{\alpha_1 \beta_2 - \alpha_2 \beta_1}{\alpha_2 \beta_1 \theta} \right\}$ is an attractor if and only if $\alpha_2 \beta_1 < \alpha_1 \beta_2$

6. In this case, equilibria of the form $\left(x_1, 0, N_1, \frac{\beta_3}{\alpha_3}\right)$, $x_1 > 0$ has undetermined general stability conditions, however the eigenvalues can be obtained by solving a cubic function.

7. The object $W_7 = W_{7c}^s \cup W_{7r}^s$ is an attractor if and only if $\alpha_2\beta_1 < \alpha_1\beta_2$ and $\alpha_3\beta_1 < \alpha_1\beta_3$. In this case, we have that $W_{7c}^s = \left\{ \left(\frac{\alpha_1\beta_2 - \alpha_2\beta_1}{\alpha_2\beta_1\theta}, x_2, 0, \frac{\beta_1}{\alpha_1} \right) : 0 < x_2 < P_+ \right\}$, while $W_{7r}^s = \left\{ \left(\frac{\alpha_1\beta_2 - \alpha_2\beta_1}{\alpha_2\beta_1\theta}, x_2, 0, \frac{\beta_1}{\alpha_1} \right) : \max \left\{ P_+, \frac{\alpha_1^2(\alpha_1\beta_2 - \alpha_2\beta_1)}{\alpha_2\theta(\alpha_1^2\beta_2 + \alpha_2\beta_1^2\theta)} \right\} < x_2 \right\}$.

8. In this case, equilibria of the form $\left(K + M\sqrt{N}, x_2, N_1, \frac{\beta_3}{\alpha_3}\right)$, are like in case 6, i.e.it has undetermined general stability conditions; however, the eigenvalues can be obtained by solving a cubic function.

Note that also this model has multi-stability in certain cases. Specifically, W_1 and W_2 are always attractors. Nonetheless, W_3 cannot be an attractor simultaneously neither with the object W_5 nor with W_7 .

Specifically, from case 7 we obtain that it is possible that species x_1 and x_2 coexist, eventually expelling the invasive species x_3 , as long as the model parameters are appropriately chosen.

In general, the system can converge to the local extinction of all species (case 1), to the survival of one species only (cases 2, 3 and 5), or to the coexistence of species x_1 and x_2 (case 7). The coexistence of species x_3 is, in general, not possible.

Qualitative long-term behaviour of model II-B with nominal parameters

We assume following nominal values for the parameters

$$\begin{aligned} \alpha_1 &= 0.00137, & \beta_1 &= 0.07, & \gamma_1 &= 0.01, & \mu_1 &= 0.01, \\ \alpha_2 &= 0.0011, & \beta_2 &= 0.29, & \gamma_2 &= 0.01, & \mu_2 &= 0.01, \\ \alpha_3 &= 0.001, & \beta_3 &= 0.1, & \theta &= 0.0995, & ST &= 146.9 \end{aligned}$$

the conservation equation

$$x_4(t_0) = ST - x_1(t_0) - x_2(t_0) - x_3(t_0)$$

and an initial time-point corresponding to the measurements for year 1990, i.e., $t_0 = 1990$ as:

$$x_1(t_0) \approx 15.4666911395349, \quad x_2(t_0) \approx 0.07896, \quad x_3(t_0) \approx 8,9326$$

Variables x_1, x_2, x_3 are in units of occupied area, normalized by the known parameter ST , due to the relation

$$x_1(t) + x_2(t) + x_3(t) + x_4(t) = ST \quad (88)$$

Equilibrium conditions

We will look case by case if the equilibrium points derived previously are stable for these parameter values.

Case 1

We have that

$$\min \left\{ \frac{\beta_1}{\alpha_1}, \frac{\beta_2}{\alpha_2}, \frac{\beta_3}{\alpha_3} \right\} = 51.095, \quad \max \left\{ \frac{\beta_1}{\alpha_1}, \frac{\beta_2}{\alpha_2}, \frac{\beta_3}{\alpha_3} \right\} = 263,64$$

Given relation (88), and that in this case $x_1 = x_2 = x_3 = 0$, then

$$\min \left\{ \frac{\beta_1}{\alpha_1}, \frac{\beta_2}{\alpha_2}, \frac{\beta_3}{\alpha_3} \right\} = 51.095 < x_4 = ST = 146.9 < 263.64 = \max \left\{ \frac{\beta_1}{\alpha_1}, \frac{\beta_2}{\alpha_2}, \frac{\beta_3}{\alpha_3} \right\}$$

And therefore, equilibrium point $(0, 0, 0, ST)$ is neither an attractor nor a repeller.

Case 2

For this case we have

$$N_1 = 5.9327, \quad N_2 = -15.9176$$

Given that, in this case, the equilibrium point corresponds to $\left(0, 0, x_3, \frac{\beta_3}{\alpha_3} \right)$, where, because of (88), x_3 satisfies

$$x_3 = ST - \frac{\beta_3}{\alpha_3} = 146.9 - 100 = 46.9$$

we obtain that

$$x_3 = 46.9 > \max \{N_1, N_2\} = 5.9327$$

and therefore, the equilibrium point $\left(0, 0, x_3, \frac{\beta_3}{\alpha_3}\right) = (0, 0, 46.9, 100)$ is stable.

Case 3

In this case we have

$$\alpha_1\beta_2 = 3.973 \cdot 10^{-4} > 7.7 \cdot 10^{-5} = \alpha_2\beta_1$$

and therefore, the associated equilibrium point is not even nonnegative.

Case 4

Here we have

$$N_2 < 0$$

and therefore, the associated equilibrium point is not even non negative.

Case 5

In this case we have

$$x_1 = ST - \frac{\beta_1}{\alpha_1} = 146.9 - 51.0949 = 95.8051$$

On the other hand,

$$\frac{\alpha_1\beta_2 - \alpha_2\beta_1}{\alpha_2\beta_1\theta} = 41.8064$$

Thus,

$$x_1 > \frac{\alpha_1\beta_2 - \alpha_2\beta_1}{\alpha_2\beta_1\theta}$$

Therefore, the equilibrium point $\left(x_1, 0, 0, \frac{\beta_1}{\alpha_1}\right) = (95.8051, 0, 0, 41.8064)$ is not stable.

Case 6

Here we have

$$x_1 = ST - N_1 - \frac{\beta_3}{\alpha_3} = 40.9673$$

Recall that in this case the eigenvalues of the Jacobian matrix are the roots of the polynomial

$$p(\lambda) = \lambda^3 - [J_{22} + J_{44}]\lambda^2 + [J_{22}J_{44} - \alpha_3N_1J_{43}]\lambda + \alpha_3N_1[J_{22}J_{43} + \mu_2x_1J_{42}]$$

where here,

$$J_{22} = 0.0398, \quad J_{44} = -0.0550, \quad J_{42} = -0.0398, \quad J_{43} = 0.7458$$

i.e.,

$$p(\lambda) = \lambda^3 + 0.0151\lambda^2 - 0.0108\lambda + 0.002$$

Thus, the roots are given by

$$\lambda_1 = -0.1189$$

$$\lambda_2 = 0.0861$$

$$\lambda_3 = 0.0177$$

Therefore, equilibrium point $\left(x_1, 0, N_1, \frac{\beta_3}{\alpha_3}\right) = (40.9673, 0, 5.9327, 100)$ is unstable.

Case 7

Here we have

$$x_2 = ST - \frac{\alpha_1\beta_2 - \alpha_2\beta_1}{\alpha_2\beta_1\theta} - \frac{\beta_1}{\alpha_1} \approx 146.9 - 51.0949 - 8.10243 = 87.70267$$

Further, in this case we have

$$\begin{aligned}\alpha_2\beta_1 &= 7.7 \cdot 10^{-5} < 3.973 \cdot 10^{-4} = \alpha_1\beta_2 \\ \alpha_3\beta_1 &= 7 \cdot 10^{-5} < 1.37 \cdot 10^{-4} = \alpha_1\beta_3\end{aligned}$$

therefore, the equilibrium point $\left(\frac{\alpha_1\beta_2 - \alpha_2\beta_1}{\alpha_2\beta_1\theta}, x_2, 0, \frac{\beta_1}{\alpha_1}\right) = (8.10243, 87.70267, 0, 51.0949)$ is stable.

Case 8

Last, in this case we have

$$x_2 = ST - (K + M \sqrt{N}) - N_1 - \frac{\beta_3}{\alpha_3} \approx 40.78685$$

Further, recall that in this case the eigenvalues of the Jacobian matrix are the roots of the polynomial

$$p(\lambda) = \lambda^3 - J_{44}\lambda^2 + [J_{14}J_{21} - \alpha_3 N_1 J_{43}]\lambda + \alpha_3 N_1 J_{13} J_{21}$$

where

$$J_{13} = 2.0248 \cdot 10^{-3}, \quad J_{14} = 2.33371 \cdot 10^{-4}, \quad J_{21} = 0.42141, \quad J_{43} = 0.1317 \quad J_{44} = -0.055297$$

i.e.,

$$p(\lambda) = \lambda^3 + 0.0611\lambda^2 - 0.0014\lambda - 5.0622 \cdot 10^{-6}$$

Therefore, the eigenvalues are

$$\lambda_1 = -0.0778$$

$$\lambda_2 = 0.0217$$

$$\lambda_3 = -0.0050$$

Therefore, the equilibrium point $\left(K + M \sqrt{N}, x_2, N_1, \frac{\beta_3}{\alpha_3}\right) = (0.18045, 40.78685, 5.9327, 100)$ is not stable.

In summary, we found 6 equilibrium points, from which 2 are stable, namely point

$$\left(0, 0, x_3, \frac{\beta_3}{\alpha_3}\right) = (0, 0, 46.9, 100) \text{ (case 2), and point}$$

$$\left(\frac{\alpha_1\beta_2 - \alpha_2\beta_1}{\alpha_2\beta_1\theta}, x_2, 0, \frac{\beta_1}{\alpha_1}\right) = (8.10243, 87.70267, 0, 51.0949) \text{ (case 7).}$$

Discusión general

La formalización de conceptos ecológicos a partir de la teoría matemática no sólo permite un punto de partida formal para analizar a los ecosistemas, a sus dinámicas y a sus subsistemas, sino que también abre un abanico de herramientas matemáticas y computacionales cuyos resultados pueden ser interpretados a la luz de la ecología y la conservación. Aunque sabemos que los modelos son representaciones de la realidad, pueden generar conocimiento e intuición que, al ser aplicados, generan numerosos beneficios. En este sentido, los modelos permiten responder algunas preguntas que abren el camino hacia nuevas incógnitas. Con ello, los tomadores de decisiones en el plan de manejo de la REPSA, y de otras áreas naturales protegidas y de otros ecosistemas importantes y amenazados, tendrán más elementos para elegir cuál es la mejor estrategia a seguir. Sabemos también que un modelo es en sí mismo un sistema en evolución, por lo que si varias de las propuestas derivadas de él son implementadas, es necesario evaluar los resultados y, de ser el caso, proponer un modelo más adecuado.

Entre más modelación ecológica se haga, habrá más elementos para criticarla. Por ello, es importante plantear diversas metodologías que permitan un diálogo entre la ecología y la teoría de sistemas dinámicos. Entre más interacciones haya entre estas dos áreas del conocimiento, surgirán más herramientas y oportunidades para proponer estrategias que resuelvan los grandes problemas ecológicos. Un ejemplo de los es la resiliencia, que ha sido un tema central en las agendas ambientales en la actualidad. Sin embargo, ha sido un reto medirla, por lo que nuestro modelo es un aporte a la modelación de sistemas ecológicos donde se puede evaluar la resiliencia. Esperamos que este trabajo ayude a implementar este concepto en el plan de manejo de la REPSA. También, esperamos que esto estimule a más ecólogos a realizar modelación con sistemas dinámicos.

Cualquier proceso biótico puede ser modelado. Por ello, es muy importante que los ecólogos conozcan todos los tipos de modelos que permite usar la teoría de sistemas dinámicos para poder elegir el más adecuado (Schuwirth et al., 2019). Sin embargo, no basta con saber cuál es el tipo de modelo más adecuado para responder a nuestra pregunta ecológica. La modelación requiere un análisis profundo y crítico sobre la interpretación de los procesos ecosistémicos a la luz no solo de la ciencia, sino con frecuencia de los procesos históricos de desarrollo de ideas. Un ejemplo de ello es la dominación de la interacción competitiva en los modelos de ensamble de especies.

Por ello, después de hacer un análisis de la literatura de las tres especies focales de este estudio, fue natural elegir dos versiones de los modelos que propusimos, dos en las que solo interviene la competencia y dos en los que se considera una interacción de facilitación entre las plantas nativas. La evidencia bibliográfica y las observaciones en campo sugieren que los modelos que incorporan la

facilitación son los más verosímiles. Esta visión es congruente con la importancia de la facilitación en las comunidades señalada por Callaway (1995), Bruno et al. (2003) y Valiente-Banuet y Verdú (2007). A diferencia de la competencia, no existe una base tan grande de datos cuantitativos que sustente la relevancia de la facilitación. Sin embargo, esto no se debe a su ausencia en la naturaleza. Su sesgo tiene que ver con el desarrollo histórico de los conceptos de competencia, de apoyo mutuo y de sucesión ecológica.

Al proponer la inclusión de una interacción mutualista en dos de los modelos pudimos encontrar evidencia matemática de que la facilitación está directamente relacionada con el estado estable de coexistencia de las especies. Por el contrario, cuando la competencia domina, es mucho más probable encontrar estados estables dominados por una sola especie. Probablemente el número de escenarios donde pudiera ocurrir la coexistencia aumentaría si aumentáramos el número de regulaciones positivas dadas por otras interacciones ecológicas directas e indirectas, tales como cambios en el ambiente, en la disponibilidad de recursos, en las interacciones con polinizadores, con hervíboros y con patógenos. Sería interesante explorar la posibilidad de que el *palo loco* tenga también algún tipo de regulación positiva sobre el *tepozán*. Sin embargo, estas posibilidades tendrán que ser examinadas con experimentos. Nuestros resultados pueden sentar las bases para la realización de estudios experimentales en el futuro que pongan a prueba la existencia de interacciones de facilitación en comunidades ecológicas, así como su papel como estructuradores del ensamble de especies. Sin embargo, no basta con proponer experimentos, sino que además hay que tener un amplio conocimiento del sistema para poder determinar cuáles son las especies clave en las que se deben enfocar los esfuerzos.

Con miras al fortalecimiento y el mejoramiento de los modelos construidos en esta tesis, otro aspecto sumamente importante sería la incorporación en futuros modelos de la REPSA de la dinámica poblacional y las interacciones ecológicas de especies nativas clave, como el arbusto *Verbesina virgata*, el pasto *Muhlenbergia robusta* y la hierba *Dahlia coccinea*. Estas especies hacen un gran aporte de biomasa al ecosistema y pueden estar relacionadas íntimamente con el funcionamiento actual de la REPSA (Cano-Santana, 1994a). Por otro lado, también sería importante incorporar la influencia y dinámica del pasto exótico invasivo proveniente de África oriental, *Cenchrus clandestinus*. Pasando al ámbito del componente animal de este ecosistema, otra especie clave en la REPSA, por su importancia en el flujo de materia y energía, es el chapulín *Sphenarum purpurascens* (Cano-Santana, 1994a). Por esta razón, incorporarlo como regulador del crecimiento de las plantas y como recurso para muchas especies de animales nos daría una visión mucho más realista de la dinámica ecosistémica de la REPSA. Otra de las especies más importantes por su efecto positivo sobre el funcionamiento de la reserva es el conejo castellano *Sylvilagus floridanus* (Lagomorpha), el herviboro más grande de la

REPSA (Dorantes, 2017). Algunas características que lo hacen un candidato ideal para integrarlo a modelos futuros son *i*) su aporte de materia orgánica por acumulación heces en el suelo dirige los flujos de materia y energía, *ii*) su dispersión de semillas através de las heces y *iii*) su aporte como alimento a los depredadores de gran talla (Cano-Santana, 1994b; Dorantes, 2017; Glebskiy, 2019). Su consumo de materia vegetal aérea en algunas zonas de las REPSA ronda entre el 12% y el 18 % (Dorantes, 2017), mientras que un toda la reserva consume entre 2.3 y 5.4 % de la PPNA (Glebskiy, 2016). Sin embargo, una complicación de aumentar la complejidad al incorporar a todas estas especies sugeridas podría hacer que el sistema sea difícil de analizar y que produzca resultados poco verosímiles y con baja aplicabilidad.

En cuanto a las recomendaciones sobre el manejo de esta reserva ecológica derivadas del modelo de tres especies con facilitación, es importante enfatizar que su aplicación debe ser eurística y no tratar de seguir las como reglas rígidas. De hecho, una de las recomendaciones más importantes es la relacionada con el control del eucalipto. Para poder estar en la cuenca de coexistencia, proponemos cortar una cierta área de eucaliptos hasta llegar a una cobertura donde se limite su expansión. En el artículo se hizo la recomendación de plantar tepozanes, sin embargo, éstos presentan altas tasas de colonización en sitios sujetos a restauración (Villeda-Hernández, 2010; González-Rebeles, 2012; Gonzalez-Jaramillo, 2018). Por ejemplo, en una area sujeta a restauración de la reserva con remoción de plantas exóticas su cobertura pasó del 21.5% en 2006 al 40.1% al siguiente año (Villeda-Hernández, 2010). Por ello, en vez que plantar tepozanes los esfuerzos deberían estar dirigidos en evaluar las condiciones del suelo para determinar si es necesaria alguna intervención ya que los tapetes de hojas y las sustancias alelopáticas podrían permanecer en el sitio y afectar su crecimiento. De esta forma, por un lado estaríamos limitando el crecimiento de los eucaliptos al eliminarlos directamente y, por el otro, aumentaríamos la competencia con los tepozanes. Predecimos que el efecto de estas dos medidas sería el mantenimiento de la cuenca de coexistencia con una mayor resiliencia. Sin embargo, una de las mayores críticas que se le pueden hacer a nuestro modelo es el no haber considerado la estructura espacial de las poblaciones de las especies focales, sobre todo considerando que los eucaliptos de la REPSA en la zona núcleo únicamente están en los bordes y sumamente raro encontrarlos al interior de la reserva. En revisiones posteriores del artículo modficaremos la recomendación de planta eucaliptos por la de revisar las condiciones edáficas de los sitios con eucaliptos removidos.

Una de las mayores críticas que se le pueden hacer a nuestro modelo es el no haber considerado la estructura espacial de las poblaciones de las especies focales, sobre todo considerando que los eucaliptos de la REPSA en la zona núcleo únicamente están en los bordes y sumamente raro encontrarlos al interior. Estás imágenes pueden hacer evidente la dinámica en el borde que experimenta

el eucalipto. Esto nos permitiría agregar un término de difusión o analizar a las áreas de manera diferenciada con distintos modelos específicos.

Un elemento que podría jugar un papel determinante en la expansión del eucalipto es el psílido *Glycaspis brimblecombei* que puede infestar al eucalipto hasta llevarlo a la muerte (Romo et al., 2007). Aunque podría considerarse para el control biológico del eucalipto en la REPSA, su alta patogenedida podría salirse de control e infectar a eucaliptos que se quisieran conservar. El problema de tener a muchos eucaliptos muertos en muy poco tiempo podría desencadenar otros problemas ecológicas (Romo et al., 2007; Cantoral, 2015) si no fuera acompañado de un plan de remoción con una tasa similar a la de la muerte por el psílido. Además, existe un parasitoide específico de *G. brimblecombei*, *Psyllaephagus bliteus* (Romo et al., 2007; Cantoral, 2015). Por lo que sería interesante generar experimentos controlados donde se use al psílido como control del eucalipto y al parasitoide para modularlo. Una posible opción de control biológico podría ser infestar a los eucaliptos de los bordes de tal manera que en los bordes que colindan con áreas fuera de la REPSA se coloque al parasitoide para generar una frontera al psílido para que sólo ataque a los eucaliptos de la reserva. Sin embargo, esta propuesta se tendría que evaluar a profundidad con otros expertos de la REPSA.

Nuestro estudio, apoyado en una gran cantidad de observaciones realizadas en las calles de la Ciudad de México, proporciona elementos para proponer al *tepozán* como un árbol clave dentro de la ecología urbana. Esta especie podría permitir la regeneración del suelo y modificar las condiciones ambientales que podrían dar paso al establecimiento de plantas sucesionalmente más maduras, como los encinos, los chapulixtles o los palo dulces. Para dar sustento a esta afirmación, sería importante conocer la dinámica de los sitios donde se distribuyen los tepozanes y este tipo de árboles, para conocer su interacción y así poder predecir si un rodal de *tepozán* en la REPSA podría eventualmente permitir un estado estable encaminado a un bosque de encinos.

Finalmente, cabe hacer una breve disertación filosófica usando algunos de los argumentos de esta discusión. El neodarwinismo y la importancia desproporcionada de la competencia en la evolución permearon el desarrollo de las ideas ecológicas y de sus modelos matemáticos. Pero no se limitaron a la ciencia sino que impactaron profundamente la organización social y económica de las sociedades occidentales. En contraposición, Piotr Kropotkin (1902) propone que el apoyo mutuo es una interacción clave, al menos igual de importante que la competencia en la evolución de las especies y de las sociedades. En este sentido, nuestro modelo es congruente con Kropotkin, sin negar las ideas darwinistas. Por lo tanto, nuestro modelo, más allá de la ciencia, es una propuesta dialéctica que plantea cuestionar la dominancia de las explicaciones basadas en competencia dando también un lugar preponderante a las interacciones de facilitación. Incorporar ambas interacciones y entender su dinámica y su influencia en los distintos ecosistemas nos permitirá tener una comprensión amplia y

realista. Estas ideas nos permiten plantear hipótesis sobre las sociedades. Podemos proponer que las organizaciones sociales con mayores interacciones positivas y de apoyo mutuo pueden construir sociedades más resilientes, en las que la coexistencia sea un estado estable. Esto tendría que ser modelado y comprobado con datos reales en distintos tipos de sociedades. Si encontráramos evidencia que sostenga esta idea, tendríamos que revalorizar las ideas del apoyo mutuo de Kropotkin para construir un futuro habitable.

Conclusiones

En este trabajo se pudo reconstruir la historia ecológica de la comunidad vegetal presente en la Reserva Ecológica del Pedregal de San Ángel de los últimos 70 años. Para ello, se integraron datos heterogéneos cualitativos y cuantitativos. Los modelos simplificaron la complejidad del sistema al grado de poder tratarlo analíticamente. Se identificaron los distintos estados de cada sistema y la probabilidad de que estos se presenten. En conjunto, esta información permitió realizar experimentos *in silico*, lo que a su vez hizo posible hacer predicciones sobre el efecto de los eucaliptos sobre las especies nativas. Este procedimiento mostró la existencia de biestabilidad e incluso triestabilidad para varios estados.

A partir de un análisis de bifurcaciones se pudo determinar que si no se realiza alguna intervención para controlar al eucalipto, esta especie invasiva se volverá dominante. Esto probablemente traería consecuencias catastróficas para la diversidad de esta comunidad. Sin embargo, con la intensidad adecuada para eliminarlos es posible llevar al sistema a un estado estable donde la coexistencia de esta especie con otras plantas nativas sea más probable.

Para aumentar la solidez del modelo aquí presentado, hace falta integrar la estructura y la dinámica espacial de las poblaciones de las especies focales, para así ganar en realismo y poder de explicación. Esta investigación generó una gran cantidad de preguntas acerca de las interacciones ecológicas clave que estructuran el ensamble y la dinámica de la comunidad, que en última instancia aumentan la resiliencia ecosistémica. Transferir estos modelos a los tomadores de decisiones en los planes de manejo de esta área natural protegida y otras equivalentes podría permitir la conservación de los ecosistemas y de su recursos de una manera más eficaz y resiliente.

Referencias bibliográficas

- Andersen, T., Carstensen, J., Hernández-García, E., Duarte, C.M. 2009. Ecological thresholds and regime shifts: approaches to identification. *Trends in Ecology and Evolution* 24, 49–57.
- Angeler, D.G., Allen, C.R. 2016. Quantifying resilience. *Journal of Applied Ecology*, 53: 617–24.
- Briske, D.D., Fuhlendorf, S.D., Smeins, F.E. 2005. State-and-transition models, thresholds, and rangeland health: a synthesis of ecological concepts and perspectives. *Rangeland Ecology & Management*, 58: 1–10.
- Bruno, J.F., Stachowicz, J.J., Bertness, M.D. 2003. Inclusion of facilitation into ecological theory. *Trends in Ecology and Evolution*, 18: 119-125.
- Callaway, R.M. 1995. Positive interactions among plants. *The Botanical Review*, 61: 306-349.
- Cano-Santana, Z. 1994a. Flujo de energía a través de *Sphenarium purpurascens* (Orthoptera: Acrididae) y productividad primaria neta aérea en una comunidad xerófita. Tesis (Doctorado en Ciencias), Universidad Nacional Autónoma de México, México.
- Cano-Santana, Z. 1994b. La Reserva del Pedregal como ecosistema: estructura trófica. pp. 149- 157. In: A. Rojo (comp.). *Reserva ecológica El Pedregal de San Ángel: ecología, historia natural y manejo*, Universidad Nacional Autónoma de México, Ciudad de México.
- Cano-Santana, Z., Meave, J. 1996. Sucesión secundaria en derrames volcánicos: el caso del Xitle. *Ciencias*, 41: 58–68.
- Cantoral-Herrera, M. T. 2015. Control biológico de *Glycaspis brimblecombei* en las áreas verdes del Distrito Federal. Tesis de Maestría. Universidad Nacional Autónoma de México,
- Clements, F. 1916. Plant succession: an analysis of the development of vegetation. Carnegie Institute of Washington, Washington, Estados Unidos de América.
- Dakos, V., van Nes, E.H., Donangelo, R., Fort, H., Scheffer, M. 2010. Spatial correlation as leading indicator of catastrophic shifts. *Theoretical Ecology*, 3, 163-174.
- Dorantes, D. 2017. Distribución y abundancia del conejo castellano, *Sylvilagus floridanus* (Lagomorpha), en la Reserva del Pedregal de San Ángel, Cd. Mx., México. Tesis de licenciatura, Universidad Nacional Autónoma de México.
- Evans, M.R, M. Bithell, S., Cornell, S.J., Dall, S.R.X., Díaz, S., Emmott, S., Ernande, B., Grimm, V., Hodgson, D.J., Lewis, S.L., Mace, G.M., Morecrof, M., Moustakas, A., Murphy, E., Newbold, T., Norris, K.J., Petchey, O., Smith, M., Travis J.M.J., Benton, T.G. 2013. Predictive systems ecology. *Proceedings of the Royal Society*, 280: 20131452.

- Glebskiy, Y. 2016. Factores que afectan la distribución y abundancia del conejo castellano (*Sylvilagus floridanus*) en la Reserva Ecológica del Pedregal de San Ángel, D.F. (México). Tesis profesional. Universidad Nacional Autónoma de México.
- Glebskiy, Y. 2019. Efecto del conejo castellano (*Sylvilagus floridanus*) sobre la comunidad vegetal del Pedregal de San Ángel. Tesis de maestría. Universidad Nacional Autónoma de México.
- González-Rebeles G, G. 2012. Efecto de cinco años de restauración sobre la comunidad vegetal y dos poblaciones de artrópodos en el área A11 de la Reserva del Pedregal de San Ángel. Tesis profesional. Universidad Nacional Autónoma de México.
- González-Jaramillo, S.I. 2018. Estructura y composición de la comunidad vegetal de dos sitios sujetos a acciones de restauración durante el periodo 2005-2012 en la Reserva Ecológica del Pedregal de San Ángel, Ciudad de México, México. Tesis profesional. Universidad Nacional Autónoma de México
- Holling, C.S. 1973. Resilience and stability of ecological systems. *Annual Review of Ecology and Systematics* 4: 1–23.
- Kropotkin, P. 1902. *El Apoyo Mutuo*. Editorial Redez. Redición, agosto 2014. Ciudad de México, México.
- Larsen, L.G., Eppinga, M.B, Passalacqua, P., Getz, W.M., Rose, K.A., Liang, M. 2016. Appropriate complexity landscape modeling. *Earth-Science Reviews*, 160: 111–130.
- MacArthur, R. 1955. Fluctuations of animal populations and a measure of community stability. *Ecology*, 36: 533-536.
- Martínez-Orea, Y., Castillo Argüero, S., Guadarrama-Chávez, M., Sánchez, I. 2010. Post-fire seed bank in a xerophytic shrubland. *Botanical Sciences*, 86: 11–21.
- May, R. M. 1973. Stability and Complexity in Models Systems. Princeton University Press.
- May, R. M. 1977. Thresholds and breakpoints in ecosystems with a multiplicity of stable states. *Nature*, 269: 471-477.
- Meave, J. y E. A. Perez-García. 2013. Vegetación: caracterización y factores que determinan su distribución. pp. 470-477, In: Márquez-Guzmán, J., M. Collazo-Ortega, M. Martínez-Gordillo, A. Orozco-Segovia y S. Vázquez-Santana (eds.). *Biología de Angiospermas*, Universidad Nacional Autónoma de México, Ciudad de México.
- Mendoza Hernández, P.E. 2003. El Tepozán. *Ciencias* 70: 32-33.
- Nazarimehr, F., Jafari, S., Golpayegani, S.M.R.H., Perc, M., Sprott, J.C. 2018. Predicting tipping points of dynamical systems during a period-doubling route to chaos. *Chaos*, 28: 073102.
- Patten, B. 1966. Systems ecology: A course sequence in mathematical ecology. *BioScience*, 16: 593-598.

- Rietkerk, M., Dekker, S.C., De Ruiter, P.C., Van De Koppel, J. 2004. Self-organized patchiness and catastrophic shifts in ecosystems. *Science* 305: 1926–1929.
- Romo Lozano, J. L., García, J., Cibrián, D., Serrano, E. 2007. Análisis económico del control biológico del psílido del eucalipto en la Ciudad de México. Revista Chapingo. Serie Ciencias Forestales y del Ambiente. 13 (1), 47-52.
- Rzedowski, J. 1954. Vegetación del Pedregal de San Ángel. *Anales de la Escuela Nacional de Ciencias Biológicas, Instituto Politécnico Nacional*. 8, 59–129.
- Scheffer, M., Carpenter, S.R. 2003. Catastrophic regime shifts in ecosystems: linking theory to observation. *Trends in Ecology and Evolution* 18: 648–56.
- Scheffer, M., Carpenter, S., Foley, J.A., Folke, C., Walker, B. 2001. Catastrophic shifts in ecosystems. *Nature*, 413: 591–96.
- Schröder, A., Persson, L., De Roos, A.M. 2005. Direct experimental evidence for alternative stable states: a review. *Oikos*, 110: 3-19.
- Schuwirth, N., Borgwardt, F., Domisch, S., Friedrichs, M., Kattwinkel, M., Kneis, D., Kuemmerlen, M., Langhans, S.D., Martínez-López, J., Vermeiren, P. 2019. How to make ecological models useful for environmental management. *Ecological Modelling*, 411: 108784.
- Segura-Burciaga, S. 2009. Introducción de especies: la invasión y el control de *Eucalyptus resinifera*. In: Lot, A., Cano-Santana, Z. (eds.), Biodiversidad del Ecosistema del Pedregal de San Ángel, pp. 533–538. Universidad Nacional Autónoma de México, México.
- Segura-Burciaga, S., Meave, J. 2001. Effect of the removal of individuals of the exotic species *Eucalyptus resinifera* on the floristic composition of a protected xerophytic shrubland in southern Mexico City. In: Brundu, G., Brock, J., Camarda, I., Child, L. Wade, M. (eds.). Plant invasions: species ecology and ecosystem management, pp. 319–330. Backhuys Publishers.
- Siebe, C. 2009. La erupción del volcán Xitle y las lavas del Pedregal hace 1670 +/- 35 años AP y sus implicaciones. In: Lot, A., Cano-Santana, Z. (eds.), Biodiversidad del Ecosistema del Pedregal de San Ángel, pp. 43–49. Universidad Nacional Autónoma de México, Ciudad de México.
- Suding, K.N., Hobbs, R.J. 2009. Threshold models in restoration and conservation: a developing framework. *Trends in Ecology & Evolution*, 24: 271–79.
- Tansley, A.G. 1935. The use and abuse of vegetational concepts and terms. *Ecology* 16, 284–307.
- Valiente-Banuet, A., Verdú, M. 2007. Facilitation can increase the phylogenetic diversity of plant communities. *Ecology Letters*, 10: 1029-1036.
- van Nes, E.H., Scheffer, M. 2007. Slow recovery from perturbations as a generic indicator of a nearby catastrophic shift. *American Naturalist* 169: 738–47.

- van der Valk, A. 2013. From formation to ecosystem: Tansley's response to Clements' climax. *Journal of the History of Biology*, 47 (2): 293–321.
- Villeda-Hernández, M. 2010. Estructura de la comunidad vegetal y abundancia de *Sphenarum purpurascens* (Orthoptera) y *Peromyscus gratus* (Rodentia) en el área “Vivero Alto” de la Reserva Ecológica del Pedregal de San Ángel sujeta a acciones de restauración. Tesis profesional. Universidad Nacional Autónoma de México.
- Willis, A. J 1997. The ecosystem: an evolving concept viewed historically. *Functional Ecology*, 11: 268–271.